

The copyright of this thesis rests with the University of Cape Town. No quotation from it or information derived from it is to be published without full acknowledgement of the source. The thesis is to be used for private study or non-commercial research purposes only.



**EXPERIMENTAL INVESTIGATION OF THE SHEAR
STRENGTH CHARACTERISTICS OF A GEOSYNTHETIC
CLAY LINER AND ITS APPLICATION IN A LOCAL
LANDFILL LINING SYSTEM**

Wesley Rouncivell

Bachelor of Science (Eng. Civ.) (Hon.)
University of Cape Town, South Africa, 2005

A thesis submitted to the University of Cape Town in partial fulfilment of the requirement for the degree of Master of Science in Engineering.

**Department of Civil Engineering
University of Cape Town**

August 2007

DECLARATION

I, **Wesley Edward Rounclivell**, hereby declare that this thesis is essentially my own work, except where otherwise indicated, and has not, to the best of my knowledge, been submitted for a degree at any other university.

Signed by candidate

University of Cape Town

ACKNOWLEDGEMENTS

I would like to thank the following people and institutions for their invaluable help during the course of this research:

Dr. F. Scheele, my supervisor, for his continuous and invaluable guidance, encouragement, commitment and constructive criticism during this work. Secondly for the generous scholarship he awarded me from the University of Cape Town Geotechnical Laboratory research fund.

The UCT Civil Engineering staff in the Workshop: Eike von Guerard, Charles Nicholas, Theo Mayan. Thank-you for always being ready to help with repairs and modifications of the testing equipment.

The UCT Civil Engineering Laboratory Manager, Noor Hessen, for accommodating and supporting my extended testing schedules.

Ms.T. Marimuthu and her family for their patience, support and understanding while I dedicated so much time to this research.

Mr. Piet Meyer and Aquatan SA who donated the materials, including their delivery cost to the UCT Geotechnical laboratory, for this research.

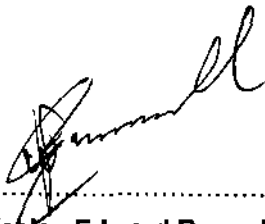
The University of Cape Town for the two University Research scholarships awarded to me, as well as organising the K W Johnston Bequest Scholarship.

Ninham Shand for the their generous post graduate scholarship.

Chris Wise, Shakira Sitarand and Suné de Klerk from Jeffares & Green who gave valuable input regarding the design of a local Cape Town landfill.

My friends, Duane, Alex, Allan, Yu-Lun, Ajith, Guy, Bone, Anthony and Victor who helped me preserve my sanity.

My sincerest gratitude,



.....
Wesley Edward Rouncivell

EXECUTIVE SUMMARY

The first geosynthetic clay liner (GCL) products were developed in the mid 1980s and have been available in South Africa since around 1995. This relatively new material is commonly incorporated in highly developed landfill liner designs which present new challenges for the geotechnical engineer. Although the GCLs primary function in a lining system is as a contaminant barrier, it has to perform structurally during construction and the project design life.

The Bellville South general waste landfill in the Western Cape, South Africa, has a lining system containing a GCL and smooth geomembrane placed against each other. The frictional strength between these materials and other interfaces in the lining are relatively low. Characterisation of the shear behaviour of all the materials and interfaces using a large direct shear device is the core objective of this study. The Civil Engineering Geotechnical Laboratory at the University of Cape Town developed this device in line with the latest international testing standards.

The specifically manufactured steel surfaces for gripping geosynthetics worked adequately over a wide range of normal stresses. Extruded bentonite on the smooth geomembrane/GCL interface at higher normal stress reduces shear strength resulting in a distinctive bilinear shear strength envelope. Extended hydration of the GCL has no significant effect on measured shear strength of the GCUsmooth geomembrane interface. 'Hook and loop' interaction in the textured geomembrane/GCL interface greatly increased the shear strength compared with the smooth geomembrane interface tests.

Combined shear strength failure envelopes were determined for different liner designs. If a smooth geomembrane is chosen then the GCUgeomembrane interface will be the critical failure plane. However, if a single-sided textured geomembrane is used, the failure plane will be shifted from the GCUgeomembrane interface to the sand/geomembrane interface at low normal stresses and to the investigated GCL at higher applied normal stresses.

In view of the combined shear strength failure envelope of the investigated landfill liner which is in principle in compliance with a wide variety of liner profiles a limit state approach to landfill slope design was developed that determines the factor of safety before and after waste placement. Partial factors of safety can easily be included into the analysis and the incorporation of a combined or multi-linear shear strength envelope is possible. If a textured geomembrane is chosen, it is shown that it is imperative that the GCL internal shear strength be reliably established.

Further testing in the large direct shear device to determine the interface shear strength parameters for other typical landfill lining interfaces is recommended. This can successfully be undertaken in the newly developed large direct shear device. The proposed design method is believed to form a good and valid basis for further work to eventually establish a design code for landfill stability assessment which should be incorporated into South African minimum standards for landfill design.

TABLE OF CONTENTS

DECLARATION	
ACKNOWLEDGEMENTS	ii
EXECUTIVE SUMMARY	
TABLE OF CONTENTS	iv
CHAPTER 1	
INTRODUCTION	1
1.1 Introduction	1
1.2 Research objectives and methodology	2
1.3 Thesis overview	3
CHAPTER 2	
HISTORICAL DEVELOPMENT	4
2.1 Introduction	4
2.2 Landfill development	4
2.3 Environmental Geotechnology	4
2.4 Geosynthetics	5
2.5 Waste treatment and disposal in South Africa	5
CHAPTER 3	
GEOSYNTHETICS IN LANDFILL DESIGN	7
3.1 Introduction	7
3.2 Geosynthetic definitions and functions	7
3.4 Landfill geometries	9
3.5 Containment liner systems	9
3.6 Geosynthetic Clay Liner	12
3.6.1 Bentonite Clay	12
3.6.2 Product development	13
3.6.3 Needle-punched GCL process	14
3.6.4 Research GCL: Bentomat ST	14
3.6.4.1 Geotextile components	15
3.6.4.2 Bentonite component	15
3.7 Local landfill	16
3.7.1 Liner system	16
3.7.2 Slope Design	18
3.8 Slope stability	18
CHAPTER 4	
LITERATURE REVIEW OF PREVIOUS RESEARCH	21
4.1 Introduction	21
4.2 Direct Shear Test Principle and Apparatus	21
4.2.1 Advantages and disadvantages of the large direct shear device	25
4.2.3 Apparatus limitations	25
4.2.4 Torsional ring shear device	26
4.2.5 Inclined plane shear	26
4.2.6 Specimen gripping system	26
4.3 GCL Internal Shear Strength	27
4.4 Interface Shear Strength	27
4.5 Specimen Preparation	28
4.5.1 Accelerated procedures	29

4.6	Shearing	30
4.6.1	Shear displacement rate	30
4.6.1.1	GCL internal shear strength	31
4.6.1.2	GCL interface shear strength	31
4.7	Bentonite Moisture Content	32
4.8	GCL Index Testing	32
4.9	Shear Strength Results	32
4.9.1	Field data	33
4.9.2	Laboratory test data	33
4.9.3	Multi-interface testing	35
4.9.3	Long term shear strength	37
4.10	Design Guidelines	38
4.10.1	South African Department of Water Affairs and Forestry	38
4.10.2	South African National Standard	38
4.11	Design Methods	39
4.11.1	Manual calculation	39
4.11.2	Pore water pressure	40
4.11.3	Numerical analyses	40
4.11.5	Modern computer solutions	42
4.12	Shear Strengths for Design	43
4.13	Research Requirements	44

CHAPTER 5

RESEARCH MATERIALS	46	
5.1	Introduction	46
5.2	Properties of the Geosynthetic Clay Liner	46
5.2.1	Geotextile components	46
5.2.2	Clay mineral	46
5.2.3	Geocomposite	47
5.2.4	Geomembrane	47
5.3	Mechanical Properties of Philippi Dune Sand	48
5.4	Micrographs of Research Materials	50

CHAPTER 6

GCL INDEX TEST INVESTIGATIONS	53	
6.1	Introduction	53
6.2	Peel test	53
6.3	Swell test	53
6.4	Mass per Unit Area test	54

CHAPTER 7

DIRECT SHEAR INVESTIGATION	55	
7.1	Introduction	55
7.2	Direct Shear Test Program	56
7.3	Large Direct Shear Device	57
7.3.1	Apparatus	57
7.3.2	Shear-box inserts	58
7.3.3	Shear device calibration	59
7.3.4	Specimen preparation	59
7.3.5	Procedures	60
7.3.6	Normal stress determination	60
7.3.6	Analysis	61

CHAPTER 8

RESULTS, ANALYSIS AND DISCUSSIONS	62
---	----

8.1	Introduction	62
8.2	Investigation of GCL property test results	62
8.2.1	Peel Test	62
8.2.2	Swell Test	63
8.2.3	Mass per unit area test	63
8.2.4	Comparison of GCL batches	63
8.3	Investigation of direct shear test results	64
8.3.1	Shear stress — horizontal displacement relationship	64
8.3.1.1	GCL internal shear strength	64
8.3.1.2	GCUsmooth geomembrane interface	66
8.3.1.2.1	Stick & Slip behaviour	68
8.3.1.3	GCL / textured geomembrane interface	68
8.3.1.4	Sand	69
8.3.1.5	Geomembrane / sand interface	70
8.3.1.6	GCL / sand interface	71
8.3.1.7	Pre-peak behaviour	72
8.3.1.8	Material damage	73
8.3.1.9	Displacement at peak	74
8.3.1.10	Bentonite moisture content	75
8.3.1.11	'Unique' tests	76
8.3.2	Shear stress — normal stress relationship	77
8.3.2.1	GCL	77
8.3.2.2	GCL /geomembrane interface	78
8.3.2.3	Sand	79
8.3.2.4	Geomembrane / sand Interface	80
8.3.2.5	GCL / Sand Interface	81
8.3.3	Comparison of direct shear interface tests	81
8.3.4	Comparison of direct shear interface tests with previous studies	83
8.3.5	Liner system shear strength	84
8.4	CONCLUSIONS	86
CHAPTER 9		
	LIMIT STATE ANALYSIS OF LANDFILL LINING SYSTEM	88
9.1	Introduction	88
9.2	Analysis methods	88
9.2.1	Partial factors of safety	89
9.3	Design parameters	91
9.4	Analysis	93
9.4.1	Verification	95
9.5	Results	95
9.6	Conclusion	96
CHAPTER 10		
	CONCLUSION	97
10.1	Introduction	97
10.2	Experimental investigation	97
10.3	Limit state analysis	98
10.4	Recommendations	99
	REFERENCES	100
	Appendix A. Test Procedures	108
	Appendix B. Large Direct Shear Devices	126
	Appendix C. Scanning Electron Microscope Images	129

Appendix D. Test Work Sheets	134
Appendix E. Direct Shear Test Raw Data	139
Appendix F. Landfill Design	141

List of Figures

Figure 1.1 Example of a Geosynthetic Clay Liner	1
Figure 3.1 Landfill cross sectional geometries (after Rathje & Bray, 2001)	9
Figure 3.2 Example of a general waste landfill liner system (after DWAF, 1998)	10
Figure 3.3 Theoretical structure of smectite molecules according to Hofmann, Endell and Wilm (1933), Marshall (1935), and Hendricks (1942). (after Grim, 1968; Cetco Poland, 2006)	13
Figure 3.4 Geosynthetic Clay Liner manufacturing process (after Naue, 2004)	14
Figure 3.5 Bellville South landfill — existing waste	16
Figure 3.6 Bellville South Landfill liner system installation	16
Figure 3.7 Bellville South landfill liner system (after Jeffares & Green, 2006)	17
Figure 3.8 Belleville South Landfill liner slope	19
Figure 3.9 Landfill boundary slope with liner	19
Figure 4.1 Direct shear device load application configuration a) sand test b) geosynthetic / sand interface test c) geosynthetic / geosynthetic interface test	22
Figure 4.2 Typical shear stress-displacement relationship for an internal shear test of a hydrated GCL (after Fox & Stark, 2004)	23
Figure 4.3 Gripping system of this investigation	27
Figure 4.4 Peak and residual shear strength failure envelopes for composite specimens (Eid, 2002).	37
Figure 4.5 Typical landfill two dimensional geometry	41
Figure 5.1 Grain size distribution of Phillipi Dune and Cape Flats sands	48
Figure 5.2 Dry density — moisture content relationship of Phillipi Dune and Cape Flats sand	49
Figure 5.3 Micrographs of research materials a) Phillipi Dune sand b) Non-woven geotextile c) Non- woven geotextile fibres d) Woven geosynthetic with needle punched non-woven fibres e) Bentonite — granular	51
Figure 5.4 Bentonite: 11% moisture content	52
Figure 6.1 a) Peel strength test in progress, b) Swell test sample showing upper bentonite level	54

Figure 7.1 Large Direct Shear Device	55
Figure 7.2 GCUgeomembrane interface test setup	57
Figure 7.3 Normal stress loading system	58
Figure 7.4 Component parts of the large direct shear box with inserts a) Vertically guided load plate b) Upper and lower shear-boxes c) GCL specimen d) Base plate for sand test e) Drop hammer f) Upper spacer plate g) Upper grip plate with geomembrane h) Lower grip plate showing textured surface i) Lower spacer plate	59
Figure 8.1 Summary of Peel Strength Tests for GCL A	62
Figure 8.2 Shear stress versus horizontal displacement of the GCL internal interface at indicated peak normal stresses	65
Figure 8.3 Shear stress versus horizontal displacement of the GCL / smooth geomembrane interface	67
Figure 8.4 Shear stress versus horizontal displacement of the GCL / smooth geomembrane interface after long hydration periods	67
Figure 8.5 GCL textured geomembrane interface showing hook and loop interaction	68
Figure 8.6 Shear stress versus horizontal displacement of the GU/ textured geomembrane interface	69
Figure 8.7 Shear stress versus horizontal displacement of the tests on sand	70
Figure 8.8 Shear stress versus horizontal displacement of the geomembrane / sand interface	71
Figure 8.9 Shear stress versus horizontal displacement of the GCL / sand interface	72
Figure 8.10 Normal stress versus shear stress relationship of the pre- peak shear stress reduction of the GCL and GCL / smooth geomembrane interface	72
Figure 8.11 Smooth geomembrane damage after GCL interface test at 433kPa peak normal stress	73
Figure 8.12 a) Geomembrane damage after dry sand interface test (433kPa peak normal stress) ..	74
Figure 8.12 b) Geomembrane damage after hydrated sand interface test (436kPa peak normal stress)	74
Figure 8.13 Displacement versus normal stress at peak shear stress conditions of all investigated interfaces	74
Figure 8.14 Bentonite moisture contents after direct shear interface tests.	75

Figure 8.15 Shear stress versus horizontal displacement of the unsuccessful GCL / sand interface tests.....	76
Figure 8.16 Shear stress versus horizontal displacement of the unsuccessful GCL / textured geomembrane interface tests	77
Figure 8.17 Shear strength diagram of GCLs	78
Figure 8.18 Shear strength diagram of the dry and hydrated GCL / geomembrane interface	79
Figure 8.19 Shear strength diagram of the GCL geomembrane interface investigating extended hydration	79
Figure 8.20 Shear strength diagram of the dry and hydrated sand tests	80
Figure 8.21 Shear strength diagram of the dry and hydrated geomembrane / sand interface	80
Figure 8.22 Shear strength diagram of the GCL / sand interface	81
Figure 8.23 Peak shear strength diagram summary of all the investigated interfaces	82
Figure 8.24 Large displacement shear strength diagram of all the investigated interfaces	83
Figure 8.25 Combined shear strength diagram of case 1	85
Figure 8.26 Combined shear strength diagram of case 2	85
Figure 8.27 Combined shear strength diagram of case 3	85
Figure 9.1 Determination of side slope interface shear strength	94

List of Tables

Table 3.1 Properties of compacted clay liners	11
Table 3.2 Bellville South landfill liner layers	17
Table 4.1 Summary of investigations of interface shear strength associated with materials used in landfill liners	34
Table 4.2 Summary of shear strength properties of materials used in landfill liners	36
Table 4.3 Summary of limit state analyses	41
Table 5.1 Properties of BENTOMAT®ST Geotextiles (CETCO specifications, 2006)	46
Table 5.2 Properties of BENTOMA®ST (CETCO specifications, 2006)	47
Table 5.3 Properties of HI-DRILINE® Smooth (HDPE) (Aquatana specifications, 2007)	48
Table 5.4 Soil mechanical properties of Philippi Dune sand	49
Table 5.5 Summary of direct shear test results	50

Table 6.1 GCL property test program	53
Table 7.1 Direct shear test program	56
Table 8.1 Summary of Peel Strength Tests for GCL A	62
Table 8.2 Summary of Swell Tests of GCL A bentonite	63
Table 8.3 Mass per unit area of synthetic components of GCL A	63
Table 8.4 Summary of mass per unit area tests	63
Table 8.5 Summary of GCL characteristics	64
Table 8.6 Summary of GCL internal shear tests	65
Table 8.7 Summary of GCL / smooth geomembrane shear tests	66
Table 8.8 Summary of GCUtextured geomembrane shear tests	68
Table 8.9 Summary of sand shear tests	69
Table 8.10 Summary of geomembrane /sand shear tests	70
Table 8.11 Summary of GCL / sand shear tests	71
Table 8.12 Summary of sand properties of the GCL / sand shear tests	71
Table 8.13 Summary of unsuccessful shear tests	76
Table 8.14 Summary of GCL shear strength results	77
Table 8.15 Summary of GCL / geomembrane shear strength results	78
Table 8.16 Summary of GCL / textured geomembrane shear strength results	78
Table 8.17 Summary of sand shear strength results	79
Table 8.18 Summary of geomembrane / sand shear strength results	81
Table 8.19 Summary of GCU sand shear strength results	81
Table 8.20 Summary of interface shear strength results	82
Table 9.1 Summary of partial safety factors	91
Table 9.2 Landfill cases	92
Table 9.3 Interface shear strength properties	92
Table 9.4 Revised interface shear strength properties	92
Table 9.5 Material properties	92
Table 9.6 Weighted material properties	93
Table 9.7 Verification examples	95
Table 9.8 Summary of results	95

CHAPTER 1

INTRODUCTION

1.1 Introduction

Landfill liners aim to prevent leakage of contaminants from stored waste into the geological environment and groundwater. There are a wide variety of lining systems in use depending on site conditions and the type of waste involved. In general they are made up of a leakage detection layer between a primary and secondary liner. The main barrier material is traditionally a thick compacted clay layer.

The high cost, scarce availability and often questionable effectiveness of the clay prompted the development of thinner, more predictable alternatives. This included compacted clay/sand mixes, plastic geomembranes and the advent of Geosynthetic Clay Liners (GCLs) in the 1980s. A GCL is a thin clay layer combined with one or two layers of geosynthetics, a typical example is shown in Figure 1.1.

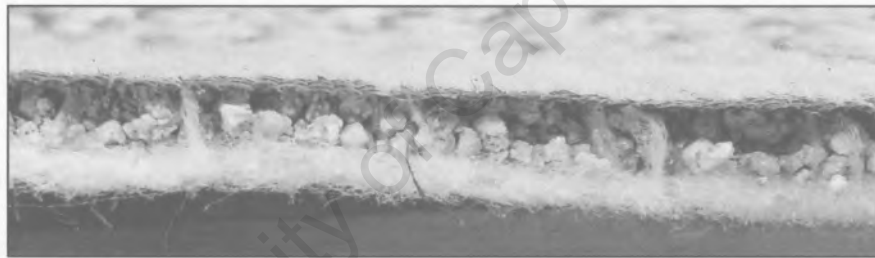


Figure 1.1 Example of a Geosynthetic Clay Liner

Many improvements to the first GCLs have been made by various manufacturers and a wide product range has been established. The needlepunched reinforced type has become the more common choice in the US for lining systems (Fox & Stark, 2004) especially where steep slopes are part of the design. GCLs are also becoming more and more accepted as a reliable option for lining systems of landfills and mining waste facilities in South Africa.

The Department of Water Affairs and Forestry (DWAF) has not yet standardised a liner design incorporating a GCL, but the profession is able to apply for its use which the DWAF will review. Reinforced GCLs have been used in one of South Africa's most hazardous mining dumps — manganese waste — and in most cells of the largest landfill in the City of Cape Town, among others. The use of GCLs in large scale projects is therefore becoming widely accepted as an attractive solution in landfill barrier problems. However, due to the complexity of the products' structure and properties, numerous aspects of its use in design are lacking.

A GCL is commonly used hand in hand with plastic membranes. These geomembranes are generally placed in direct contact with the GCL. The intimate contact prevents contaminants spreading over a

large area of the GCL if a hole develops in the overlying geomembrane. There is, however, a serious drawback of this combination: the low frictional strength at the interface, especially if a smooth geomembrane is used. The underside of the GCL is generally placed on sand which acts as a leakage detection layer. The mechanical behaviour of this interface has, to the author's knowledge, only superficially been investigated.

The internal shear strength of the GCL is a critical aspect of the GCL itself. Most research has been conducted in this area; this is more surprising since there are no known cases of slope failure caused by this mechanism (Bouzza, 2002). Only one study has been published (Triplett & Fox, 2001) on the GCL/geomembrane interface behaviour using a large interface area as required by the current US testing standards (ASTM D 6243).

Although the GCL and geomembrane's primary function in a lining system is as a contaminant barrier, it has to perform structurally during construction and the project design life. Slope stability is dependent on the steepness of the slope, the shear strength characteristics of the various materials and the frictional behaviour of the respective interfaces. If excessive displacements occur the integrity of the lining system components can be detrimentally affected or even the geosynthetics primary function compromised.

It is the shear strength characteristics of a primary landfill lining system in a local landfill site containing both a geomembrane and a GCL that are investigated in this study.

1.2 Research objectives and methodology

As mentioned previously, the internal and interface frictional strength of the lining materials is critical for the safe design of side slopes in waste containment facilities.

The core objective is to characterize the shear behaviour of all the materials and interfaces in a local landfill lining system using a large direct shear device as required by the latest international testing standards (ASTM D 6243; ASTM D 5321)

Another goal of the study is to objectively confirm the properties of the chosen GCL. This is to be done by conducting the most common standard index tests for the material as well as assessing its internal shear strength.

A microscopic investigation of all the research materials is also an objective since micrographs are essential for understanding the microstructure and thus the behaviour of the involved materials.

An interesting side objective of the study is to investigate how different direct shear test procedures and testing conditions may influence the measured shear strength over a large range of normal stresses. In general, commercial testing laboratories prefer the fastest and least labour intensive test methods and procedures.

The final objective is to use the interface shear strength results to assess the stability of the local landfill design as well as to identify the slope geometry critically by considering the interfaces tested in this study.

1.3 Thesis overview

Chapter 2 explores the historical development of modern lining systems and the unique materials which make them possible. Chapter 3 demonstrates how geosynthetics are incorporated in these lining systems, with focus on a South African example. A review of previous studies is presented in Chapter 4. This includes an overview of the laboratory test procedure, landfill limit state analyses and South African landfill minimum design requirements. Chapter 5 discusses the materials of the components of the primary lining system investigated in this study.

The measurement of various properties of the GCL and its component parts are briefly discussed in Chapter 6. Chapter 7 deals with the method of investigation of the shear strength of the liner system interfaces using the large direct shear device. Chapter 8 presents all the results of the GCL index tests and the direct shear tests of the various liner interfaces. Chapter 9 proposes a landfill limit state design method to hopefully set the groundwork for a comprehensive South African standard for landfill liner systems containing geosynthetics. A summary of the conclusions of the experimental study and design analysis, as well as recommendations for further investigations are presented in Chapter 10.

CHAPTER 2

HISTORICAL DEVELOPMENT

2.1 Introduction

The development of modern lining systems for landfills grew out of an increased awareness of the need to contain contaminants to protect public health and the environment. Towards the end of the 20th century improved geotechnical knowledge and innovations of the polymer industries made the sophisticated designs of landfill liners possible. This chapter explores the history of these aspects, the way they evolved and their current effect on waste management solutions in South Africa.

2.2 Landfill development

In the USA waste disposal laws were passed as early as 1795 (Williams, 1998) and all US cities provided a waste collection system by 1930 (Neal & Schubel, 1987). In the UK, the threat to human health was addressed by the Nuisance Removal and Disease Prevention Acts of 1875 and 1936 (British Medical Association, 1991). Landfilling, the controlled tipping of waste, was the dominant waste treatment and disposal method due to its cost effectiveness. Waste incineration was the main alternative to landfilling, but like most other disposal methods residues invariably reach landfills.

The years between 1940 and 1960 saw an enormous expansion of manufacturing capacity in industrialized countries (Daniel, 1993) resulting in vast quantities of industrial and hazardous waste. The rapidly growing world population simultaneously increased municipal solid waste production and growing cities brought people closer to abandoned and new landfill sites. Thus, a move from merely dumping or minimal landfill planning led to landfill design. Increased waste quantity and various incidents, from cyanide dumping in Germany (1971) to toxic leachates and vapour leakages in a housing development in New York State (1977), drove legislators to evolve sophisticated containment designs and cleanup protocols for new and existing sites (Daniel, 1993). Geosynthetics became increasingly popular in such systems due to their reliable quality and cost effectiveness. The use of geosynthetics reduced the thickness of the lining system and greatly improved its performance if installed properly.

2.3 Environmental Geotechnology

Great advances were made in Geotechnical Engineering in the 1950s and 1960s but there was Me emphasis on environmental matters. Clayey soils were thought to *be* impermeable and the mere existence of such materials in a lining system of a waste containment facility was thought to be adequate to protect the environment. In the 1970s geotechnical engineers became involved in large scale considerations of the environment for the first time, producing environmental impact statements for nuclear power plants in the US.

The sophisticated landfill designs developed by legislators in the late 1970s presented new challenges for the geotechnical engineer and made the landfill into a veritable engineering structure to be managed over its full design life.

2.4 Geosynthetics

The synthetic materials used in geotechnical engineering are termed geosynthetics, defined as a 'product manufactured wholly or in part from polymeric material used with soil, rock, earth, or other geotechnical engineering related material as an integral part of a project, structure or system' (ASTM 4469). The development of modern liner materials, including geotextiles and geomembranes, is intrinsically linked to the development of the polymer industry (Williams, 1998). Two of the main synthetics used as geosynthetic materials are polyethylene (PE) and polypropylene (PP) which were discovered in 1933 and 1954, respectively (Huang & Gao, 2001).

According to Staff (1984) the earliest type of thin prefabricated polymer sheets placed on a prepared soil base was the use of polyvinylchloride (PVC) as swimming pool liners in the early 1930's. Research into using large polymer membranes in lining water canals was undertaken by the US Bureau of Reclamation in the 1950's (Hickey, 1957). The industry grew rapidly thereafter. West Germany and South Africa were heavily involved with the development of polyethylene liners in the 1980's (Williams, 1998).

One of the earliest documented cases of the use of woven geotextiles was for a waterfront structure in Florida in 1958. The first non-woven geotextile was developed in 1968 by the Rhone Poulenc company in France which was used in a dam construction in 1970 (Huang & Gao, 2001).

The first geosynthetic clay liner (GCL) products were developed in 1986 (Stark & Eid, 1996). In 1987 the German company NAUE developed a reinforced GCL and patented its needlepunching process. At about the same time the Colloid Environment Technologies Co. (CETCO) in America produced a similar product. These manufacturers remain the chief producers and innovators in this field. GCLs are not just used for waste containment but for, inter alia pond liners, concrete protection barriers and secondary liners of underground fuel storage tanks. GCL products have been freely available in South Africa since around 1995 (Davies & Legge, 2002).

2.5 Waste treatment and disposal in South Africa

Landfilling remains the dominant disposal route for South Africa. Historically, many landfills in South Africa have been badly sited, designed and operated with minimum legislative control (DWAF, 1998). The Environment Conservation Act of 1989: 'The Control and Management of General Communal and General Small Waste Disposal Sites' was the first framework of standards, procedures and policies to control waste disposal in South Africa. The Act instituted a permit system applying to new and existing landfills. In 1994, the Minimum Requirements for Waste Disposal by Landfills South African national standard was instituted. This was part of the new democratic Government's Reconstruction and Developed Programme — the provision of a clean and healthy environment for all South Africans.

The standards were less stringent than those adopted in the Northern Hemisphere at the time. However, the high costs of demanding standards were considered to be difficult to accommodate in a country with so many other social and economic development objectives. The development of these standards was viewed as 'work in progress' (DWAF, 1994) and the second edition, with certain revisions, was issued in 1998.

In 1994, geotextiles were made a requirement in the higher risk landfills, including the large general waste sites. Geomembranes were only specified for the most hazardous landfills. Since 1998, however, geomembranes played a role in low hazardous landfills as well. Also, the option to use a GCL in place of the thick, compacted clay layers was introduced, subject to review by the Department of Water Affairs and Forestry.

University of Cape Town

CHAPTER 3

GEOSYNTHETICS IN LANDFILL DESIGN

3.1 Introduction

This chapter deals with geosynthetics and their use in the field as part of lining systems for landfills. In general, in-situ soils at landfill sites have relatively high permeability properties, even when heavily compacted. Thus, seepage of contaminants from the waste into the hydrogeological environment is inevitable. The modern lining system is a sophisticated combination of soil and synthetic materials which together serve the function of containing contaminants from the environment and controlling their drainage to allow the waste to degrade.

The objective of this chapter is to define different geosynthetics and their various functions. A generic landfill lining system, in line with South African standards, is presented to demonstrate how geosynthetics are incorporated. The Geosynthetic Clay Liner's manufacturing process, the properties and typical applications are explained. The combined use of the geosynthetics in a specific local lining design is discussed and the importance of the frictional behaviour is demonstrated for a selected 'lined' landfill slope.

3.2 Geosynthetic definitions and functions

There are various types of geosynthetics, each designed for a specialised geotechnical function. Only the types considered in this study are defined:

Geotextile: a permeable geosynthetic, comprised solely of textiles (ASTM D 4439).

Geomembrane: an essentially impermeable geosynthetic, composed of one or more synthetic sheets (ASTM D 4439). Common synthetics are high density polyethylene (HDPE) and linear low density polyethylene (LLDPE).

Geosynthetic Clay Liner: a manufactured hydraulic barrier, consisting of clay bonded to a layer or layers of geosynthetic material (materials) (ASTM D 6243).

These end-use functions can be summarised into five basic groups (adapted from Kalumba, 1998):

Reinforcement: The geosynthetic (typically a geotextile or geogrid) imparts tensile strength to a soil/geosynthetic system, potentially resulting in increased structural stability.

Separation: The geosynthetic (typically a geotextile) forms a boundary between different soil types or rock materials, thereby segregating two or more grain or particle sizes.

Filtration: The geosynthetic (typically a geotextile or geodrain) retains particles while allowing water to flow through with little or no increase in pore water pressure to the surrounding soil.

Drainage: The geosynthetic (typically a geotextile, pozidrain or geonet) allows water to flow in the plane of the geosynthetic, thus allowing drainage of water away from a structure or system.

Barrier: The geosynthetic (typically a geomembrane, asphalt impregnated geotextile or GCL) forms a barrier which impedes the flow of moisture or gas through a system.

In a geotechnical application these primary functions may also serve as secondary functions to complement each other. In the case of a landfill lining system all functions are required and therefore geosynthetics are integral to the operation of a modern lining system.

3.3 Landfill types

The type of landfill directly dictates the performance requirements and therefore the design of the lining system. Landfills are categorised according to their size, waste type and climatic environment. These characteristics affect the type and amount of contaminant production that will occur over the life of the facility. Once a choice is made about how effectively the contaminants must be contained, a lining system can be designed in accordance with these requirements.

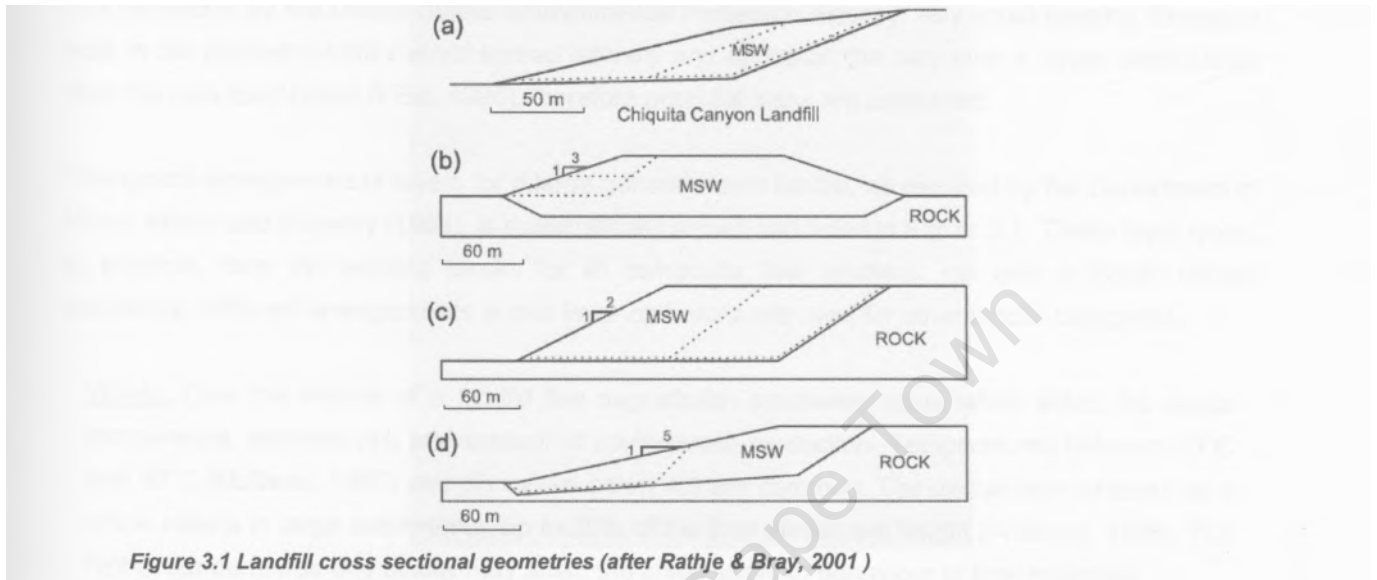
Attenuate and disperse landfills slowly and uncontrollably release leachate (solution containing dissolved and/or suspended contaminants produced by leaching of water through the waste material) into the geological and hydrogeological environment whereby the contaminants are first diluted by the groundwater then attenuated (polluting potential reduced) by natural biological, physical and chemical processes in the surrounding environment (Williams, 1998). At the opposite end of the spectrum is the entombment (dry) landfill, which aims to completely contain relatively dry waste indefinitely, preventing biodegradation and thus, leachate and gas generation. However, inevitably its liner will eventually fail (which may take centuries) and release contaminants.

Proper liner design, being adopted more and more in the developed world, incorporates a robust primary liner with a leachate collection system above it. The waste can slowly degrade to stabilisation and effective monitoring of the landfill is possible. The system also prevents groundwater seeping into the waste and subsequently increasing the leachate levels.

The most sustainable (yet least understood) landfill type is the controlled flushing bioreactor. Leachate is recirculated through the waste to accelerate biodegradation and hence stabilisation of the waste within a generation (Reinhart, 2007). However, this requires higher capacity leachate removal systems, a recirculation system, waste temperature control and certain waste density requirements (Williams, 1998).

3.4 Landfill geometries

The landfill profile is what predominantly affects the liner stability considerations. Construction can either be above or below natural ground level (see Figure 3.1 (b) and (d)). A combination of these is also possible as well as construction within a valley or an abandoned excavation. Above grade design is necessary in areas where there is a shallow water table. The final profile can be an 'eyesore' and may take up valuable land space.



The Chiquita landfill in Los Angeles (see Figure 3.1 (a)) shows the potential sliding surfaces in dotted lines. Bellville South landfill in Cape Town is similar to the Figure 3.1 (b) configuration. Configuration (d) due to embedment into the rock at the waste slope toe is relatively stable.

Below-ground geometries may be of higher initial costs but the excavated soil can be used for daily covering of the waste material and more volume is available for waste disposal. The end product is less visible and possibly functional as a new land use. The below-grade liner system requires pumping to remove leachate. Excavation and valley designs result in steeper slopes and geometries that are more critical in terms of waste stability and lining integrity (see Figure 3.1 (a) and (c)). The Kettleman Hills landfill failure in the late 1980s was of this configuration (Chang, 2005).

All geometries require a gentle sloping base to ensure leachate drainage under gravity to a sump area or drain.

3.5 Containment liner systems

Modern containment designs include layers of low permeability materials (natural or synthetic) and leachate management and detection systems. The liner system should also be resistant to the variety of chemicals in the leachate throughout the lifetime of the site, which may be centuries.

The first liner option is to site the landfill in an area where there is naturally occurring low permeability soil. These soils are generally termed clays and vary widely in composition and effectiveness.

Another option is adding pure clay with high swell characteristics to fill most of the voids of the coarser in-situ soil or chosen fill material. These materials are compacted into thick layers to form compacted clay liners (CCLs). Thirdly, geosynthetic clay liners (GCLs) can be incorporated to create very low permeability barriers.

Generally, if a GCL is used it will be placed directly below a geomembrane. This was originally recommended by the United States Environmental Protection Agency. Any liquid passing through a hole in the geomembrane cannot spread laterally and approach the clay over a larger wetted area than the hole itself (Stark & Eid, 1996), therefore potential leaks are contained.

The typical arrangement of layers for a large general waste landfill, as required by the Department of Water Affairs and Forestry (1998), is schematically shown and listed in Figure 3.1. These layer types, in principle, form the building blocks for all composite liner systems, not only in South African conditions. Different arrangements and/or layer omissions are used for other landfill categories.

Waste: Over the lifetime of a landfill five degradation processes occur which affect the waste temperature, leachate pH, and amount of contaminant production. Temperatures between 30°C and 90°C (McBean, 1995) and pH values below 4.0 are common. The degradation process as a whole results in large settlements, up to 30% of the final placement height (Williams, 1998). The higher temperatures and acidity may affect the shear strength behaviour of liner materials.

A layer: Leachate collection layer comprising a 150mm thick layer of single-sized gravel or crushed stone having a size between 38mm and 50mm. Leachate flows to a sump area where it is removed by a submersible pump. This drainage system prevents the build-up of leachate above the sealing system.

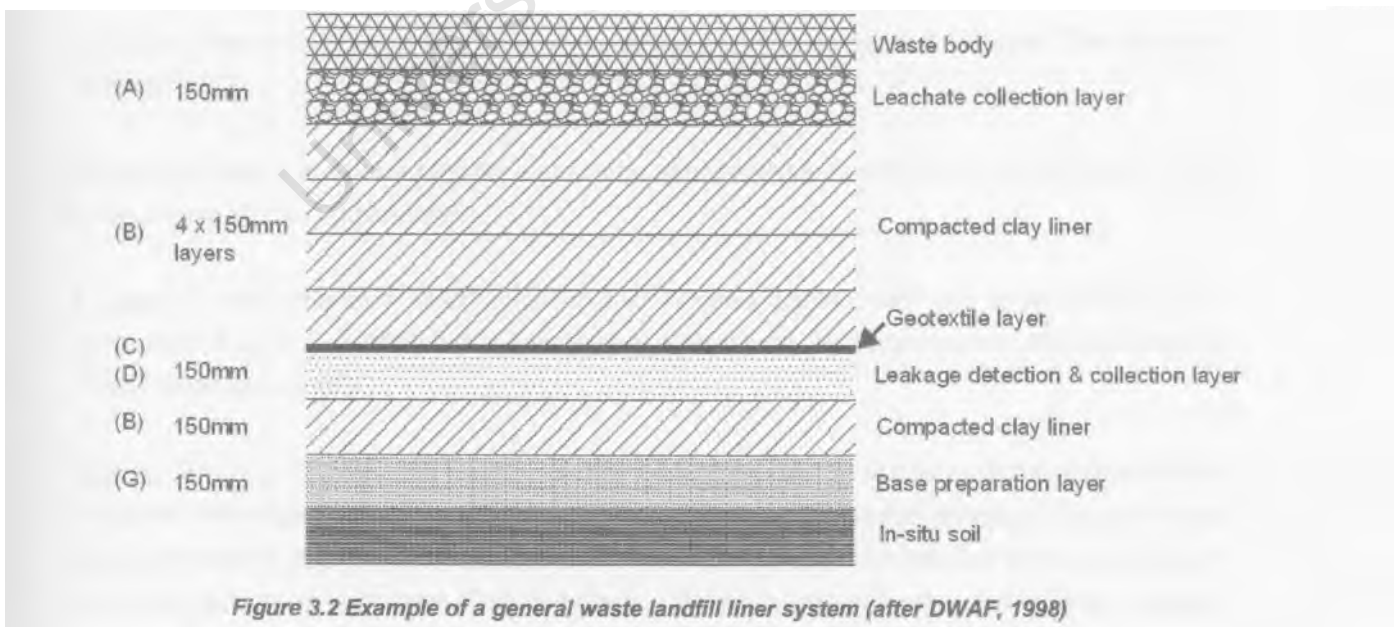


Figure 3.2 Example of a general waste landfill liner system (after DWAF, 1998)

B Layer: A 150mm thick compacted clay (or a multiple of that depending on the location within the liner). Typical properties of a CCL are listed in Table 3.1. The surface of every clay layer must be graded towards the leachate collection drain or sumps at a minimum gradient of 2%. At the

discretion of the Department of Water Affairs and Forestry, B layers may be replaced by a geomembrane, a GCL, or a composite liner. Williams (1998) indicated that hydraulic asphalt has also been used as a B layer.

Table 3.1 Properties of compacted clay liners

Property	Unit	Daniel (1993)	DWAF (1998)
Fines`		20 - 30	-
Plasticity Index		7 - 10	10 (min)8, (max)
Gravel		530	—
Max.particiesize	mm	25 - 50	<25

t% dry weight passing 75 micron sieve

**maximum that will not result in excessive desiccation cracking

C Layer: This is a separation layer of geotextile placed on top of any D layer (and A layer if required) to protect it from contamination by fine materials.

D Layer: A leakage detection and collection layer. It has a minimum thickness of 150mm and consists of single sized gravel or crushed stone having a size of between 38mm and 50mm. Leachate must gravitationally flow to its own sump area and be removed by a submersible pump using smaller diameter pipes than for the primary leachate collection layer (A layer).

G layer: This is a base preparation layer consisting of a compacted layer of reworked in-situ soil with a minimum thickness of 150mm. It is constructed to the same compaction standards as a B layer. Where the permeability of a G layer can be proven to be of the same standard as a B layer it may replace the lowest B layer. The surface of a G layer must be graded towards a leachate collection drain or sump from which sporadic leachate can be collected if it occurs. The minimum gradient is 2%.

The following layers are not a requirement for the general waste landfill according to DWAF (1998), but are discussed for completeness:

F Layer: A geomembrane which must be laid in direct contact with the upper surface of a compacted B layer. The thickness is specified as 1.5mm for a low hazardous landfill and 2mm for a high hazardous landfill.

Elam: This is a 100mm thick cushion of fine to medium sand or similar suitable material which is placed immediately above any F layer to protect it from mechanical damage. The protective layer permanently distributes concentrated stresses on the geomembrane due to the angularity of the drainage blanket aggregate. This layer below the waste plus the primary leachate collection gravel layer also ensure lower temperatures within the geosynthetics and mineral sealing layer (German Geotechnical Society, 1993).

3.6 Geosynthetic Clay Liner

The latest addition to the liner system materials option is the GCL. This unique combination of geotextiles and natural clay is a viable option to replace thick Compacted Clay Liners (B layer).

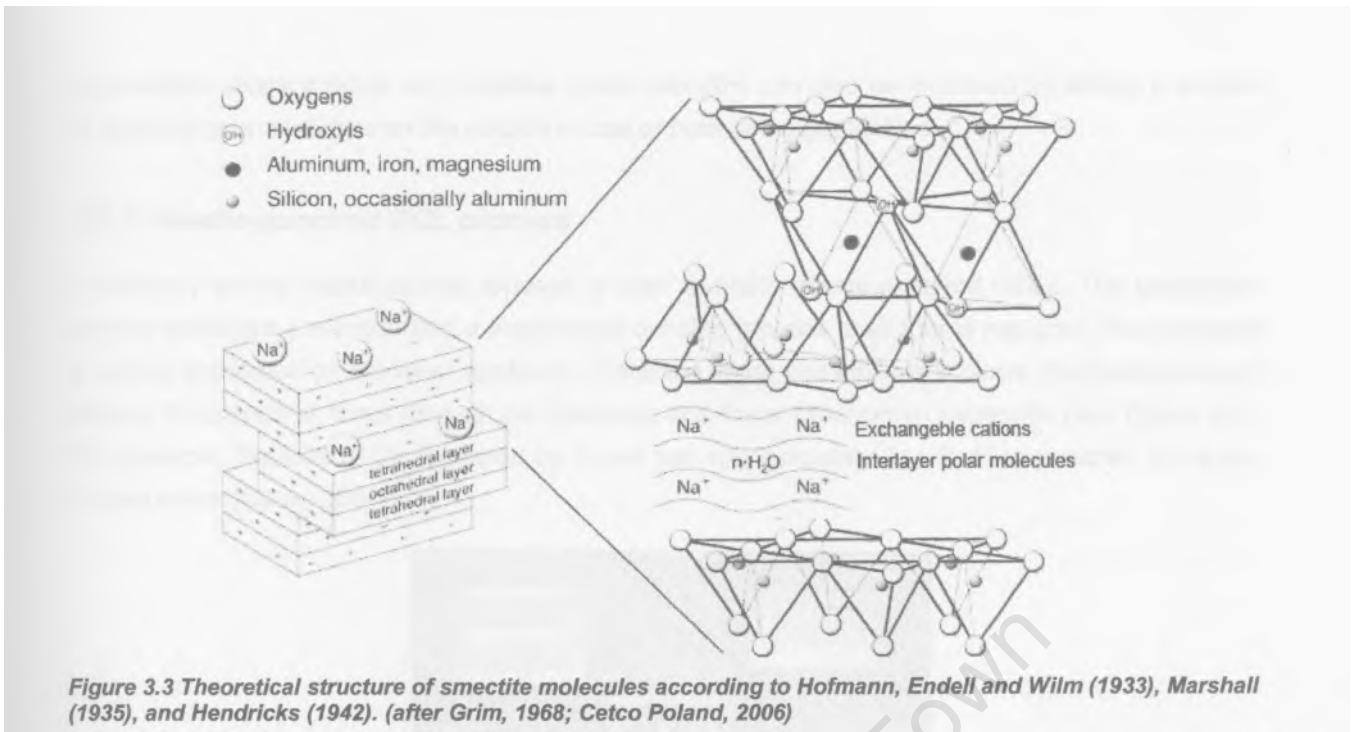
Comprehensive lists of advantages and disadvantages of GCLs are provided in the literature (Sharma and Lewis, 1994; Bouazza, 2002; Bogchi, 1994). The main benefits when used in a lining system are its easy and rapid installation, more waste volume, self-healing ability, resistance to fracturing or cracking. The hydraulic conductivity to water is very low; between 2×10^{-10} and 2×10^{-8} m/s depending on the confining pressure (Bouazza, 2002). This is approximately one thousand times lower than a typical CCL (CETCO, 2004). The main problems are potentially low internal and interface shear strengths depending on the GCL type.

In addition to their application in landfills, GCLs are also used in transport facilities (roads and railways) and in the context of accidental chemical spills from road accidents as environmental protection barriers. GCLs are also used as secondary liners for underground storage tanks at fuel stations for underground protection. Also, they are installed as single liners for canals, ponds or surface impoundments (Bouazza, 2002). Certain robust GCLs are used to seal underground reinforced concrete structures from water penetration (Naue, 2004).

3.6.1 Bentonite Clay

Grim (1968) defines clay as a natural, earthy, fine-grained material which develops plasticity when mixed with a limited amount of water. Many types of clay exist, but the best clay material for reducing permeability is sodium bentonite. This naturally occurring material geologically was formed from volcanic ash approximately 100 million years ago. Since it is naturally formed, it is stable for long term geotechnical applications. Once it is hydrated, it swells into a gel like substance that is practically impervious (Naue, 2004). Its major constituent is sodium montmorillonite, a clay mineral of the smectite group.

Montmorillonites are three-layered minerals consisting of a central octahedral sheet/layer sandwiched between two tetrahedral sheets/layers forming approximately 1nm thick platelets (see Figure 3.2). Their areal diameter to thickness ratio is 100:1 to 300:1. There is a slight excess negative charge on the surface of the platelets which is balanced by free-moving cations, in this case sodium, which move between them (CETCO Poland, 2006). Extended sheets of this arrangement group together like a pack of cards when dry. The theoretical surface area of the dry powdered material is $800\text{m}^2/\text{g}$ (Grim, 1968).



The sodium enables large amounts of water to be absorbed between the platelets. A high quality sodium bentonite will absorb 25 to 50 water layers (Grim, 1968) which translates to the absorption of up to five times its weight in water and up to 15 times its dry volume. This high swelling characteristic gives it its low permeability characteristics and thus, only thin layers are needed to form a barrier. This also gives the material the ability to seal around penetrations.

3.6.2 Product development

All GCLs can be subdivided into two categories: reinforced and unreinforced products. In their development, early types were geomembrane-supported: a thin bentonite layer bonded to the geomembrane using an adhesive and a thin open weave spun-bound geotextile is adhered to the bentonite for protection during installation. The recent more popular GCL is the geotextile-supported product which consists of a layer of bentonite between two layers of woven or non-woven geotextiles.

The geotextiles contain the bentonite, forming a thin uniform bentonite layer in dry and/or hydrated conditions. Reinforcement can be in the form of an adhesive, stitchbonded or needlepunched form (Bouazza, 2002). Nowadays, the needlepunched variety is the more common choice in the US (Fox & Stark, 2004). This reinforcement holds the geotextiles in place and helps to contain the bentonite if the GCL is not flat in the field, but its chief function is to provide internal strength. The additional confinement provided by the needlepunched fibres decreases the water content of the hydrated bentonite and the potential for lateral bentonite migration (Fox & Stark, 2004).

Manufacturers have improved this basic design. For instance the bentonite can be artificially improved (i.e. allow higher swelling; be more resistant to contaminants), the sides of the roll can be modified to automatically seal at overlaps and some manufacturers heat-treat the anchoring geotextile after needlepunching to fuse the geotextile and/or punched fibres (Bouazza, 2002). The

permeability characteristics and interface shear strengths can also be improved by adding a smooth or textured geomembrane on the outside of one or both of the geotextiles.

3.6.3 Needle punched GCL process

A relatively simple manufacturing process is used to make needle-punched GCLs. The geotextiles and bentonite are pre-made and a mechanical bonding process is all that is required. The bentonite is evenly distributed on the lower geotextile. Once the upper geotextile is in place, the needlepuncher pierces thousands of fibres through the bentonite and lower (anchoring) geotextile (see Figure 3.3). For example, Bentofix (GCL produced by Naue) has approximately 2 to 3million punched fibres per square meter (Naue, 2004).

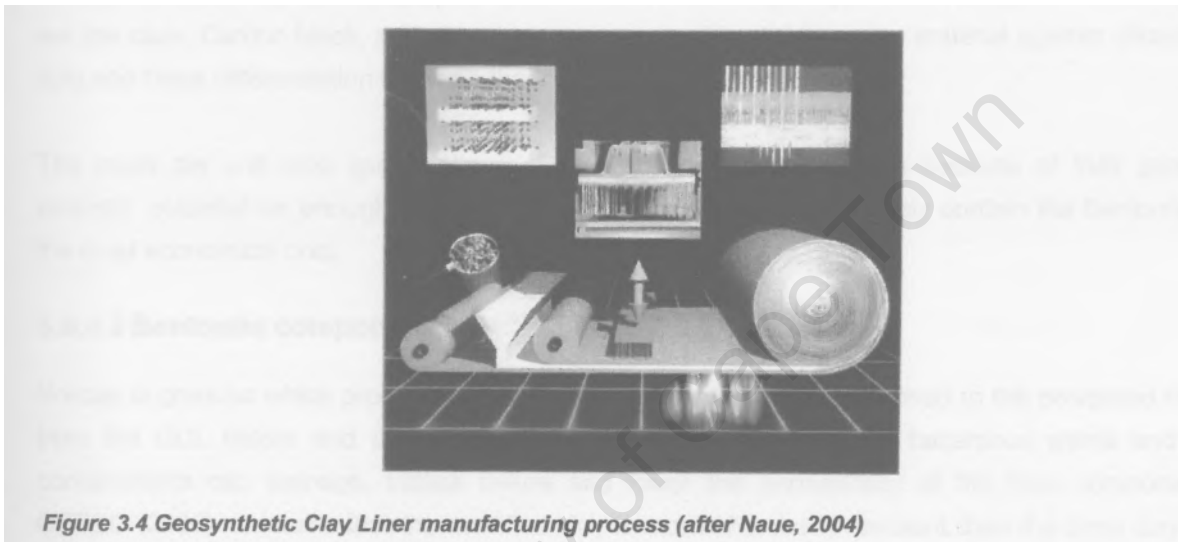


Figure 3.4 Geosynthetic Clay Liner manufacturing process (after Naue, 2004)

The punched fibres stay in place due to friction and entanglement but also may be heat treated to aid anchoring. The GCL is rolled up and packaged. Typical dimensions of a single panel are approximately 4.5m x 45m. The resulting rolls have a diameter of over half a meter and weigh over a ton.

3.6.4 Research GCL: Bentomat ST

The GCL chosen for this study is extensively used internationally and was recently used in a local Cape Town landfill. Bentomat® ST is one of seven GCL reinforced and unreinforced products manufactured by CETCO (2006), each product tailored to a specific function by varying the type of geosynthetic components used.

CETCO (2006) describes Bentomat ST as "a reinforced GCL consisting of a layer of Volclay sodium bentonite encapsulated between two geotextiles, needlepunched together for maximum performance under a wide variety of field conditions Bentomat ST has a woven upper geotextile for maximizing intimate contact in composite liner systems." This is the only CETCO product utilizing a woven geotextile. Volclay is the trade name of the granular modified sodium bentonite they use in all their GCLs.

3.6.4.1 Geotextile components

The geotextiles are made of polypropylene which is a light, stiff synthetic suitable for fibres. Polypropylene (**PP**) consists of non-polar molecules resulting in excellent chemical resistance. It is a durable, strong and cost effective structural component.

A non-woven geotextile must be used since fibres are required for punching through the bentonite layer and second geotextile, where the fibres are anchored. The main reason for the woven geotextiles, as stated by CETCO (2006), is that it allows an intimate contact between the GCL and a geomembrane, thus preventing any spread of water if a hole develops in the geomembrane. This, however, may not be optimal from a stability perspective. More bentonite tends to be extruded through the woven geotextile (Triplett & Fox, 2001) and marginally lower interface shear strengths are the case. Carbon black, added to the woven geotextile, stabilizes the material against ultraviolet light and helps differentiation between the top and bottom of the GCL.

The mass per unit area specifications of the geotextiles were chosen because of their general strength, potential for enough punched fibres and the ability to adequately contain the bentonite at the most economical cost.

3.6.4.2 Bentonite component

Volclay is granular which probably results in less bentonite loss (as apposed to the powdered form) from the GCL before and during construction. Many landfills contain hazardous waste and the contaminants can damage, induce failure and lower the permeability of the liner components. CETCO (2006) maintains that the modified clay is more chemically resistant than the base day but should be tested for site specific contaminants if required. Not only is it more chemically resistant but the free swell is increased through the Volclay process which results in lower permeability.

A high quality (tetrahedral inversions and inter-lattice ionic substitutions are minimal) base day is selected. The following additives, in the proper proportion, work synergistically and provide significant contaminant resistance and improved performance.

Firstly, polymers are added to promote the disaggregation of clay platelets during hydration. Since a greater fraction of the clay is exposed and thus hydrated, it is believed to become more effective than untreated clays in buffering the potentially damaging effects of chemical contaminants. The polymer chains also form mechanical protective encapsulations around hydrated bentonite platelets.

Secondly, dispersants are added to reverse platelet edge charges. Grim (1968) mentioned that chemical dispersing agents almost certainly alter the base exchange composition of the material and they agitate and split/deave the natural particles. The entire day platelet then becomes negatively charged and edge-to-face bonding between platelets is prevented. Thus, the spacing between platelets increases, allowing thicker adsorbed water layers. Possible disruptive effects on the water layers by the positive edge charge are also removed. Some dispersant remains in the unadsorbed water and can neutralise potentially deleterious cations in the leachate (CETCO Poland, 2006).

3.7 Local landfill

Bellville South, a local landfill in the Western Cape, has a lining system containing the GCL Bentomat ST. Jeffares & Green (Pty) Ltd., Consulting Engineers, the responsible company, was briefed on various aspects of the project (Wise, 2006). The landfill is a general waste, large (more than 500 tons per day) facility with a positive water balance. It is currently Cape Town's main general waste landfill and will be in operation till 2013. The landfill is above grade, thus the liner slopes are gentle and the maximum allowable waste height is 35m with an outer slope gradient of 1:4 (see also Figure 3.4).



Figure 3.5 Bellville South landfill – existing waste

Three new waste cells are being constructed, each approximately 100m x 120m in size on plan. Figure 3.5 shows the first cell's liner system installation.



Figure 3.6 Bellville South Landfill liner system installation

3.7.1 Liner system

The Bellville South liner design does not fit exactly into the generic recommended type of the South African Department of Water Affairs and Forestry (DWAF). Due to specific local site conditions — relatively high water table and windy weather - the design was adapted. The consultancy showed the economic and design benefits of using a GCL and its use was approved by the DWAF for the latest cells. The GCL was accepted on the condition that a minimum of 4000g of bentonite was guaranteed

per square meter. The GCL was placed with the woven side at the bottom against the sand base material. The non-woven GCL geotextile against the geomembrane was considered to have less potential to slip than the GCL woven geotextile/geomembrane interface.

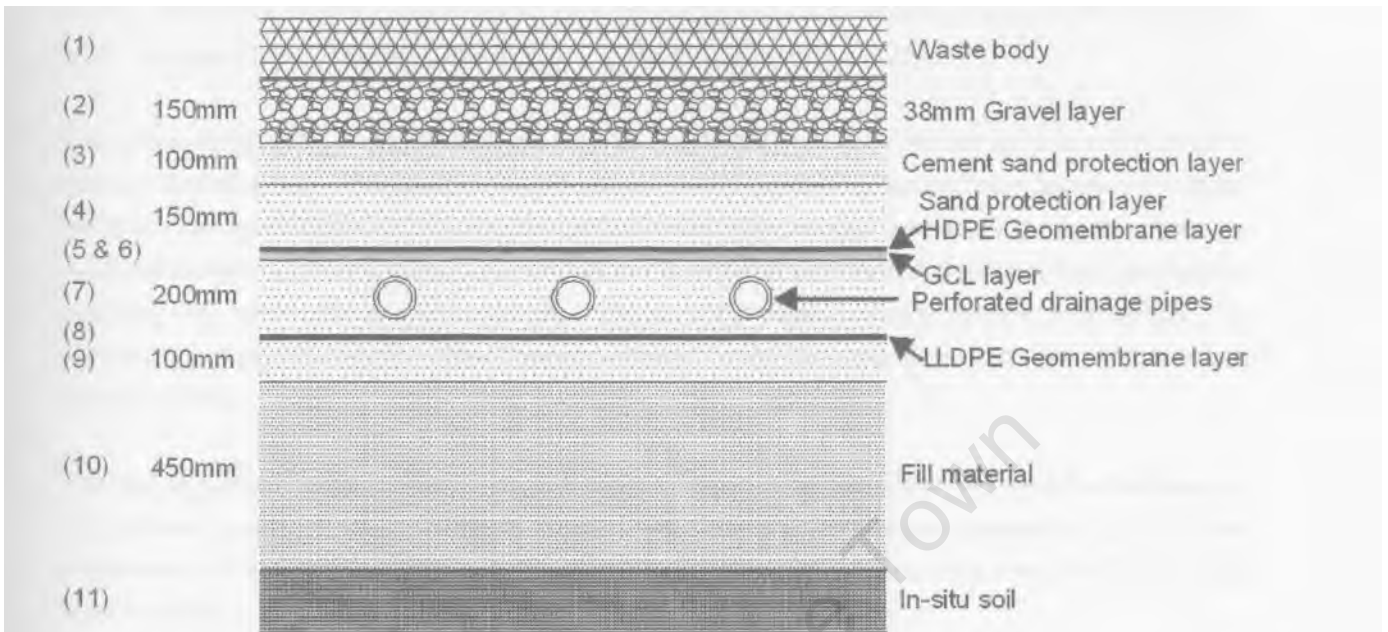


Figure 3.7 Bellville South landfill liner system (after Jeffares & Green, 2006)

Table 3.2 Bellville South landfill liner layers

Layer No.	Layer type	Description
(1)	Waste	General waste
(2)	A	38mm crushed stone
(3)	E	Clean sand + 5% cement
(4)	E	Clean sand - lightly compacted
(5)	F	1mm smooth HDPE
(6)	B	Reinforced GCL
(7)	D	Clean sand + slotted pipe - uncompacted
(8)	F	1mm smooth LLDPE – secondary liner
(9)	E	Clean sand - lightly compacted
(10)	G	95% Proctor (100% for sand) density
(11)	in-situ	100% Proctor density

The cell interior has a gradient of 2 to 3% for drainage purposes and the steepest side slope is 1:10 at the side adjacent to the existing waste cell. The lining system consists of a primary and secondary liner separated by a sand leak detection layer.

A 1mm smooth **HDPE** (high density polyethylene) geomembrane is used above the GCL to reduce the primary liners permeability. A textured geomembrane, which may provide more stability, was not warranted for this project because relatively gentle slopes were used. These two geosynthetics form the primary liner system. A non-woven geotextile above the geomembrane has been incorporated in the newer cells to protect the geomembrane.

Also, a cement stabilized sand layer above the soil protection cushion is an addition to the minimum standard. This layer prevents excessive stone embedment into the sand cushion and prevents excessive dispersion of the underlying sand layer by heavy winds. A secondary liner incorporating a LLDPE (linear low density polyethylene) geomembrane was used above a lightly compacted sand layer. This sand layer provides protection and a level surface for the LLDPE.

Cape Flats sand is the in-situ material at Bellville South and was used for the sand cushion and the leakage detection layer. The sand is uncompacted for the leakage detection layer because this layer contains drainage pipes and is lightly compacted (two roller passes) for the sand cushion. There is no target moisture content, only a moist condition is required for the leak detection layer so that the overlying GCL can hydrate once in place. If the sand becomes saturated before construction, it is drained by cutting grooves for water flow and allowed to dry for a few days, then resurfaced before laying the GCL.

The use of geosynthetics instead of compacted clay layers was beneficial because the thickness of the liner was greatly reduced and more airspace was thus available. More importantly, the increased performance of the geosynthetics provides better protection of the groundwater and the City of Cape Town's aquifer.

3.7.2 Slope Design

The limit state design method used for the landfill slopes was based on Koerner's (1998) method for designing soil slopes containing a geomembrane. Wise (2006) mentioned that the GCUgeomembrane interface was considered critical.

The interface shear strength design values were obtained from tests of similar geotextiles, geomembranes and sand. These tests were conducted by the University of Cape Town on a 100mm x 100mm shear device in the 1990s. No tests have been performed with the GCL itself.

3.8 Slope stability

The Bellville South landfill liner only incorporates gradual slopes (see Figure 3.7). However, if such a lining system, specifically the HDPE geomembrane/GCL combination, were to be used in a future landfill with steeper slopes, sliding along the geosynthetics would need serious consideration. Williams (1993) mentioned that to his knowledge in all primary leachate collection systems, natural soil was used, but problems were encountered keeping the sands and gravels on side slopes especially when using smooth geomembranes. Not only is the soil/geomembrane interface a possible sliding surface, but when a GCL is incorporated the GCL internal shear strength, GCUgeomembrane and GCUsand interfaces should also be investigated.



Figure 3.8 Belleville South Landfill liner slope

Since liner slopes can be very long for a large landfill the stability along a specific interface can be conservatively approximated by the limit equilibrium equation for an infinite slope. The factor of safety is expressed as the ratio of resisting to driving forces. If the resisting forces are larger than the driving forces then the factor of safety is above one which indicates safe conditions.

For the case of an infinite slope:

$$FS = \frac{\text{resisting}}{\text{driving}} = \frac{F}{W \cdot \sin \beta} = \frac{N \cdot \tan \delta}{W \cdot \sin \beta} = \frac{W \cdot \cos \beta \cdot \tan \delta}{W \cdot \sin \beta} = \frac{\tan \delta}{\tan \beta}$$

Where:

W = waste weight

N = normal waste weight component on interface

β = slope angle

δ = friction angle of the interface

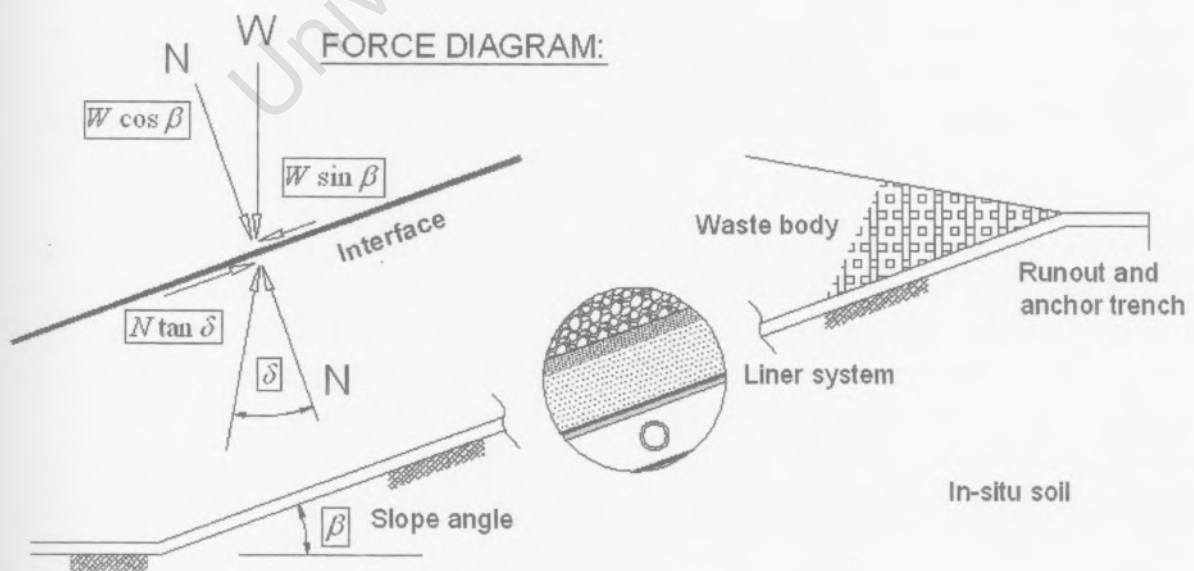


Figure 3.9 Landfill boundary slope with liner

The infinite slope equation highlights the importance of the slope and interface friction angle in landfill liner slope design. If the interface friction angle is known, a safe slope angle can be determined. However, in practice numerous other aspects need to be considered and designed.

More complex analyses are required to take the soil buttressing effect at the bottom of the slope and the geosynthetic tension above the slip surface into account. The geosynthetics are held at the crest of the lining system to prevent displacements down the slope. The methods used are a horizontal runout section covered with a sand layer and a vertical trench to anchor the geosynthetic. The force of the sand causes friction between the underside of the geosynthetic and the crest along the runout length. Only the underside friction force is considered because the overlying sand will move with the geosynthetic. If a higher anchoring force is required and restricted space for a runout section is available a trench is dug in which the end of the geosynthetic is buried. The complete system is generally designed such that the geosynthetic will pull out of the anchor before it tears. This ensures holes don't develop in the lining even if large, though still undesirable, displacements occur down the liner slope.

Further analysis of the system when waste is placed in layers as well as long-term stability once dumping is complete should also be investigated. In the long term, degradation of the waste causes large settlements which can increase displacements along the lining interfaces. Pore water pressures due to leachate collection on the liner may also have to be taken into account. The GCLs internal shear strength will deteriorate with time due to creep and degradation of the needlepunched fibres. This reduction may be significant for the safe design of the landfill liner geometry over the full design life.

CHAPTER 4

LITERATURE REVIEW OF PREVIOUS RESEARCH

4.1 Introduction

The use of Geosynthetic Clay Liners (GCLs) in relatively steep embankments of a lining system requires careful assessment of the internal shear strength of the GCL and the interface shear strength between the GCL and its contact materials. A large direct shear device, developed by the Civil Engineering Department at the University of Cape Town, South Africa, was used to characterize the shear behaviour of all interfaces of a lining system of a local landfill which incorporated a GCL and smooth geomembranes.

Various researchers have investigated the same GCL used in this study. This includes direct shear tests of the GCL itself as well as the GCL in contact with other liner materials. Different test setups, procedures and their results are summarized and compared.

The direct shear test procedure in the laboratory is firstly defined followed by a review of previous experimental direct shear investigations of lining materials as well as limit equilibrium analyses of specific landfill geometries where those lining materials were involved. South African design requirements for general geosynthetic as well as landfill design approaches are presented and finally, the relevant research requirements in liner design are identified.

4.2 Direct Shear Test Principle and Apparatus

The direct shear test is a procedure in which the shear strength of a soil is determined by shearing the soil along an enforced shear plane under a known normal stress. The use of the test is limited since stress and strain conditions within the soil are not uniform and pore water pressures cannot be measured. However, the test is widely used to determine the effective shear strength, in terms of the angle of internal friction and cohesion of a soil.

The test procedure is also used for the determination of the internal shear strength of a GCL as well as the frictional resistance between the GCL and adjacent materials. The international standard for this test method is ASTM 6243 (1998) which defines the direct shear friction test for GCLs as a procedure in which the internal GCL or the interface between a GCL and any other surface, under a range of normal stresses specified by the user, is stressed to failure by the relative movement of one surface against the other. ASTM 5321 (1992) was the forerunner to this test method; it presented the standard for testing general geosynthetic interfaces.

ASTM 6243 (1998) defines the following properties of the tested materials which are determined by the test procedure:

- *The angle of friction* is "the angle whose tangent is the ratio between the limiting value of the shear stress that resists slippage between two solid bodies at rest with respect to each other and the normal stress across the contact surface."
- *The coefficient of friction* is "a constant proportionality factor relating normal stress and the corresponding critical shear stress for a defined failure condition."
- *Cohesion* is "the portion of the internal shear strength indicated by the term c , in Coulomb's equation $c \text{ and } \tan(\phi)$."
- *Adhesion* is "the shearing resistance between two unlike materials under zero normal stress."

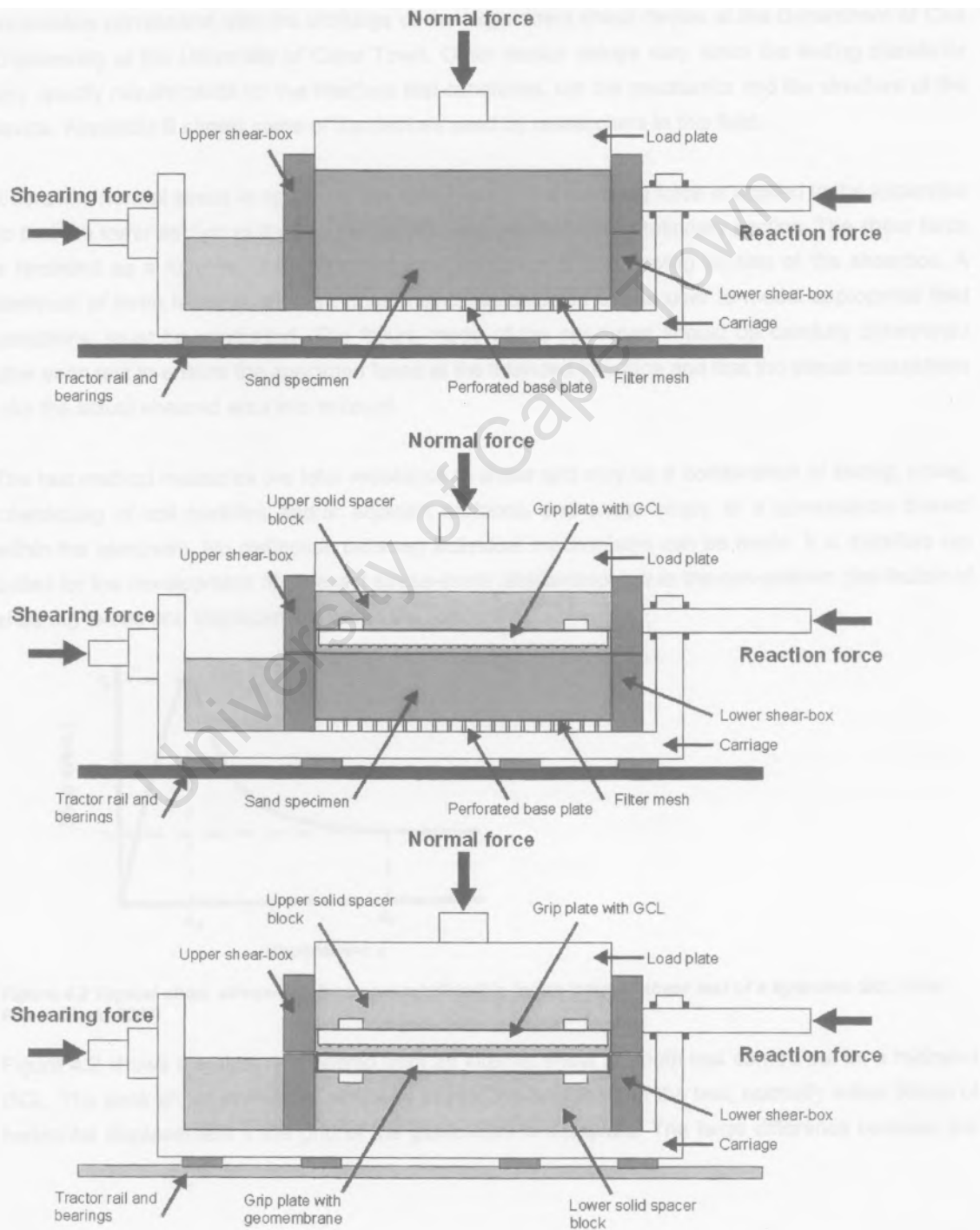


Figure 4.1 Direct shear device load application configuration a) sand test b) geosynthetic / sand interface test c) geosynthetic / geosynthetic interface test

Conventionally, soil testing is conducted using a 60mm x 60mm or 100mm x 100mm direct shearbox. This, however, is not large enough for testing geosynthetics due to boundary effects and relatively large structural characteristics of certain geosynthetics. Therefore the ASTM standards require a large direct shearbox apparatus with internal dimensions of at least 300mm x 300mm (on plan).

Figure 4.1 shows schematics of three possible tests using the large direct shearbox; soil test, geosynthetic against soil friction test and geosynthetic against geosynthetic friction test. The internal shear strength test of a GCL is not shown but is similar to the geosynthetic/geosynthetic test; the two geotextile layers encapsulating the bentonite are each connected to a separate grip plate. These schematics correspond with the workings of the large direct shear device at the Department of Civil Engineering at the University of Cape Town. Other device setups vary since the testing standards only specify requirements for the interface test conditions, not the mechanics and the structure of the device. Appendix B shows some of the devices used by researchers in this field.

A constant normal stress is applied to the specimen, and a shearing force is applied to the apparatus so that the lower section of the box moves in relation to the upper stationary section. The shear force is recorded as a function of the horizontal displacement of the moving section of the shearbox. A minimum of three tests, at different normal stresses selected by the user to model appropriate field conditions, must be conducted. The failure mode of the specimen should be carefully determined after each test to ensure the specimen failed at the intended interface and that the stress calculations take the actual sheared area into account.

The test method measures the total resistance to shear and may be a combination of sliding, rolling, interlocking of soil particles and/or adjacent surfaces, and shear strain, or a combination thereof within the specimen. No distinction between individual mechanisms can be made. It is therefore not suited for the development of an exact stress-strain relationship due to the non-uniform distribution of shearing forces and displacement within the specimen.

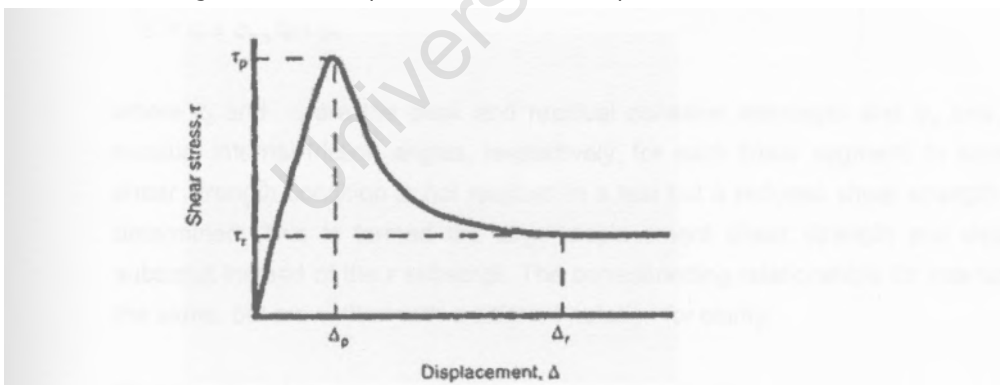


Figure 4.2 Typical shear stress-displacement relationship for an internal shear test of a hydrated GCL (after Fox & Stark, 2004)

Figure 4.2 shows a typical relationship from an internal shear strength test carried out on a hydrated GCL. The peak shear strength is achieved toward the beginning of the test, normally within 50mm of horizontal displacement if the grip of the geotextiles is adequate. The large difference between the

peak and residual shear stress of the internal shear strength test is due to the fact that once the geotextile fibres failed, only the low strength of the bentonite remains.

All GCLs and most GCL interface tests show a post peak strength reduction to a point where no further strength reduction occurs — the residual strength condition. This strength reduction is caused by numerous mechanisms, including clay particle reorientation at the failure surface, volume increase of soil material within the shear zone, loss of interface roughness of geosynthetic materials, and failure of reinforcement or supporting geotextiles. The direct shear machine used by Fox et al. (1998) could shear up to 203mm. In some tests residual strength was not reached until the very end of the test indicating that true residual strengths *are* difficult to determine without large horizontal displacements.

Generally, all peak interface shear strengths are smaller and all large-displacement strengths are larger than for the internal shear strength of the GCL considered. Little to no post-peak strength reduction has been shown for direct shear tests conducted on dry sand/needlepunched GCL interfaces (Garcin et al., 1995).

Using the shear stress and normal stress results at failure, the shear stress and normal stress can be plotted in a diagram to determine the shear strength parameters of the soil or interface at failure. This Mohr-Coulomb relationship is used to characterize linear and multi-linear failure envelopes.

Peak internal failure envelope:

$$\tau_p = c_p + \sigma_{n,s} \tan \phi_p$$

Residual internal failure envelope:

$$\tau_r = c_r + \sigma_{n,s} \tan \phi_r$$

where c_p and c_r are the peak and residual cohesion intercepts and (ϕ_p and ϕ_r are the peak and residual internal friction angles, respectively, for each linear segment. In some cases the residual shear strength condition is not reached in a test but a reduced shear strength condition can still be determined. This is termed the large displacement shear strength and designated with the *LD* subscript instead of the *r* subscript. The corresponding relationships for interface shear strength are the same, but are written with a different notation for clarity:

Peak interface failure envelope:

$$\tau_p = a_p + \sigma_{n,s} \tan \delta_p$$

Residual interface failure envelope:

$$\tau_r = a_r + \sigma_{n,s} \tan \delta_r$$

where a_p and a , are the peak and residual adhesion intercepts, and b_p and b_r are the peak and residual interface friction angles, respectively, for each linear segment. The notation for large displacement shear strengths is the same as for the internal failure envelope.

4.2.1 Advantages and disadvantages of the large direct shear device

Fox & Stark (2004) highlighted that the advantages outweigh the disadvantages for commercial testing using a large direct shear procedure. Shearing occurs in a single direction, simulating field behaviour and the specimens are large which minimizes boundary effects. Shear displacement are theoretically uniform over the specimen which minimizes progressive failure and promotes accurate peak strength measurement.

However, the horizontal shear displacement is limited and normally not sufficient to measure residual shear strengths, especially when using upper and lower containers of the same size. The area of the failure surface decreases during the test thus an area correction is necessary for data analysis. Also, it can be difficult to attain very high normal stresses over such a large surface area.

The fact that residual internal shear strengths of all hydrated GCLs are known to be essentially the same as that of hydrated bentonite (Fox et al., 1998) partially eliminates the disadvantage of limited shear displacement. Backpressure cannot be applied; therefore the effective measurement of pore water pressure is not possible.

4.2.3 Apparatus limitations

Adherence to a single test method in all universities and commercial laboratories across the world would be ideal for further research. This uniformity would allow reliable comparisons and joint research initiatives. However, this is not the case due to a wide range of reasons.

ASTM 6243 was only developed in 1998, allowing little time for laboratories to change their apparatus. Due to the large forces involved in a 300mm by 300mm shear area, especially at high compressive stresses, machines must be massive and therefore expensive. ASTM 6243 only prescribes conditions for testing and is still undecided on certain aspects of the test setup. Thus, there is no standardisation of direct shear machines. The large amount of work and time required to perform a single test has also possibly discourages extensive research on aspects of this topic.

This has resulted in almost all the studies using different machines and procedures, making comparisons difficult. Since the available literature on GCL testing using the appropriate large direct shear machine as specified by the standard is limited, various other test results from other test methods are included in this thesis. This provided valuable insight into certain aspects of GCL behaviour not readily available when using the direct shear machine.

4.2.4 Torsional ring shear device

This device consists of a mechanism to grip and rotate a circular specimen continuously. Stark (1996) tested specimens with inner and outer diameters 40mm and 100mm, respectively. Unlimited shear displacement allows measurement of residual shear strengths and the area of the failure surface is constant throughout the test.

However, the shear displacement does not occur in one material direction therefore anisotropic materials cannot be tested. Since needlepunched GCLs are isotropic materials they can be tested in such a device. Specimen preparation is complex and shear displacement is not uniform across the width of the specimen, resulting in progressive failure (Fox & Stark, 2004).

4.2.5 Inclined plane shear

This test setup uses gravity to induce shear and normal stresses into the specimen. The angle of a rigid board on which the specimen rests is increased at a specific rate until failure occurs. Specimens can be much larger than those used in a Large Direct Shear Device, but normal stresses are limited (typically below 50kPa) due to a dead weight loading system on the sloping board. Post peak stresses are not measured in the standard test and as the tilt increases the stress conditions on the failure surface become increasingly non-uniform. However, this test is well suited to creep investigations simulating landfill cover systems (Fox & Stark, 2004).

4.2.6 Specimen gripping system

An essential requirement for reliable test results in a direct shear machine is a proper grip of the geosynthetic specimen within the shearframe; if specimens are not solidly fixed to the grip plate shear does not take place in the desired interface. Fox & Stark (2004) identify this as the single most important source of error in current production GCL shear testing. Side clamping systems are used to secure the ends of a test specimen but should not significantly participate in the shearing process as they may introduce tensile forces in the textiles and thus promote progressive failure.

ASTM 6243 (1998) states that "work is still in progress to define the best type of rough surfaces" and that "a textured steel gripping surface made of wood working rasps has been found to work". These surfaces should allow good drainage and not interfere with measured shear strength over a wide range of normal stresses. Stapling or gluing geosynthetics can alter the material behaviour on the intended interface. Indications of poor gripping apparatus are double peaks, poor similarity, undulations, and/or very wide peaks in shear stress (Fox & Stark, 2004).

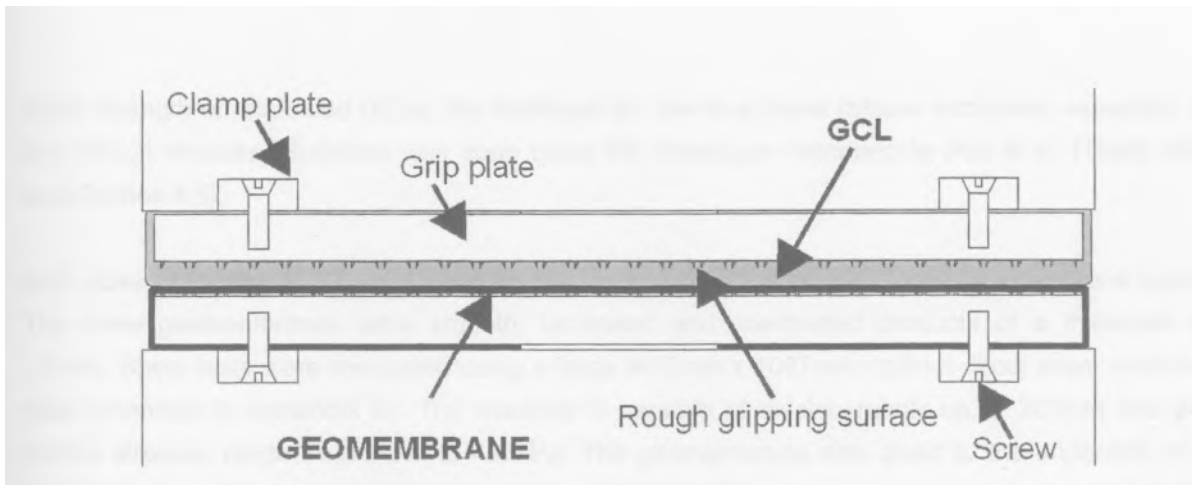


Figure 4.3 *Gripping system of this investigation*

Figure 4.3 shows the gripping system which was developed for the current study of GCL / geomembrane interfaces. Other studies have demonstrated adequate surfaces which appear to give accurate results. Nail plates moulded in epoxy with 1nail/cm² density, short sharp nails, protruding 2mm have worked well (Zanzinger & Alexiew, 2000). A textured steel grip made up of wood working rasps with 1-2mm high teeth (1 tooth/1.1cm²) has also been satisfactory (Fox & Stark, 2004). Geomembranes may be glued, as shown by Triplett & Fox (2001) but this limits the normal stress range, since slipping along the adhesive interface may start at relatively low shear stresses.

4.3 GCL Internal Shear Strength

Internal failure is typically a concern when a textured geomembrane is placed in contact with a GCL (Eid et al., 1999; Stark, 1996). Extensive testing has been carried out on the internal shear strength of reinforced GCL's. Fox et al. (1998) investigated three different GCL's, including Bentomat ST, using a large pullout shear machine. The specimen size was 406mm x 1067mm.

The largest source of data for internal shear strength testing is a commercial testing laboratory' which adhered to ASTM D6243 Standards even before it was released in 1998. 414 large direct shear tests of GCL internal shear strength, conducted over twelve years, were analysed by Zornberg et al. (2005). A wide variety of GCL products, including Bentomat ST, were tested. The equipment used consisted of a top and bottom shearbox measuring 305mm x 305mm in plan. The apparatus included a water bath to test under submerged conditions, but it was rarely used. The geotextiles were gripped adequately using textured steel plates (Zornberg, 2005).

The exact failure surface internal to the GCL has been observed by numerous authors (Fox et al., 1998; Eid et al., 1999; Zornberg, 2005). The failure surface was between the bentonite layer and woven carrier geotextile and not within the hydrated bentonite.

4.4 Interface Shear Strength

The only published comprehensive study into interface shear strength between a GCL and different geomembrane types was conducted by Triplett & Fox (2001). Due to improvements in the internal

shear strength of reinforced GCLs, the likelihood for interface shear failures increases, especially at low normal stresses. Hydration was done using the procedure described by Fox et al. (1998) (see also Section 4.5).

Both sides of Bentomat ST were used for the tests in combination with three geomembrane types. The three geomembranes were smooth, laminated and coextruded products of a thickness of 1.0mm. Shear tests were conducted using a large (406mm x 1067mm) pullout direct shear machine (see schematic in Appendix B). The machine is capable of displacements up to 203mm and the normal stresses range from 1kPa to 486kPa. The geomembrane was glued to the underside of a horizontal steel pullout plate. This is sheared against the GCL which was secured to the floor of the test chamber with sharp metal plates. Normal stress was transferred through steel balls on the pullout plate from an air bag to the sample. Vertical displacements and pore pressures were measured at the centre of the shearing specimen (Triplett & Fox, 2001).

Horizontal displacements at peak strength were small, less than 3mm, and increased with increasing normal stress. The large displacement strength ratio (stress at large displacement divided by stress at peak) decreased with increasing normal stress. Relatively small positive pore pressures were measured for all interfaces at peak failure stress. This suggests that the current practice of preparing failure envelopes based on total normal stress is conservative. However, pore water pressure measurements only indicate qualitative trends as no back pressure was used in the study (Triplett & Fox, 2001).

The main difference between geomembrane/geotextile interface strength and geomembrane/GCL interface strength is due to the presence of extruded bentonite at the interface. Generally, more extruded bentonite was observed for woven than for non-woven interfaces and increased with higher normal stresses and lesser amounts of extruded bentonite was observed along smooth geomembrane interfaces. Triplett and Fox (2001) found that bentonite extrusion through woven and non-woven geotextiles onto the adjacent geomembrane probably reduces the frictional resistance between the two. Little or no damage due to shear was observed for the smooth geomembrane (Triplett & Fox, 2001).

Fox & Stark (2004) state that at that time there was no information available on displacement rate effects for any interfaces except the Geomembrane/GCL interface.

4.5 Specimen Preparation

Internal GCL and GCL interface shear strengths are affected by hydration liquid, extent of hydration and hydration/consolidation procedure. Therefore, if hydration is expected in the field, which is normally the case, tests should be conducted under hydrated conditions (Fox & Stark, 2004).

The GCL is a unique geosynthetic material since it contains clay — a natural mineral with swelling characteristics. Thus, particular attention must be given to the hydration and consolidation of the specimen. Tap water is normally used because its chemistry is similar to that of pore water in most

soils. Koerner (1998) obtained shear strengths for various different hydration liquids such as diesel fuel and harsh leachate which showed higher shear strength values than for tap water. Therefore tap water appears to be a conservative choice regarding shear strength.

GCL specimens should be hydrated under the normal stress expected in the field at the time of hydration. Daniel et al. (1993) and Stark et al. (1998) showed that hydration of non-encapsulated GCLs occurs relatively quickly, within a few days or weeks, when placed next to damp soil or a compacted clay liner. However, this is difficult to simulate in the laboratory since hydration and loading may occur slowly and only to a certain extent. The conservative approach is to fully submerge the specimen as well as its contact materials.

Ideally, GCL specimens should be hydrated to equilibrium i.e. no volume change. But this may take as long as three weeks (Stark & Eid, 1996). Gilbert et al. (1997) proposed considering a GCL adequately hydrated when the change in thickness is less than 5% over a 12h period. But this may still require extended hydration times. Stark & Eid (1996) hydrated Bentofix GCL specimens outside the testing machine at 17kPa (simulating field conditions) until the end of primary swelling as defined by ASTM D 4546. Thereafter the specimen was incrementally loaded in the machine to the desired normal stress for the test. A load increment ratio (increase in normal stress divided by the existing normal stress) of 0.1 was used. 3 to 13 days were required to complete this consolidation stage.

4.5.1 Accelerated procedures

Most production laboratories only hydrate GCLs for up to two days due to time and cost implications. However, incomplete hydration may lead to unconservative results. Thus, various accelerated hydration procedures that do not alter measured shear strength have been investigated by researchers.

Some direct shear devices have separate shearing frames and shear box assemblies so that multiple GCL specimens can be hydrated and consolidated simultaneously outside the shearing machine. Another alternative is a two stage procedure used to reduce in-machine time. This approach was used successfully by Fox et al. (1998) and Triplett and Fox (2001).

Sufficient tap water was added to the specimen to arrive at the final water content expected for the test. This was done in a shallow pan and left for two days without any normal stress for the needlepunched GCL. Thereafter, the specimen was placed in the shear machine, the test normal stress applied and hydrated for two further days. It was shown that this two stage procedure reduced in-machine time to reach vertical equilibrium. No significant impact on measured shear strength was recorded (Fox et al., 1998).

Zomberg (2005) reported a similar procedure used by a commercial testing laboratory. The specimen and rigid substrates were placed under a specified normal stress outside the direct shear device and soaked in tap water for a specified time. This assembly was then transferred to the direct shear device. If the shearing normal stress was higher than the hydration normal stress the normal

stress was slowly ramped up to the required value, allowing pore pressures to dissipate during a consolidation time.

A single rapid normal stress change from hydration normal stress to test condition normal stress is inappropriate for hydrated specimens unless the change is relatively small or simulates a field condition (Fox & Stark, 2004). If consolidation loads are not applied incrementally excessive bentonite extrusion and the presence of positive pore water pressures at the start of the test may occur. Merrill and O'Brien (1997) reported that consolidation was effectively completed within 10h for a needlepunched GCL subjected to a normal stress increment from 69kPa to 138kPa (Fox & Stark, 2004). Additional comparative studies are needed to determine the effect of hydration/consolidation procedure on the shear strength of various GCLs and GCL interfaces (Fox & Stark, 2004).

4.6 Shearing

4.6.1 Shear displacement rate

The most important aspect of the shearing stage is the choice of the shear displacement rate (SDR). The SDR affects the measured shear strength of the GCL and most interfaces. For example a faster rate may promote tearing over pullout or slipping of geosynthetic fibres. Unless a specific application requires rapid shearing to simulate field conditions (e.g. seismic loading), maximum allowable SDRs have been established with the intent of minimizing the generation of pore pressures on the failure surface during shear (Fox & Stark, 2004).

The choice of SDR is also important from a time *and* cost perspective, especially with regard to commercial testing. The acceptance and marketability of GCLs may also be affected (Stark & Eid, 1996).

Equation (1) from ASTM D6243 (1998) can lead to very slow SDRs.

$$R = \frac{d_f}{50 \cdot t_{50} \cdot \eta} \quad (1)$$

where:

R = rate of horizontal displacement, mm/min,

d_f = estimated horizontal displacement at peak shear stress or at the residual shear strength as requested by the user, mm,

t_{50} = time required for specimen to reach 50 % consolidation under the current normal stress increment determined from methods described in Test Method D 2435 with double drainage, min, and

η = factor to account for drainage conditions on the shear plane (use 1 for internal shear of GCL with drainage at both boundaries)

Shan (1993) estimated that rates based on consolidation data from four GCL products would range from 0.001mm/min to 0.0001mm/min. Shear tests conducted to 50mm at these rates would require 34.7 and 347 days, respectively. Equation 1 assumes that failure occurs throughout the centre of the bentonite layer. This has however been shown to not to happen in numerous studies showing failure at the bentonite - woven geotextile interface. The geotextile interface can be considered drained and shear-induced pore pressures relatively small. Due to the inappropriateness of the given equation, many production laboratories justify a shearing rate of 1mm/min (Fox & Stark, 2004) for GCL testing.

4.6.1.1 GCL internal shear strength

Stark & Eid (1996) tested the GCL Bentofix at different SDRs at a normal stress of 17kPa. Tests were conducted using a modified Bromhead torsional ring shear device at rates between 0.015mm/min and 36.5mm/min. Tests with the bentonite removed showed higher shear strength values. An SDR of 0.04mm/min was considered satisfactorily slow to eliminate negative shear effects. The residual internal shear stress was shown to be independent of SDR.

Eid et al. (1999) used the same apparatus, GCL, hydration time and SDRs as Stark & Eid (1996) to investigate higher normal stresses conditions, i.e. 100kPa, 200kPa and 400kPa. The measured GCL peak internal shear strength at normal shear stresses between 200kPa and 400kPa were less sensitive to SDR than shear strengths at lower normal stresses. The shear displacement rate had little influence on residual internal shear strength at any normal stress.

The same result as Stark & Eid (1996) was shown by Zornberg (2005) at a normal stress of 50kPa (with a 24h hydration period) at rates of between 0.01mm/min and 1.0 mm/min. However, the opposite result is shown at a high normal stress of 520kPa (312h hydration period) at SDRs of between 0.0015mm/min and 1.0 mm/min.

The effect was significant on peak stress at low normal stresses (50kPa — 40% decrease per log cycle of SDR), but at higher normal stresses it was less significant (520kPa — 10% decrease per log cycle of SDR). Zornberg (2005) concluded that at relatively high normal stresses a comparatively high SDR will lead to conservative shear strength values. However, at lower normal stresses a sufficiently low SDR (e.g. 0.1mm/min) should be specified.

Fox et al. (1998) performed tests using a pullout shear machine at 72.2kPa normal stress with displacement rates between 0.01mm/min and 10mm/min. In contradiction to the abovementioned studies he showed a decrease in shear strength of approximately 3% to 5% of the corresponding values at 0.1mm/min per log cycle of SDR. This decrease of strength with decreasing SDR applied to both, the peak and residual shear strengths.

4.6.1.2 GCL interface shear strength

Triplett & Fox (2001) used SDRs of between 0.01mm/min and 10mm/min for tests at 72.2kPa normal stress to measure the effect of SDR on measured interface shear strength. They found that the SDR had no effect, on average, for interface shear strengths between the woven side of a needle-punched GCL and various HDPE geomembranes. This is in agreement with Stark et al. (1996). Triplett & Fox

(2001) suggest that a rate of 1mm/min is acceptable for hydrated geomembrane/needlepunched GCL interfaces for production testing, though a slower rate, such as 0.01mm/min, may be ideal.

The interaction between textured geomembranes and non-woven geotextiles is governed by the hook and loop interaction phenomenon, like the product Velcro. This is the case between a needle-punched GCL and a structured geomembrane. Hebder S al. (2005) investigated this behaviour but with a plane non-woven geotextile, not a GCL. The advantage of using textured geomembranes is that it increases the friction angle and the additional interaction between the materials during installation requires minimal or no supplemental restraints during placement and seaming. However other practitioners note that this large interaction greatly restricts realignment after the initial placement.

4.7 Bentonite Moisture Content

Final moisture contents of the GCL specimen and soil (if applicable) are generally taken after shearing to assess the level and uniformity of hydration during the test. A minimum of five water content samples is recommended by Fox & Stark (2004).

Eid et al. (1999) measured the average water content for the GCL Bentofix after each internal shear test using a torsional ring shear device. The water content decreased from approximately 145% to less than 70% for normal stresses ranging from 17kPa to 400kPa, respectively. Fox et al. (1998), using a direct shear device, also reported similar data. Both results showed a decrease in bentonite moisture content with increasing normal stress. Fox et al. (1998) fitted a power function to his data.

4.8 GCL Index Testing

GCL index tests assess the quality of a product. Researchers of the GCL shear strength generally only report the peel strength since this is possibly related to the internal shear strength of the GCL. No mention of the amount, type and characteristics of the bentonite are made. However, tests conducted on an unreinforced GCL yielded enough variability to conclude that the variability of the bentonite is also relevant (Zornberg, 2005).

Zornberg (2005) investigated 15 GCL batches (of Bentomat ST) from 2002 where the peel strength specified by the manufacturer was 65N/m. However, his peel strength results varied significantly, from 43N/m to 225N/m. The peel strength was shown not to be a good indicator of the peak shear strength. However, the study by Fox et al. (1998) concluded that the shear strength did correlate with the peel strength.

4.9 Shear Strength Results

As stated by many authors in this field including (Fox & Stark, 2004; Bouazza, 2002; Eid et al., 1999), project-specific materials and interface shear strengths must be used for design purposes.

4.9.1 Field data

Field tests, due to their large scale, are expensive but they can demonstrate the real behaviour of GCL interfaces. Daniel et al. (1998) reported failure modes for different slopes and different GCL types in the cover system. All 3H:1V test slopes, as opposed to 2H:1V, performed satisfactorily. The critical surface was found to be the GCL / smooth geomembrane for the reinforced GCL test plots. Two failures occurred on the 2H:1V slopes (20days and 50days after construction) due to a reduction in shear strength caused by bentonite extrusion through a woven geotextile.

No full scale field investigation has been undertaken for a liner system since excavating tens of metres of waste or soil material to observe the liner system condition post loading is not feasible. However, valuable information has been inferred from landfill liner failures.

Numerous authors have investigated the stability of the landfill lining system especially since lining failures in the early days of rigorous lining design standards in the 1980's. The most popular of these is probably the Kettleman Hills Landfill slope failure of 1988. The description and analysis of the failure has been well documented (Seed et al., 1990; Byrne et al., 1994; Gilbert et al., 1998; Chang, 2005; Koerner & Soong, 1997). Failure occurred between the secondary geomembrane and secondary clay layer along the base and lower portion of the side slopes. Excessive sliding also occurred along the primary geomembrane and secondary geotextile along the upper portion of the side slopes.

4.9.2 Laboratory test data

High-quality test data are available in the open literature for GCL internal shear strengths and geomembrane/GCL interface shear strengths. Much less information is available on shear strength behaviour for other common GCL interfaces (Chiu and Fox, 2004). A list of research work applicable to this study is given in Table 4.1. The test setup and specimen size refer to the type of machine used and the maximum size of the shear area of the tested materials listed under the 'interface materials' column. The 'pullout' shear device is shown in Appendix B. The test shear displacement rate (SDR) and pressure range (normal stress range) define the test conditions. The rate of 6.5°sec by Izgin & Wasti (1998) refers to the rate of the increase of tilt of the inclined board. A very brief indication of what was investigated appears in the final column.

The most pertinent research, which incorporated the GCL BENTOMAT[®]ST, is listed first. These are followed by geomembrane/geotextile interface, geomembrane/clay and geomembrane/sand interface tests and a multi-interface test study. Finally, results of two publications, which concerned numerical analyses of landfills, are included. These are listed to indicate which interface shear strength parameters were chosen for the respective numerical investigations.

The specimen size is constant if one of the shearboxes is sufficiently larger than the other. Only the tests considered by Zornberg (2005) make use of a large direct shear device where the area changes during testing. The shear displacement rate indicated is the rate for the corresponding result

Table 4.1 Summary of investigations of interface shear strength associated with materials used in landfill liners

Researcher	Test setup	Specimen size (l x b) mm	Test rate mm/min	Pressure range kPa	Interface materials	Studied influence of ...
Fox, et al. 1998	Pullout (direct shear)	1067 x 406 (constant)	0.1	17-279	GCL - Bentomat®ST	Shear displacement rate Product type
Zornberg 2005	Direct	300 x 300	0.1 1	35-310 97-2759	GCL - Bentomat®ST	Shear displacement rate Product type
Triplett & Fox 2001	Pullout	1067 x 406 (constant)	0.1	6.9 - 487	Smooth 1mm HDPE GM* GCL - Bentomat®ST (NW side)	Shear displacement rate Bentonite extrusion, GM texturing
Wasti & Ozduzgun 1999	Direct	300 x 300	18	111-400	Smooth GM 500g/m ² NW** Polyester geotextile	Material type Test setup
Jones & Dixon 1998	Direct	300 x 300	3	25 - 200	Smooth GM 750g/m ² polypropylene geotextile	Geotextile type Cover soil
Hebeler, et al. 2005	Direct	100 x 100 (constant)	5	0.4 - 312	Structured 1.5mm GM 203g/m ² NW geotextile	Investigation of Hook Loop behaviour
Hsieh & Hsieh 2002	Direct	300 x 300	1	49.1- 196.2	Smooth GM 1.9mm Sand - uniform, dry ¹	Load plate rigidity GM type
Izgin & Wasti 1998	Inclined Board	300 x 300	6.5°/sec	0 - 25	Smooth GM Sand - Ottawa ²	Size of specimen Test setup
Stark & Eid 1996	Torsional Ring	40 int. diameter 100 outer diameter	0.5	17	GCL - Bentofix textured 1.5mm GM	Shear displacement rate Bentonite
Eid 2002	Torsional Ring	40 int. diameter 100 outer diameter	0.015	17 - 400	Textured GM GCL - Bentofix, soil	Multi interface test setup
Filz, et al. 2001	Approximated average values from other research and back analyses of failed landfill				smooth GM , Geotextile Clay	- Numerical study - Progressive failure
Jones & Dixon 2005	No details			25 - 200	Textured GM NW Geotextile	- Numerical study - Waste settlement

*GM = Geomembrane

**NW = Non-woven

¹ D85 = 1.0, Cu = 1.01, Dr = 24% $\phi = 38^\circ$

² D60 = 0.55, Cu = 1.375, Cz = 1.05, loose $\phi = 33^\circ$

shown. The applied normal stress/pressure varies a lot between researchers with only Zornberg (2005) achieving normal stresses above 500kPa. The GCL interface refers to the internal shear strength of the GCL itself. Only the main aspects the researcher focused on and their affect on the test results are indicated. Eid (2002) incorporates three test materials in a multi-interface test arrangement. The details of this test are discussed in Section 4.9.3.

Table 4.2 is an extension of Table 4.1 and summarises the peak and residual shear strength parameters of the investigated interfaces. The failure envelope line was linear for most tests. Those that were not, were linearly approximated between the specified range of normal stress. Eid (2002) had a trilinear result as a consequence of the three interfaces investigated in the multi-interface test.

Esterhuizen et al. (2001) (not listed in the tables) conducted large direct shear tests between a smooth geomembrane and clay material (LL= 55%, PI = 29, 96% passing 200-mesh U.S. standard sieve, $w = 27.4\%$, dry density = 14.6kN/m^3) at 35kPa and 345kPa normal stress. The residual condition was reached at displacements of 100mm to 150mm. The peak and residual shear strength parameters at low normal stresses were 26.8° and 18.4° with an effective cohesion of 0kPa. As the normal stress increased the shear strength decreased. They expected that the failure envelope will eventually become horizontal at very high normal stresses as the partially saturated clay adjacent to the geomembrane approaches saturation.

4.9.3 Multi-interface testing

It is possible to test various interface at the same time. Which interface will fail is dependent on the normal stress conditions of the test. Research studies on this test method are rare due to its complexity and there is no real requirement by industry.

The main disadvantage of this form of testing is that the combination failure envelope does not show how close other material interfaces are to failure. Secondly, cumulative displacements are measured and it is difficult to estimate the individual surface displacement contributions at peak failure. Thirdly, this test is difficult to set up, perform and interpret which lends itself to more erroneous assumptions (Fox & Stark, 2004).

Eid (2002) performed this type of test to study the interactive shear strength behaviour of the components of a landfill composite liner system. The typical field alignment of the different components was simulated in a modified Bromhead ring shear device. This consisted of the compacted silty clay underneath a needlepunched GCL (Bentofix) — woven side upwards, which in tum was overlain with a textured geomembrane. The hydration and consolidation procedures were similar to those published in Eid et al. (1999).

Failure occurred along the soil/GCL non-woven geotextile side interface at normal stresses of 17kPa, 25kPa, 50kPa and 75kPa. The failure surface moved to the textured geomembrane/GCL woven geotextile side interface in shearing at normal stresses of 100kPa, 150kPa, 200kPa and 250kPa. For specimens sheared at normal stresses of 300kPa or higher, internal failure occurred through the

Table 4.2 Summary of shear strength properties of materials used in landfill liners

Researcher	Failure envelope	Displacement at peak (mm)	Peak shear strength		Displacement at LD [†] (mm)	LD shear strength	
			c' (kPa)	φ' (degrees)		c' (kPa)	φ' (degrees)
Fox, et al. 1998	non-linear	16.5 -25.8	98.2 42.3	32.6* 41.9**	-	-	-
Zornberg 2001	non-linear	10.0 -25	20.6 102.4	25.2 11.9	60	15.5	9.4
Triplett & Fox 2001	Linear: peak LD: Bi-linear	0.5 - 2.5	0.4	9.9	200	(6.9 - 127kPa) 0.6 (127 - 486kPa) 5.8	9.2 6.9
Wasti & Ozduzgun 1999	linear	0	3.3	12.3		0	
Jones & Dixon 1998	linear	2 mm (approximately)	3.2	8.4		0	
Hebeler, et al. 2005	linear	8mm	0	35.1	80		
Hsieh & Hsieh 2002	linear	1.0-2.0	0	24.2	run till residual	0	18.9
Izgin & Wasti 1998	linear	-	0 0	19	-	-	-
Stark & Eid 1996	linear	10.0-15.0		22.5 (interface)			15 (interface) 22 (unfilled) 8 (bentonite filled)
Eid 2002	Trilinear ^{††}	5.0-15	Soil/GM: 0 GCL: 43 GM/GCL 0	(0-95kPa) 25.5 (260-400kPa) 13 (95-260kPa) 22-25		70	20 7 14
Filz, et al. 2001	linear		0 (low normal stresses)	26.8		0 (low normal stresses)	18.4
Jones & Dixon 2005	linear	5-9mm	3.2	24.5	90mm	2.5	12.8

† LD = Large displacement

†† Combination failure envelope

* peel strength = 160N

** peel strength = 85N

GCL (Eid, 2002). It was observed that the extrusion of bentonite increased with higher normal stresses and was generally more for woven geotextile interfaces than for non-woven geotextile interfaces.

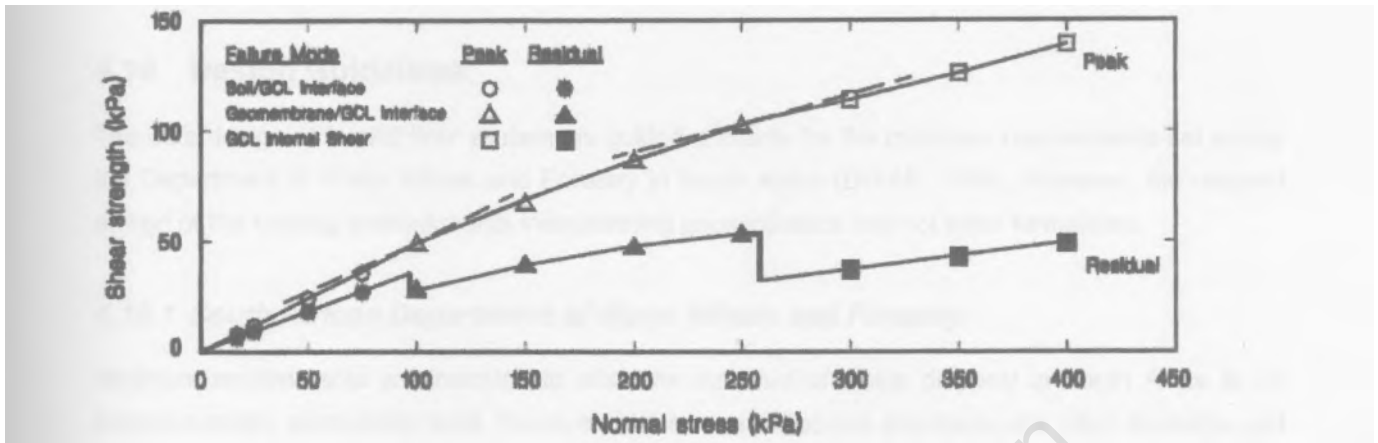


Figure 4.4 Peak and residual shear strength failure envelopes for composite specimens (Eid, 2002).

The result is a tri-linear peak strength failure envelope and a corresponding residual shear strength failure envelope, as shown in Figure 4.4. Eid (2002) conjectures that the non-linearity of the geomembrane/GCL interface may be attributed to the extrusion of more hydrated bentonite at higher normal stresses. This failure envelope could also be developed by test results from investigating each interface separately.

This type of comprehensive failure envelope should be used for design to account for the effect of changing normal stresses acting on the liner interfaces as well as for a shear strength reduction due to strain incompatibility with a 'soil' material consisting of Municipal Solid Waste (MSW) and also for progressive failure. MSW peak shear strength is mobilized at approximately 40mm as apposed to about 20mm for the liner interfaces (Eid, 2002). Thus, when looking at a comprehensive failure condition in a landfill system, the residual shear strength may be critical.

4.9.3 Long term shear strength

The direct shear test is a short term test. But in practice, GCLs sustain shear loads for the full design life of the facility which could be hundreds of years. The long-term performance of GCLs and GCL interfaces under sustained loads remains largely unknown (Fox & Stark, 2004).

Since these facilities have only recently been constructed it is not possible to predict the long term behaviour of geosynthetic materials. For design, the use of reduction factors may be used to take account of creep and durability. Marr & Christopher (2003) proposed an approach to estimate long term internal shear strength reduction due to creep and durability over the life of a landfill facility. Only the needle-punched polymeric fibres provide the shear strength above the residual shear strength. Reduction factors of 3.0 for creep and 1.1 for durability for a 100y design life are recommended, giving a total reduction factor of 3.3. This is applied to the difference between the peak and residual shear strengths at each normal stress level of the short term shear test results. The internal residual shear strength parameters of the GCL is almost the same as bentonite – friction

angle between 4° and 5° and a cohesion of 0 kPa. Discussion of the derivation of such reduction factors is beyond the scope of this work, however their use in landfill design is considered in Chapter 9.

4.10 Design Guidelines

The safe design of landfill liner systems is guided primarily by the minimum requirements set out by the Department of Water Affairs and Forestry in South Africa (DWA, 1998). However, the detailed design of the sloping embankments incorporating geosynthetics has not been formalised.

4.10.1 South African Department of Water Affairs and Forestry

Minimum requirements are intended to raise the standard of waste disposal in South Africa to an environmentally acceptable level. However, higher waste disposal standards are often desirable and appropriate.

Landfills are classified according to their waste type, size and climatic water balance. A significant leachate generating site is where the water balance is positive for more than 1 in 5 years. The minimum requirements define general waste (domestic, certain industrial, and builders rubble) as waste that does not pose a significant threat to public health or the environment if properly managed.

The main design guidelines regarding landfill liner stability are as follows:

- The side slopes should be such that it is possible to lay the required liner geosynthetic (if used). Interfacial friction of the liner system components must be determined.
- Design should be based on residual shear strengths measured under saturated conditions. These should be measured with a ring shear device to a shear deformation of at least 360°.
- Slopes must be graded to achieve a global factor of safety of at least 1.3. This must take into account pore pressures due to leachate head on the liner. There is no mention of the permissible level of head.
- Where adequate data is not available, geomembranes, composite liners and geotextiles will have to be tested for strength, interface friction, durability and compatibility with identified components of waste and leachate.

The minimum permissible physical separation, excluding the lining system, between the proposed waste body and the wet season high elevation of the groundwater must be at least 2m (whether excavated or not).

4.10.2 South African National Standard

Though the minimum requirements for landfill design exist in South Africa, no official code of practice for the design of liner and cover systems of waste containment facilities is available. Koerner's (1998) method for designing soil slopes containing a geomembrane has been used by local consultancies to assess landfill stability. However, the use of this method is open to interpretation and a formalised

limit state method specific to landfills would be beneficial. The most useful reference in this regard is the South African National Standard: *The design and construction of reinforced soils and tills* (SANS 207, 2006). This code provides international approaches (i.e. BS 8006, 1995) to designing with geosynthetics.

In geotechnical engineering in SA the application of partial factors of safety to the various geotechnical parameters has not been found practical in general design and overall factors of safety are still in use (SANS 207, 2006). However, with the use of structural elements in soil systems partial factors are appropriate and take account of all aspects of the components of the design.

The standard considers ultimate and serviceability limit states in the design of geotechnical structures. The ultimate limit state concerns structural failure where driving forces are equal to or larger than resisting forces. Serviceability limit states occur if the magnitude of deformation exceeds prescribed limits during the structures design life. Safety factors are built into the ultimate limit state design using partial material and load factors. For serviceability, these factors (except for the reinforcements) are set to unity and the deformations computed. Partial factors of safety to take account of the economic consequences of failure are also incorporated.

In a landfill the geosynthetics do not play a reinforcing role, but do have a containment function. However, the geosynthetics must sustain shear forces to maintain integrity of the lining system. Since the design life is very long for these facilities geosynthetics will creep and internal shear strength will decrease with time. Thus, the application of partial safety factors to these components is imperative.

4.11 Design Methods

The strength parameters determined by the direct shear test is used by the engineer for the safe design of geosynthetic layered systems such as those occurring in modern landfill liner and cover systems. Various tools of varying levels of sophistication are available for this task. This includes manual calculation, numerical applications and finite element programs.

4.11.1 Manual calculation

Giroud & Ahline (1984) set forth a general method for complex geometries, which is rather tedious for typically layered systems of uniform thickness. Martin & Koerner (1985) proposed an infinite slope analysis for systems of uniform thickness and a two-wedge analysis for non-uniform thickness systems. Giroud & Beech (1989) provided a detailed analysis of all three mechanisms involved in the stability of sloped and layered systems: i) the interface friction along the slip surface, ii) the toe buttressing effect and iii) the tension of geosynthetics above the slip surface using a two-wedge analysis. However, cohesion- and adhesionless conditions above the slip surface were assumed and an explicit factor of safety was not presented .

Koerner & Hwu (1991) presented a similar two-wedge analysis, but the calculation of the factor of safety, though explicitly stated, is more complex (involving a quadratic equation) and the factor of

safety related to tension of the geosynthetic is calculated separately. In Giroud et al. (1995) the shortfalls of the work done by Giroud & Beech (1989) are addressed. Cohesive and adhesive conditions are incorporated above the slip surface and the factor of safety is expressed explicitly in a user friendly and clear manner (effects of each design parameter are shown separately). This method gives almost the same factor of safety in most practical situations as Koerner & Hwu (1991), yet is elegant, succinct and takes geosynthetic tension into account directly. Giroud et al. (1995) note that if the actual layered system has more than one soil layer above the considered slip surface, the total thickness above the slip surface must be used and the properties (γ , c , p) of the various soil layers must be averaged. A brief overview of the method is shown in Appendix F.

Chang (2005) conducted a three dimensional limit state analysis of the Kettleman Hills landfill slope failure based on the observed sliding-block mechanism. The field investigations showed the waste slope moved essentially as a sliding block unit along the interfaces of the underlying liner system (Byrne et al., 1994). The 3D study showed slightly higher computed factors of safety than the associated 2D values indicating that 2D analyses are conservative. Chang (2005) considered the mobilization of different interfaces as a function of the normal stress level, thus incorporating a combined failure envelope.

No explicit 2D analytical method was found that directly assesses the stability of a landfill with waste fill.

4.11.2 Pore water pressure

Few papers have addressed the influence of leachate on the stability of the waste mass. The piping and pumps within the sump are generally designed so that not more than 300 mm of leachate head are on the liner system. However, generally low initial hydraulic conductivity of leachate collection systems, the build-up of particulates and micro-organisms and crushed pipes tend to decrease the hydraulic conductivity in time (Koerner et al., 1994).

Koerner (1994) discussed various different leachate scenarios in a landfill including discontinuous leachate, localized leachate, excess pore water pressure, gas entrapment and leachate head on the liner. Of all scenarios, leachate head on the liner is probably the most common. Koerner et al. (1994) found four landfills with significantly higher heads than anticipated, up to 20m. Since it acts hydrostatically it can readily be incorporated into stability analyses.

4.11.3 Numerical analyses

Analytical methods have been automated by various software developers for the speedy computation of circular and plane failure surfaces in geotechnical systems. No paper was found that dealt specifically with landfill analyses, but some finite element method focussed studies incorporated a comparative numerical limit state analysis.

Filz et al. (2001) used the software UTEXAS3 (Wright, 1991) which uses Spencer's method. Reddy et al. (1996) used PCSLTAB4 (Lovell et al., 1983) which uses the simplified Janbu method for non-

circular surfaces. Jones & Dixon (2005) conducted analyses of the waste fill using SLOPE-W which uses the Morgenstern and Price method.

Table 4.3 summarises the properties of the materials and interfaces used for the limit equilibrium analyses (LEA) by the respective authors. L is the length of the landfill base and H is the height of the waste fill as shown in Figure 4.5. The gradient of the outer waste slope for each geometry analysis is 1V:3H and the liner slope is varied. For the Finite Element analyses, the stiffness of the waste had to be specified. This value was varied to simulate soft or stiff waste. The waste fill properties of Filz et al. (2001) were for the Kettleman Hills landfill. Parametric analyses were also conducted with lower unit weights and internal friction angles as part of the investigation.

Table 4.3 Summary of limit state analyses

Author	Critical interface	Geometry analysed			Waste properties		
		L(m)	H(m)	liner slope	c' (kPa)	ϕ' (degrees)	γ (kN/m ³)
Filz, et al. (2001)	Smooth GM NW Geotextile Clay	153	21.3 to 27	1:2	10	38	17.3
Reddy, et al. (1996)	Smooth GM Textured GM NW Geotextile	91.5	30.5	1:2	1.4	11	10.2
Jones & Dixon (2005)	Textured GM NW Geotextile	100	30 to 60	1:1; 1:2; 1:3	5	25	12.2

NW – nonwoven



Figure 4.5 Typical landfill two dimensional geometry

Due to various waste types and difficulty in testing such a material, often composed of large items, a wide range of values have been published. Landva & Clark (1990) reported values of cohesion and internal shear angles varying from 0 – 23kPa and 24° - 41° respectively. Internal friction angles as low as 19° (Fang et al., 1977) and as high as 81° (Siegel et al., 1990) have been reported. DWAf recommends cohesion and an internal friction angle of 25kPa and 15°, respectively, for the preliminary assessment of the stability of an outer waste slope.

Previous studies of the Kettleman Hills failure showed sliding occurred as a result of reaching a critical waste height (Chang, 2005). Different factors of safety between authors for the same 2D Kettleman analyses were caused by the adoption of different interface strength data, highlighting the importance of applying project specific values. Even though the Kettleman Hills landfill has a 2%

base gradient, Filz et al. (2001) assumed a flat base for the analyses. Global factors of safety to take into account the variability and uncertainty in the materials and construction procedures were used. The use of residual on the base and the side slope approximated the actual failure waste height well. However, the use of peak on the base and the residual on the sides overestimated the safe landfill height.

Jones & Dixon (2005) consider waste settlement along a single strain softening interface. The textured geomembrane/non-woven geotextile interface was used but the shear strength is relatively high compared with using a smooth geomembrane. This practice is common in the UK. Jones & Dixon (2005) initially analysed four cases each with varied liner side slope angle and waste height. Assuming base peak and side residual and a liner slope angle of 1:3 they determined factors of safety of 2.6 and 1.4 for 30m and 60m, respectively. After completing the Finite Element Method analyses they calculated the actual mobilized interface shear stresses based on weighted average formulation. Using these values in a Limit Equilibrium Analysis very similar results to the base peak side residual assumption were obtained. Thus, the approach of using residual shear parameters on the slope and peak shear parameters on the base is valid for assessing global stability of the waste body.

The following aspects are generally not taken into consideration in a limit state analysis:

- Geosynthetic tension
- Waste strength/stiffness properties
- Waste settlements
- Partial factors of safety
- Seepage
- Progressive failure (versus development of a continuous failure plane.)

However, if the above aspects are well understood they can be indirectly incorporated.

4.11.5 Modern computer solutions

The finite element method (FEM) has increasingly become popular in all disciplines of engineering since the 1950's as computers became more powerful. The FEM method can help make recommendations for selecting the appropriate interface shear strengths for safe landfill design.

From a mathematical perspective FEM is "An approximate method for solving differential equations utilizing a variational principle and piecewise polynomial approximation (Babuska, 2001)." Physically, FEM is the approximation of the change in the stress and strain field of a system due to imposed loads or displacements. However, this is an expensive tool and not warranted for most projects in developing countries. DiBiagio & Flaate (2000) quote Ralph Peck, pointing out that "Simple calculations based on a range of variables are better than elaborate ones based on limited input" Reddy et al. (1996) noted that caution should be exercised because the accuracy of the finite element analyses depends on the accuracy of the model for the actual interface shear stress/shear

displacement behaviour as well as the stress-strain behaviour of the Waste material. However, well conducted analyses help to understand the behaviour of the liner system and hence aid designers using simpler calculation methods.

Byrne (1994) analysed the Kettleman Hills failure using a finite difference method. Filz, et al. (2001) analysed two interfaces simultaneously and incorporated bar elements to simulate the soil and geosynthetic layers between the two Kettleman Hills critical interfaces. Slippages were confirmed on the side slopes of the liner system at the early stages of waste filling.

Long et al. (1995) considered interface and axial load displacement behaviour of all components, but the waste loading was simulated by an assumed loading profile. Reddy et al. (1996) investigated a single interface showing shear stresses and displacements along the interface. The stiffness of the MSW was shown to be a major factor determining composite liner interface shear stress and shear displacement distribution. Villard et al. (1999) considered strain softening interfaces as well as tensile stresses in the geosynthetics. However, the study was limited to the placement of a thin single gravel layer over the interface.

Filz, et al. (2001) concluded that progressive failure effects greatly reduce available shearing resistance and that values only slightly higher than that of residual shear strength are representative. Thus, limit equilibrium analyses using only peak shear strength is illogical and slightly increasing the shear strength (by applying a specific factor) or using the residual shear strength with a reduced required factor of safety is appropriate.

Jones & Dixon (2005) considered waste settlement along a single strain softening interface. Final surface settlements of up to 20% of the initial waste thickness generally occur (UK Waste Management Paper 26B, 1995). Displacements and shear stresses along the interface are considered but not the tension in the geosynthetics. The analysis concluded that the approach of using residual shear parameters on the slope and peak shear parameters on the base is valid for assessing global stability of the waste body.

None of the approaches can be used to assess all the aspects of the lining system behaviour. Jones & Dixon (2005) points out that Numerical analyses that incorporate multiple geosynthetic and mineral layers that are numerically stable when large displacements occur are required to assess the possibility of tensile failure of components." The results of these limited finite element analyses help to understand the behaviour of the liner system and hence the approach to manual calculations can be improved.

4.12 Shear Strengths for Design

The Mohr-Coulomb shear strength failure envelope can be determined for each interface of the lining system. A combined peak and residual failure envelope can be constructed such as the one in Figure 4.4.

A combination design failure envelope can be constructed from segments of the individual failure envelopes of the liner system Interfaces. The peak envelope represents the lowest peak shear strength at each normal stress. The combination large displacement envelope does not represent the lowest large displacement shear strength at each normal stress but corresponds to the peak envelope.

In finite element analyses there is a limitation in modelling strain softening behaviour and other analytical methods require the precise specification of shear strength and respective interface since displacements are not taken into account. The following approaches have been suggested:

- Assign residual shear strengths to the side slopes and peak shear strengths to the base of the liner system, and satisfy a factor of safety greater than 1.5 (Stark & Poeppel, 1994).
- The use of residual shear parameters on the slope and peak shear parameters on the base is valid for assessing global stability of the waste body (Jones & Dixon, 2005).
- Assign residual shear strengths to the side slopes and base of the liner system and satisfy a factor of safety greater than 1.0. A factor of safety of 1.1 should be satisfied if large displacement shear strengths are used instead of residual values (Stark & Poeppel, 1994).
- Use the residual shear strength with a reduced required factor of safety (Filz et al., 2001).
- The use of peak strengths with an adequate factor of safety for all non-seismic conditions (Koerner, 2000).

Two approaches are possible, firstly to assign different shear strengths to the base and slope of the liner system. The methodology of using residual shear strength on the slopes assumes that large displacements occur within a bottom liner system and failure progresses from the side slopes to the base liner. Secondly, to assign the same shear strength parameters to the entire interface and satisfy an appropriate factor of safety.

4.13 Research Requirements

Based on this literature review a number of possible research requirements were identified that could be undertaken with the current resources. Aspects such as long term strength and improved finite element analyses are therefore not discussed, though equally important.

- Effectiveness of a new specimen gripping system.
- Large Direct Shear testing of all interfaces of a landfill liner system to provide an additional comparative study.
- Effectiveness and influence of the hydration and consolidation procedure on measured shear strength.
- Impact of bentonite properties on test results.
- Shear behaviour of the GCL / sand liner interface.
- Development of a limit state liner design approach for the full life of a landfill.

Although project-specific testing should always be carried out, additional comparative studies are needed to illustrate strength behaviour of a multiple liner system. A simple yet reliable manual limit state design approach would be beneficial for designers who have no access and/or the knowledge to use sophisticated software.

University of Cape Town

CHAPTER 5

RESEARCH MATERIALS

5.1 Introduction

In this chapter the materials of the components of a primary lining system used in the investigation which include a Geosynthetic Clay Liner, a HDPE geomembrane and Philippi Dune sand are discussed. The main physical properties of the geosynthetics were obtained from the manufacturer's specification pamphlets. Additional information, e.g. visual characteristics on microscale and a check of the manufacturer's specifications is given by using appropriate test devices and procedures.

Results of previously conducted tests on the sand material, relevant to this investigation, are also included. Further mechanical tests were undertaken on the sand to fully understand the current material. The results of the microscopic analysis undertaken on all the research materials are presented and discussed.

5.2 Properties of the Geosynthetic Clay Liner

The GCL product used in this study was BENTOMAT[®]ST, manufactured by CETCO Lining Technologies in the USA (CETCO, 2006) and distributed in South Africa by AQUATAN (Pty) Ltd in Johannesburg.

5.2.1 Geotextile components

The woven geotextile consists of 99% Polypropylene and 1% carbon black. The non-woven geotextiles, composed of 100% Polypropylene, is white. Carbon black stabilizes the material against ultraviolet light improving its weather resistance as well as helps to distinguish between the woven and non-woven (white) side. The individual fibres are 60mm to 90mm long and of 4.5 to 11 denier diameter specification. The manufacturer guarantees the specifications listed in Table 5.1.

Table 5.1 Properties of BENTOMA[®]ST Geotextiles (CETCO specifications, 2006)

<i>Physical property (machine direction)</i>	<i>Unit</i>	<i>Woven</i>	<i>Non-Woven</i>
Mass per unit area	g/m ²	110	200
Grab strength (force)	N	540	300
Grab elongation	%	20 nominal	50 nominal
Puncture (force)	N	311	800

5.2.2 Clay mineral

The clay mineral is Volclay[®], a granular modified sodium bentonite produced by Volclay Dongming Industrial Minerals Co. Ltd in Jianping, China. The bentonite enhancement includes additions of polymer and dispersant chemicals in a CETCO patented treatment process. This increases the swell and contaminant resistant properties of an already high quality base clay.

The material has a moisture content, at delivery, of up to 12%. The free swell index is at least 24ml/2g. The swell index of the specific bentonite of the GCLs of this study were tested and high magnification images of the bentonite in the dry and hydrated state were taken. Unfortunately the X-RAY Diffraction device at the University of Cape Town was in disrepair at the time of this research, thus identification of the mineral make-up of the clay was not undertaken.

5.2.3 Geocomposite

The GCL is a special arrangement of the geotextiles and bentonite discussed earlier and has its own properties. All the certified properties of BENTOMAT®ST are summarized in Table 5.2.

Table 5.2 Properties of BENTOMA®ST (CETCO specifications, 2006)

Material Property	ASTM Test method	Unit	Required values
Bentonite Swell Index	D 5890	ml/2g	24 min.
Bentonite Fluid Loss	D 5891	ml	18 max.
Bentonite Dry Mass/Area	D 5993	kg/m ²	3.6 min.
GCL Grab Strength	D 6768	N/cm	40 MARV
GCL Peel Strength	D 6469	N/cm	4.4 min.
GCL Index Flux	D 5887	m ³ /m ² /s	1x10 ⁻⁸ max.
GCL Hydraulic Conductivity	D 5887	cm/s	5 x 10 ⁻⁹ max.
GCL Hydrated Internal Shear Strength	D 5321 D 6243	kPa	24 @ = 9.6

BENTOMAT®ST comes in panels with dimensions of 4.6m x 45.7m weighing in at 1180 kg per roll. (CETCO, 2006).

Two batches of this GCL were used in the study, received in 2005 and 2006, respectively. The second batch was the focus of this study in terms of interface shear strength tests. The specific results of these interface tests and the index and internal shear strength of both batches are presented in Chapter 8.

5.2.4 Geomembrane

A smooth and textured geomembranes were investigated for shearing against the other lining materials. HI-DRILINE® Smooth, is a High Density Polyethylene (HDPE) membrane manufactured by AQUATAN Lining Systems in South Africa. The geomembrane is smooth on both sides, contains approximately 97.5% Polyethylene, 2.5% carbon black, and trace amounts of anti-oxidants and heat stabilizers, which improve weather resistance. Although a 1mm geomembrane was used in the local landfill the thickness of 2mm was chosen for this study since this type, in general, is used internationally. The main physical product specifications (AQUATAN Data Sheet, 2007) are presented in Table 5.3. Properties such as the melt flow index and low temperature brittleness are not presented since these are not relevant to this study.

A structured HDPE geomembrane of 1.5mm thickness, with 1mm high texturing (3 protrusions per cm²), on one side was used in a number of tests for comparison with the smooth geomembrane.

Table 5.3 Properties of HI-DRILINE® Smooth (HDPE) (Aquatun specifications, 2007)

Material Property	ASTM Test method	Unit	Nominal values
Density		g/cm ³	>0.94
Tensile properties (each direction)	D 638 & D 6693 Type IV		
Strength at yield	50mm/min	N/mm	32
Elongation at yield	10 = 33mm		16
Strength at break	200mm/min	N/mm	66
Elongation at break	10 = 50mm		800
Tear resistance	D 1004	N	275
Puncture resistance	D 4833	N	980

5.3 Mechanical Properties of Philippi Dune Sand

The sand was sourced from a local quarry and form part of the Cape Flats Sand group. The soil mechanical properties were determined by conducting standard tests in the Geotechnical laboratory of the Department of Civil Engineering, University of Cape Town. The tests included the determination of dry density/moisture content relationship, particle size distribution and shear strength in terms of angle of internal friction and cohesion.

Figure 5.1 presents the grading curve of the research sand. Included is the grain size distribution curve of Cape Flats sand by Kalumba (1998) for comparison. The results indicate a uniformly graded sand.

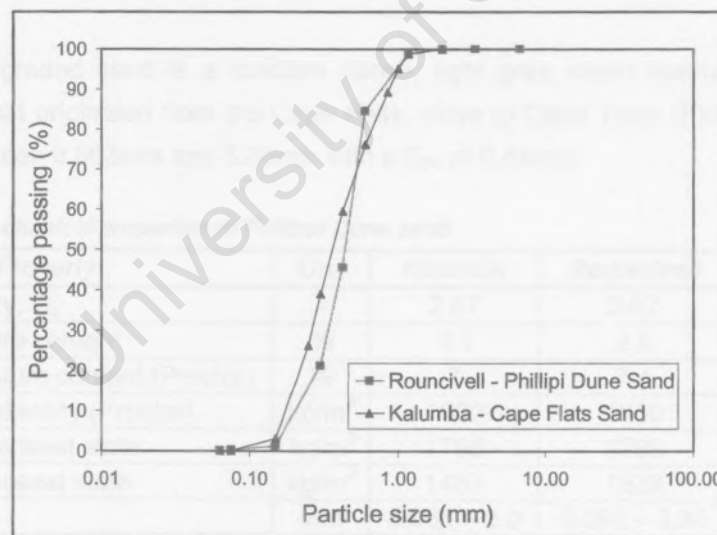


Figure 5.1 Grain size distribution of Phillipi Dune and Cape Flats sands

The standard Proctor compaction test procedure (Appendix A.3) was followed to determine the dry density/moisture content relationship. The resulting curve is shown together with Kalumba's (1998) results for Cape Flats sand in Figure 5.2.

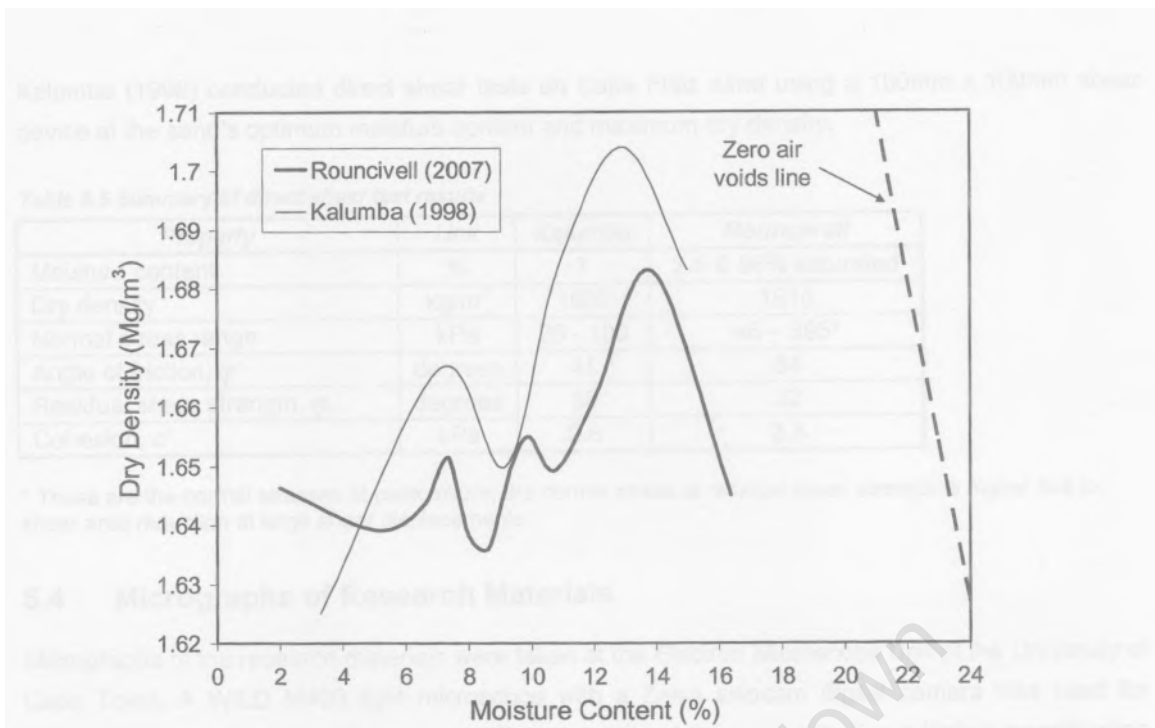


Figure 5.2 Dry density— moisture content relationship of Philippi Dune and Cape Flats sand

The Philippi Dune sand compaction relationship curve is consistent with the relatively flat, multiple peak compaction curve of Kalumba (1998). The natural moisture content of the sand was determined using various samples taken from the point of excavation at the Philippi Quarry near Cape Town, S.A.

The uniformly graded sand is a medium dense, light grey, clean quartz, subround-grained silty aeolian sand that originated from the Cape Flats, close to Cape Town (Kalumba, 1998). The grain sizes vary between 0.063mm and 3.35mm with a D_{50} of 0.44mm.

Table 5.4 Soil mechanical properties of Philippi Dune sand

Property	Unit	Kalumba	Rouncivell
Specific Gravity, G_s			2.67
Natural moisture content	%	3.1	2.5
Optimum moisture content (Proctor)	%	7	7.4
Maximum dry density (Proctor)	kg/m ³	1660	1650
Average dry densest state	kg/m ³	1765	1789
Average dry loosest state	kg/m ³	1487	1532
Particle range	mm	0.063 — 2.0	0.063 — 3.35
Mean grain size, D_{50}	mm	0.365	0.44
Coefficient of uniformity, C _u		2.33	2.31
Coefficient of gradation, C _g		0.96	1.14

Chemical tests conducted by Kalumba (1998) with hydrochloric acid being applied to the sand showed traces of calcite which cement the sand particles together.

Direct shear tests using a large 300mm x 300mm direct shear device were performed on the sand at an average dry density of 1510kg/m³. Series were run at the natural moisture content as well as in a near saturated condition. The relative dry density (D_r) of this lightly compacted state was 9.7%.

Kalumba (1998) conducted direct shear tests on Cape Flats sand using a 100mm x 100mm shear device at the sand's optimum moisture content and maximum dry density.

Table 5.5 Summary of direct shear test results

Property	Unit	Kalumba	Rouncivell
Moisture content	%	7	2.5 & 86% saturated
Dry density	kg/m ³	1660	1510
Normal stress range	kPa	25 - 100	46 – 395*
Angle of friction, (ρ')	degrees	41	34
Residual shear strength, (ρ_r')	degrees	30	32
Cohesion, c'	kPa	2.8	3.8

* These are the normal stresses at peak failure; the normal stress at residual shear strength is higher due to shear area reduction at large shear displacements.

5.4 Micrographs of Research Materials

Micrographs of the research materials were taken at the Electron Microscope Unit of the University of Cape Town. A WILD M400 light microscope with a Zeiss axiocam digital camera was used for magnifications of 20x and 64x to show different details of the materials. For a higher magnification required to investigate the microtexture of the geomembrane and the bentonite platelet arrangement a Scanning Electron Microscope was used up to a magnification of 15000x using a Leo Stereoscan 440 device.

The image of the Philippi Dune sand (Figure 5.3a) shows the sub-round shape, relatively smooth surfaces and non-uniformity of the particle sizes. The non-woven geotextile images show a needlepunched hole (Figure 5.3b - top left) and the variable diameter and non-linearity of the individual fibres (Figure 5.3c). A group of needlepunched fibres through the woven geotextile shows the long needlepunched length and potential for anchoring (Figure 5.3d). The as-received bentonite grains vary in size, have an orange brown colour (Figure 5.3e) and are relatively hard.

Numerous high magnification images of the bentonite and geomembrane were taken. These are presented in Appendix C. The electron microscope produces images in black and white only with the lighter parts of the image generally higher than the darker regions. However, this may be reversed depending on the properties of the surface material. The micrographs are topographical images of the surface of the materials. Magnifications of between 500x and 15 000x were utilized.

The two sides of the smooth geomembrane appear different at high magnifications. The side sheared against the sand shows relatively smooth "ripples" orientated in the machine direction. The side sheared against the GCL exhibits a similar pattern in terms of ripples, however there seems to be a coating over the surface (black areas). Micrographs of both sides of the geomembrane after shearing with the respective materials are presented in Chapter 8.

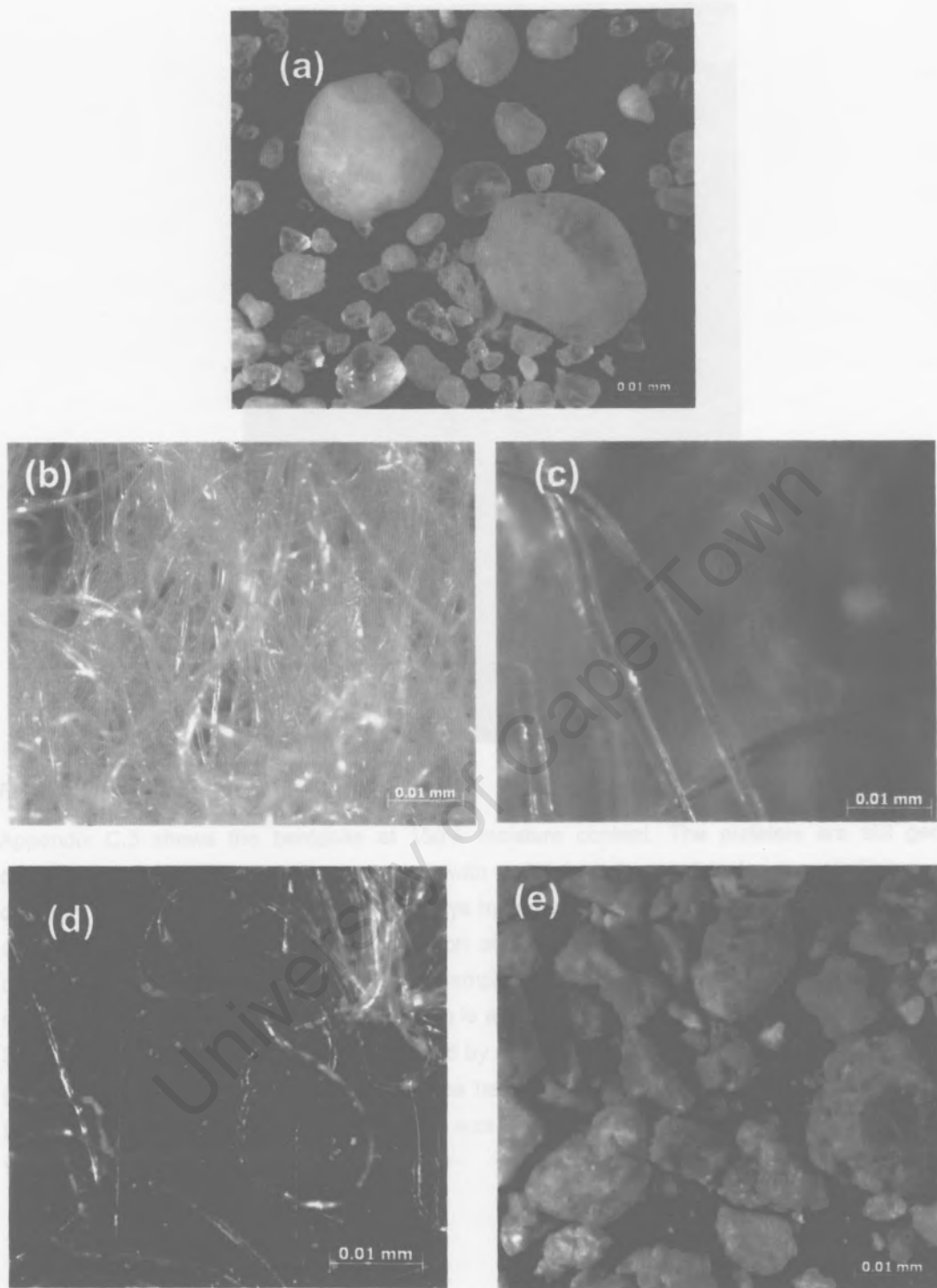


Figure 5.3 Micrographs of research materials a) Philippi Dune sand b) Non-woven geotextile c) Non-woven geotextile fibres d) Woven geosynthetic with needle punched non-woven fibres e) Bentonite – granular

The Bentonite was imaged in three different moisture content states to examine the disaggregation of the clay platelets with hydration. At 500x magnification (moisture content of 11%) the granular form of the Volclay® is shown. A higher magnification (Figure 5.4) shows the platelets, with irregular areal shapes, stacked on top of each other (black spaces are air voids). Further studies of the bentonite in a wet and near saturated condition were possible with the use of liquid nitrogen to freeze the wet specimens before placement in the electron microscope.

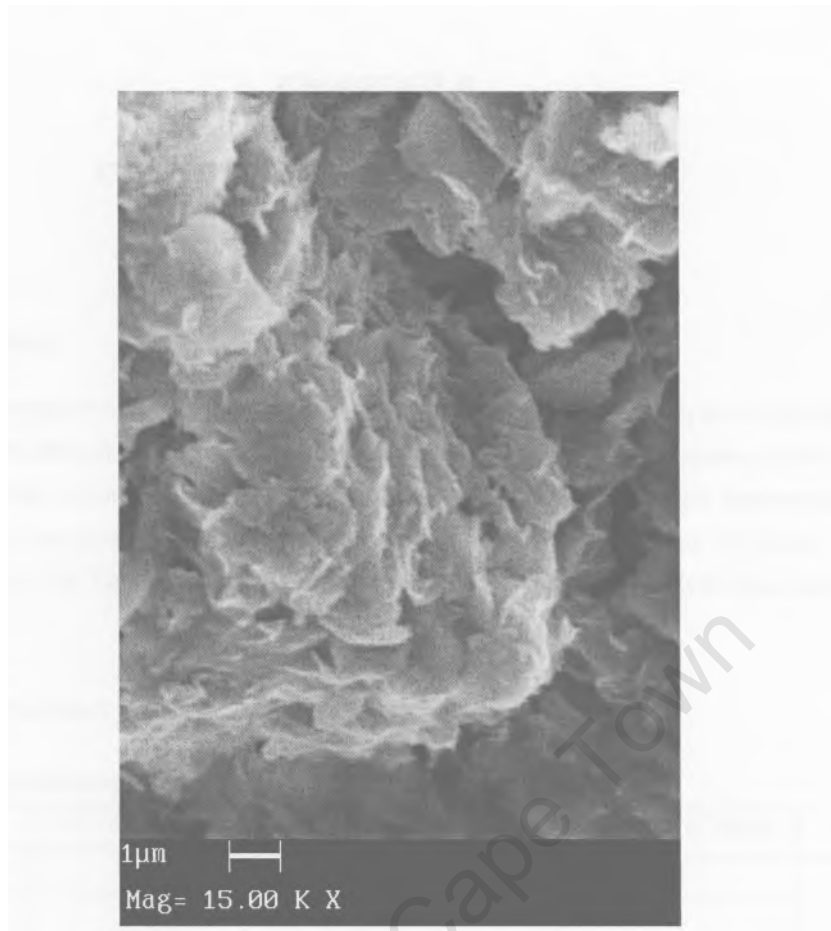


Figure 5.4 Bentonite: 11% moisture content

Appendix C.3 shows the bentonite at 150% moisture content. The platelets are still generally contiguous but disaggregation is apparent with water in between (black spaces). This moisture content condition was the result of seven days hydration and 400kPa normal stress during a direct shear interface test. The biggest separation of the platelets was observed at 3000% moisture content (see Appendix C.4). The bentonite sample had free access to water for two months with no normal stress applied. The hexagonal pattern is apparent with each hexagonal shape approximately 3.0 μm across. Similar images were observed by Kumai (1979) in a study of frozen bentonite in cold geographic regions. An investigation of these hexagonal sheet structures into the effects on their mechanical properties within the liner system was considered to be beyond the focus of the research work.

CHAPTER 6

GCL INDEX TEST INVESTIGATIONS

6.1 Introduction

In this chapter the measurement of various properties of the GCL and its component parts are briefly discussed. Since it is difficult or impossible to assess or estimate the performance of the GCL in the long-term (service life), short-term index tests serve as requirements which theoretically ensure physical integrity and performance in the field. The three most common and important index tests were carried out (listed in Table 6.1) to show the compliance of the GCLs with the manufacturer's specifications.

Details of these test methods are discussed in Appendix A.

Table 6.1 GCL property test program

<i>Test</i>	<i>ASTM Test method</i>	<i>Research material</i>	<i>Number of tests</i>	<i>Appendix</i>
Peel	D 6496	GCL	5	A.5
Swell	D 5890	Bentonite	5	A.6
Mass per unit area	D 5993	GCL	5	A.4

6.2 Peel test

The quality of the bond between the top and bottom layer of a GCL, expressed in terms of bond strength, is assessed by this index test. Five specimens of 100 mm x 200 mm are carefully cut and the top and bottom layer of the GCL separated for 50 mm. The grip setting of the tensile testing machine is adjusted so that the distance between the clamps at the start of the test was 50mm and the displacement rate is set at 300 mm/min.

The test is run till the grip separation is at least 125 mm, resulting in 100mm recorded peeling of the GCL. Figure 6.1a) shows a test in progress. The bonding peel strength is calculated for each individual specimen; that is, the average force to cause a specimen to separate completely as read directly from the test instrument expressed in N/m of width.

6.3 Swell test

Bentonite clay is the component of a GCL which functionally reduces hydraulic conductivity of moisture and gas through the GCL. An estimation of bentonite quality and thus its usefulness for permeability reduction is evaluated according to its swelling properties; clay of a higher swelling potential generally has a lower permeability.

The granular bentonite sample is ground to 100 % passing a 100 mesh U.S. Standard Sieve and a minimum of 65 % passing a 200 mesh U.S. Standard Sieve. A mass of 2.0g of the bentonite is added in 0.1 g increments, each carefully dusted over the water surface in the graduated cylinder at 10 minute intervals.

After the final increment has settled, adhering particles on the sides of the cylinder are carefully rinsed into the water column, raising the water volume to the 100 ml mark. The cylinder is allowed to stand undisturbed for 16 hours from the last incremental addition. The swell index is simply the volume level in millilitres at the top of the settled clay mineral (see Figure 6.1b)), recorded to the nearest 0.5 ml.

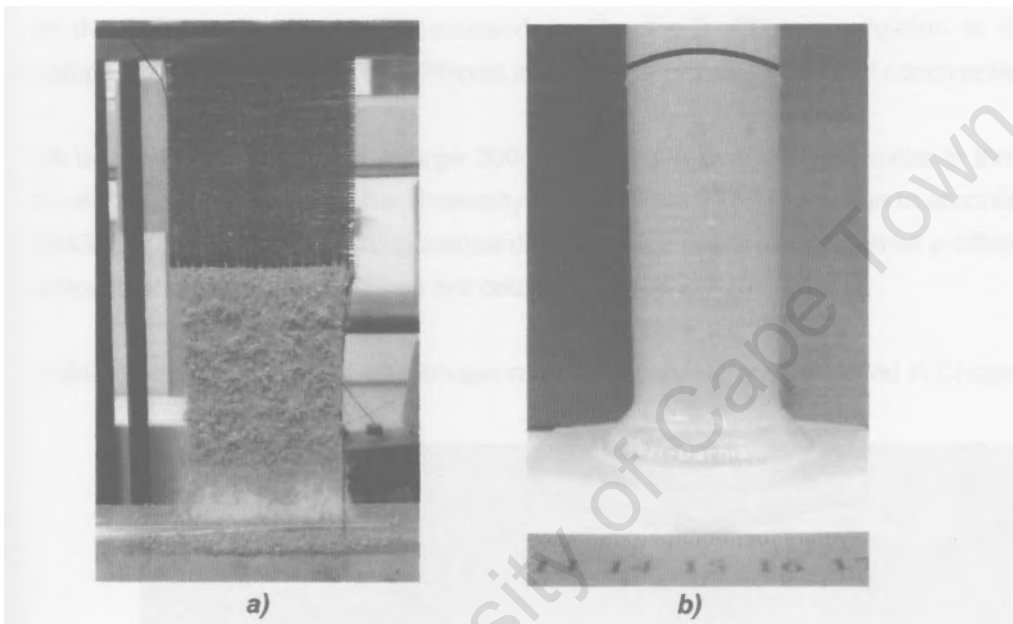


Figure 6.1 a) Peel strength test in progress, b) Swell test sample showing upper bentonite level

6.4 Mass per Unit Area test

A minimum mass per unit area of dry bentonite is required for the GCL to perform its barrier function properly.

Five test specimens of 100 mm x 200 mm are cut from the sample at different locations within the width of the GCL. The clay from the edges after removing the specimen is cleared from the cutting surface, weighed and split between the individual specimen and the discarded clay.

Specimen containers of known weight are used to dry the test specimens to constant mass conditions. The mass of the container and oven-dried material is determined. The tare of the container is subtracted from the mass of the sample to determine each samples' constant dry mass. The mass per unit area of dry bentonite itself is determined by subtracting the GCL synthetic components' mass per unit area from the total mass per unit area. This includes the woven and non-woven geotextiles of the GCL. The final mass per unit area is determined by taking the average value of the five test specimens.

CHAPTER 7

DIRECT SHEAR INVESTIGATION

7.1 Introduction

This chapter deals with the investigation of the shear strength of the GCL/sand, geomembrane/sand and GCL/geomembrane interfaces, internal shear strength of the GCL as well as the direct shear strength of the sand using the large direct shear device. The interfaces form part of the liner system of the Bellville South landfill discussed in Chapter 3. This investigation is characterizing and comparing the behaviour of the different interfaces over a wide range of compressive stress levels.

All tests were conducted in a large 300mm x 300mm direct shear device in the Civil Engineering Geotechnical Laboratory at the University of Cape Town. Tests were run in accordance with ASTM D 6243 and ASTM D 5321 testing standards. Each type of interface required a different test setup and procedure; these test procedures are detailed in Appendix A.7.

Details of the test results, their discussion and comparison, are presented in Chapter 8.

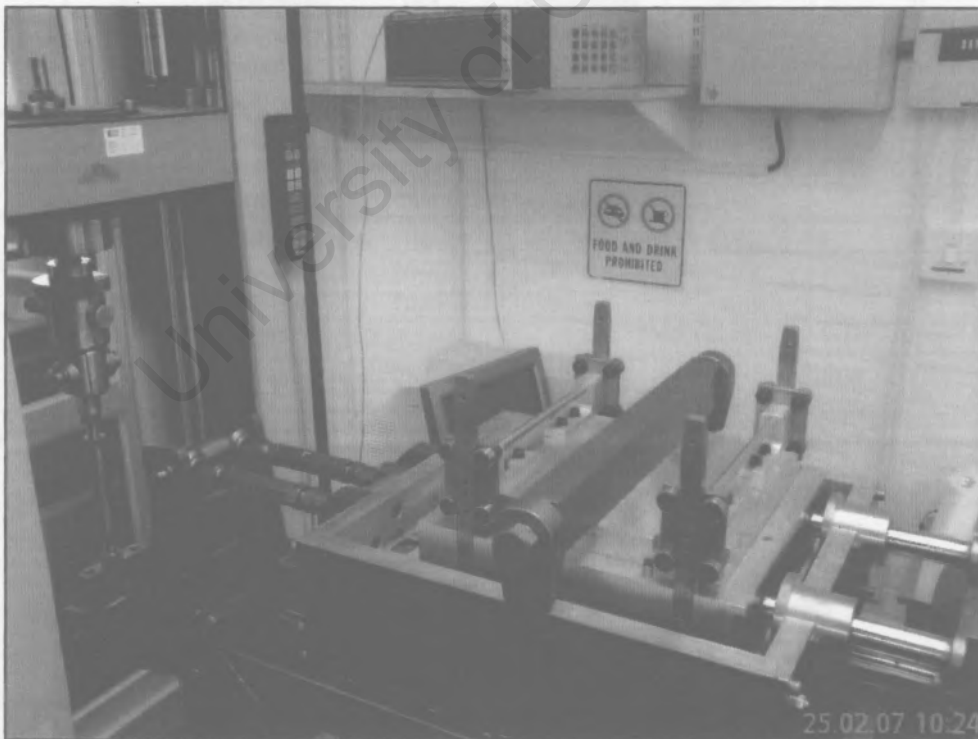


Figure 7.1 Large Direct Shear Device

7.2 Direct Shear Test Program

34 direct shear tests were conducted over a normal stress range of 25 kPa to 400 kPa. The values indicated in Table 7.1 are the peak normal stresses aimed at in the respective tests.

Table 7.1 Direct shear test program

Test interface	Test number	GCL condition	Sand condition	GCL Side	Normal Stress (kPa)	Hydration (min. period) (days)
Sand/Sand	1ss	N/A	NMC*	N/A	50	N/A
	2ss	N/A	NMC	N/A	200	N/A
	3ss	N/A	NMC	N/A	400	N/A
	4ss	N/A	Saturated	N/A	50	N/A
	5ss	N/A	Saturated	N/A	200	N/A
	6ss	N/A	Saturated	N/A	400	N/A
GCL Internal	1i	Saturated	N/A	N/A	125	4
	2i	Saturated	N/A	N/A	175	4
	3i	Saturated	N/A	N/A	225	4
GM/GCL	1	Saturated	N/A	Non-woven	25	4
	2	Saturated	N/A	Non-woven	50	4
	3	Saturated	N/A	Non-woven	100	4
	4	Saturated	N/A	Non-woven	200	4
	5	Saturated	N/A	Non-woven	400	4
	1d	as received	N/A	Non-woven	50	0
	2d	as received	N/A	Non-woven	200	0
	3d	as received	N/A	Non-woven	400	0
	11	Saturated	N/A	Non-woven	50	70
	21	Saturated	N/A	Non-woven	200	70
GMX/GCL	31	Saturated	N/A	Non-woven	400	70
	1x	Saturated	N/A	Non-woven	50	4
	2x	Saturated	N/A	Non-woven	200	4
GCL/Sand	3x	Saturated	N/A	Non-woven	400	4
	1gs	Saturated	NMC	Woven	50	4
	2gs	Saturated	NMC	Woven	200	4
GM/Sand	3gs	Saturated	NMC	Woven	400	4
	1s	N/A	Saturated	N/A	25	N/A
	2s	N/A	Saturated	N/A	50	N/A
	3s	N/A	Saturated	N/A	100	N/A
	4s	N/A	Saturated	N/A	200	N/A
	5s	N/A	Saturated	N/A	400	N/A
	6s	N/A	NMC	N/A	50	N/A
	7s	N/A	NMC	N/A	200	N/A
8s	N/A	NMC	N/A	400	N/A	

*Natural Moisture Content (NMC): $\pm 2.5\%$

Each test had a slightly different normal stress due to the variability of the loading system and the change in shear area due to the shear displacement. In fact, the normal stress range extended over 500kPa in some tests due to the area correction at large horizontal displacements. Six direct shear tests were conducted on the sand at its natural moisture content as well as in hydrated conditions. Internal shear strength tests of the GCL were run over a limited normal stress range due to the limitations of the gripping system for this type of GCL.

Fourteen of the tests involved the GCL/geomembrane interface. This included an investigation of the effect of the degree of hydration of the GCL on the shear strength as well as a study of the effects of a textured geomembrane. Three tests investigated the GCL/sand interface behaviour. The remaining tests were conducted on the geomembrane/sand interface. A prerequisite to all these tests were specific machine internal shear calibration tests (not shown in the table) for all test arrangements.

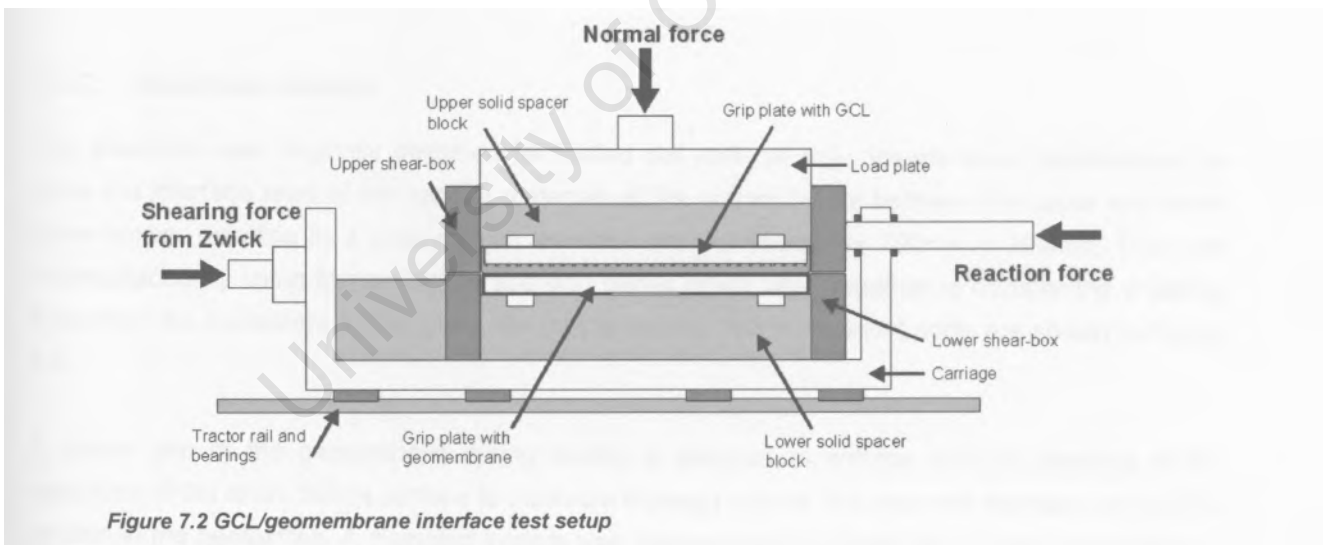
All the test set-ups, procedures and calculations are described in more detail in Appendix A.7.

7.3 Large Direct Shear Device

ASTM D 6243 and *ASTM D 5321* require a 300mm x 300mm shear area as standard for testing geosynthetic interfaces and GCL internal shear strength. Thus, a device of this magnitude was developed in the University of Cape Town Geotechnical Laboratory (see Figure 7.1). The internal dimensions of the shearbox were the specified 300mm x 300mm. This, however, meant that the interface was reduced in certain set-ups due to the components for gripping the geosynthetics being slightly smaller to fit within the shearbox. The size reduction was not substantial and the minimization of boundary effects was still accomplished with the resulting shear surface areas.

7.3.1 Apparatus

The rigid direct shear device consisted of both a stationary and moving shear-box, each with internal dimensions of 300 mm x 300 mm x 75 mm.



The shear force load is applied at a constant rate of horizontal displacement. A Zwick Universal Testing Machine was used for this function. A massive lever system was manufactured to convert the vertical movement of the Zwick machine into the horizontal displacement required by the shear device. The machine has a maximum load limit of 100kN and a test speed accuracy of 0.1% at 1 mm/min.

The normal stress loading system, consisting of a lever and pulley arrangement (as shown in Figure 7.3), maintained a relatively constant uniform normal stress, up to 600kPa, on the specimen for the

duration of the test. The normal force (up to 5 tons) on the specimen was determined using a loadcell connected to the bottom of the loading yoke. The weight pulley system was sensitive to sample movement, giving rise to minute changes in normal stress during testing, especially with the compressible hydrated bentonite in the GCL specimens. However, this was monitored throughout each test, thus, at instantaneous points in time, the normal stress could be accurately determined.



Figure 7.3 Normal stress loading system

7.3.2 Shear-box inserts

The shear-box was originally designed for testing soil material only. Inserts were manufactured to place the interface level of the various materials at the correct height between the upper and lower shear-boxes, resulting in a geosynthetic interface area of effectively 290mm x 290mm. This was accomplished by using spacer blocks and grip plates which fitted together to transfer the shearing force from the containers to the specimen during testing. The component parts are shown in Figure 7.4.

A proper grip of the geosynthetic during testing is required to enforce uniform shearing of the specimen of the entire failure surface to minimize slippage outside the intended interface and to limit tension in the geotextiles. A clamping system was incorporated to secure the ends of the specimen. Although no tests were conducted without these clamps, the gripping plates were observed to adequately hold the specimen and prevent progressive failure. These plates were also used to grip the geomembranes and found to be very effective at all normal stresses applied in the study.

Textured surfaces were used over the full shear surface area of the grip plate to prevent local displacements of the geosynthetic on the grip plate. The chosen rough surface was made of punctured stainless steel plates. The surface comprised 1.6 punctured holes per cm² with each punctured hole having four sharp points approximately 2mm high. The sharp points did not extend deeply into the geosynthetic so as to alter the interface behaviour of the geosynthetics. The plates to

which the rough surface was attached, had various holes to allow hydration and pore water pressure dissipation.

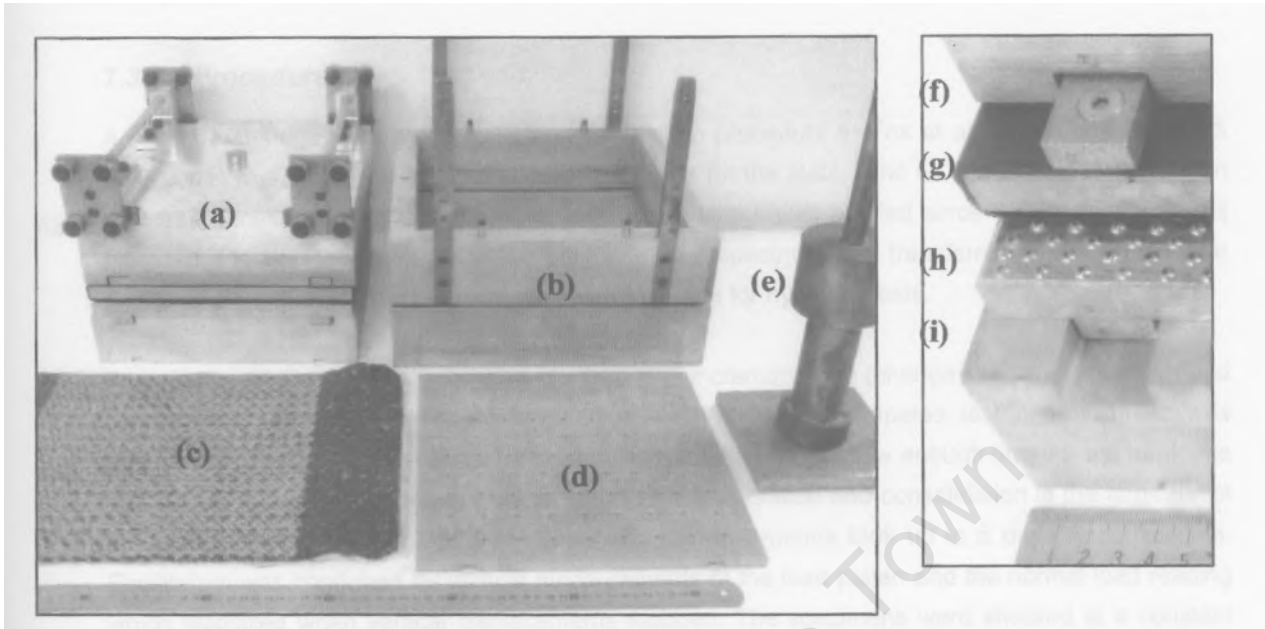


Figure 7.4 Component parts of the large direct shear box with inserts a) Vertically guided load plate b) Upper and lower shear-boxes c) GCL specimen d) Base plate for sand test e) Drop hammer f) Upper spacer plate g) Upper grip plate with geomembrane h) Lower grip plate showing textured surface i) Lower spacer plate

7.3.3 Shear device calibration

The direct shear device was calibrated to measure the internal resistance to shear caused by the mass of the travelling container, the bearings and shear loading system. Different calibration measurements were made for the different test conditions — dry, hydrated and hydrated with bentonite present.

7.3.4 Specimen preparation

The GCL was cut to dimensions of 46cm x 30cm. The specimen was placed with free access to water outside the shear machine with no normal stress for at least 48 hours. If the geomembrane was used, it was cut to dimensions of 59cm x 30cm. Holes were made for the clamping screws and the interface was cleaned with a moist soft cloth.

For the sand interface test the shear-boxes were screwed together before compacting the sand inside. A 4.533kg hammer was used, dropped from a height of 420mm onto a 151mm x 151mm stiff compaction plate. The sand was compacted in three layers (five blows per layer) into the shear-box at the required dry density and moisture content. For a sand/geosynthetic interface test the sand was compacted in two layers into the lower shear-box at the required dry density and moisture content to between 3 mm and 5.5mm above the shearing plane, depending on the normal stress for the test.

For the GCL/sand interface the sand was compacted at a lower moisture content ($\pm 0.5\%$) than the natural moisture content, since it would become more moist as water squeezed out of the GCL during consolidation.

7.3.5 Procedures

A similar two-stage GCL hydration and consolidation procedure to Fox et al. (1998) and Triplett & Fox (2001) was employed to reduce in-machine time for the tests. The GCL was hydrated in a pan with free access to water for two days. No normal stress was applied since the reinforcing fibres provided adequate confinement of the bentonite. The specimen was transferred to the direct shear device and the box flooded to above the shear interface for hydrated tests.

The specimen was incrementally loaded with a load increment ratio (change of normal stress divided by the previous normal stress) of approximately 1 until the anticipated test normal stress was reached. This was to avoid excessive bentonite extrusion and to allow enough time for the bentonite in the GCL to reach equilibrium. The minimum time of hydration and consolidation in the large direct shear device was 48 hours. Higher normal stress requirements took up to 5 days to consolidate. Equilibrium was confirmed by vertical measurements of the load platen and the normal load reading which stabilized when vertical displacements stopped. The specimens were sheared at a constant displacement rate of 1mm/min to a displacement of up to 70mm.

After shearing the specimens were removed, examined and at least five water content determinations of the bentonite undertaken. The test was repeated with at least three normal stress levels with newly prepared specimens.

7.3.6 Normal stress determination

The load cell was connected to a digital voltmeter with a five decimal place reading capability. The type of load cell was a Novatech 50kN load cell with a supply of 10V and zero balance reading of 1.8215mV/V. The normal stress, σ_n , was calculated as follows:

$$\sigma_n = (W_1 \times g + (V_1 - V_0) \times C) / A$$

where:

W_1 = dead weight, kg

g = gravitational acceleration, m/s²

V_1 = zero balance reading, mV

= voltmeter reading, mV

C = calibration factor, kN/mV

A = area of interface, m²

7.3.6 Analysis

For tests involving Philippi Dune sand and/or the GCL, the initial and final water content of the sand and bentonite was determined.

The difference between the recorded shear force and the internal shear correction of the machine was the actual shearing force applied to the specimen. Since the stationary and travelling containers have the same plan dimensions an area correction was applied to the shear as well as normal stress on the specimen (in accordance with ASTM D 6243) for each recorded shear force.

The limiting values of shear stress versus applied normal stress for each test conducted were calculated. These peak shear stress data points were connected with a best-fit straight line to define the peak failure envelope. In some cases a multi-linear envelope was more appropriate. The angle of friction and adhesion for the specific interface could then be determined. Additionally, the angle of friction was calculated based on shear stresses at some larger displacement or at the end of the test in order to determine the large displacement shear strength parameters.

University of Cape Town

CHAPTER 8

RESULTS, ANALYSIS AND DISCUSSIONS

8.1 Introduction

This chapter presents all the results of the GCL index tests and the direct shear tests of the various interfaces of the liner system. Each category of tests is presented and discussed in its own section.

8.2 Investigation of GCL property test results

The index test results are presented with a brief discussion of departures from the standard test method as well as the meaning of the results. The GCL batch obtained in 2006 (GCL A) was the focus of this study and is presented in more detail. The 2005 GCL batch (GCL B) was tested before this study and those results are only listed.

8.2.1 Peel Test

The graphical results of the index tests are shown in Figure 8.1. The 100mm displacement results range is between 25mm and 125mm.

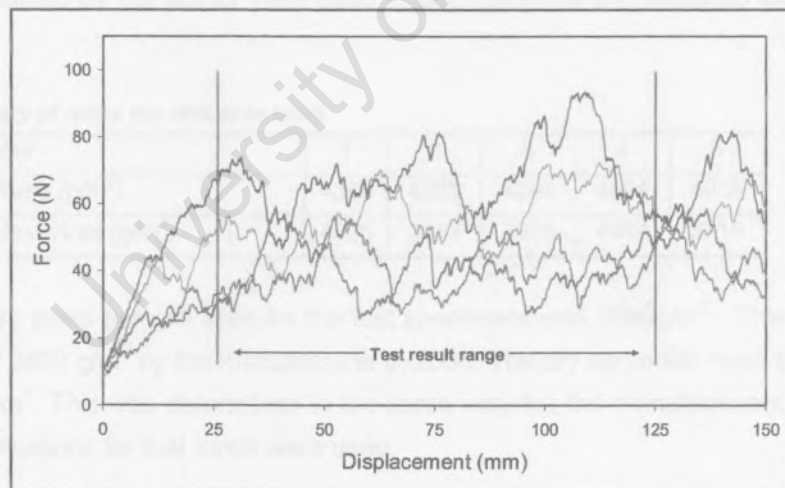


Figure 8.1 Summary of Peel Strength Tests for GCL A

The clamps held the geotextiles adequately and the results displayed a consistent pattern over the 100 mm test range. The average bonding peel strength of GCL A was 50 N/m, meeting the specification of 44 N/m by the manufacturer. GCL B had a higher peel strength of 97N/m.

Table 8.1 Summary of Peel Strength Tests for GCL A

Specimen Number	1	2	3	4	5
Average Peel Strength (N/m)	40.6	39.5	46.4	68.4	56.3

8.2.2 Swell Test

The granular bentonite of GCL A was ground to 71% passing the 200 sieve. Although the test method requires only one cylinder, five cylinders were prepared.

Table 8.2 Summary of Swell Tests of GCL A bentonite

Cylinder Number	1	2	3	4	5
Volume of Clay (ml)	31	31	31.5	32	30.5

The average swell index for GCL A bentonite after 16 hours of hydration was 30.5 ml/2g at a temperature of 22°C. GCL B had a much lower swell index of 23.5 ml/2g after the required hydration period.

8.2.3 Mass per unit area test

The nominal mass per unit area values of the geotextile components of GCL A were checked by carefully cutting, separating, measuring, cleaning and drying the synthetic components.

Table 8.3 Mass per unit area of synthetic components of GCL A

Synthetic Type	Woven	Non-woven
Dry Mass/Area (g/m ²) – Manufacturer	110	200
Dry Mass/Area (g/m ²)– Rouncivell	135	205

The results obtained by the author were used to determine the dry bentonite mass per unit area of GCL A.

Table 8.4 Summary of mass per unit area tests

Specimen Number	1	2	3	4	5
Dry GCL Mass/Area (g/m ²)	4366	4223	4245	4804	4055
Dry Bentonite Mass/Area (g/m ²)	4026	3883	3905	4464	3715

The average dry mass per unit area for the test specimens was 3999g/m². This meets the required specification of 3600 g/m² by the manufacturer in 2006. The dry bentonite mass per unit area of GCL B was 3560 g/m². This was determined in the same way but the manufacturers synthetic mass per unit area specifications for that batch were used.

8.2.4 Comparison of GCL batches

Even though GCL A and GCL B are the same GCL by trade name, certain of their characteristics vary considerably. Each project requires a certain specification but the manufacturer may change its materials and still meet most of those specifications in a cost effective manner. This emphasises the need to schedule the appropriate tests for each project and to choose the right GCL type from the outset.

Table 8.5 Summary of GCL characteristics

Characteristics	GCL A	GCL B
Peel strength (N/m)	50	97
Bentonite dry mass per unit area(g/m ²)	4000	3560
Woven geotextile (g/m ²)	135	115
Non-woven geotextile (g/m ²)	- 205	241
Swell (ml/2g)	31	23.5

The most relevant differences between GCL A and GCL B are the peel strength and swell properties of the bentonite. Higher peel strength has been shown to correlate to higher internal shear strengths by some authors including Fox et al. (1998). The swell potential may not only affect the permeability characteristics but also the moisture content of the bentonite at different compressive levels and its potential to increase interface slip behaviour.

8.3 Investigation of direct shear test results

The focus of this study was the shear strength characterisation of the GCL and various interfaces of a local liner system. The direct shear results are initially presented in the form of interface shear stress development versus horizontal displacement diagrams. Secondly, the relationship between interface shear stress and the applied normal stress for the peak and large displacement conditions are shown. Comparisons between the different interface results are made, including brief comparisons with results from certain researchers discussed in Chapter 4.

8.3.1 Shear stress – horizontal displacement relationship

The shear stress versus horizontal displacement relationships of all the interfaces tested are presented according to their test programs in Chapter 7. Depending on the interface investigated between three (the minimum requirement) and five tests at different compressive levels were conducted, each with newly prepared specimens. Other relationships, such as the displacement versus peak shear stress and the bentonite moisture content versus normal stress are also discussed.

Different test conditions are differentiated by the thickness of the test curve lines on the diagrams. Each successive curve with a higher peak shear stress is at a higher normal stress than the previous one, unless otherwise indicated. The curves on different diagrams cannot be directly compared because the normal stress was not exactly the same between tests at the same target normal stress range. The exact values of peak shear stress, displacement at peak shear stress and the normal stress level are listed in the accompanying tables.

8.3.1.1 GCL internal shear strength

Measurement of the internal shear strength requires effective gripping of both geotextiles of the GCL. GCL A was successfully tested between normal stresses of 131 kPa and 244kPa. The upper limit was due to the high compressibility of the GCL - the gripping plate teeth almost touched and sheared each other. The lower limit was determined as a result of the gripping plate teeth not adequately holding the woven side of the GCL where slipping subsequently occurred instead of inside the

specimen. The same limitations applied to GCL B, however since the internal shear strength was higher, tests below 200kPa normal stress could not be carried out successfully.

Table 8.6 Summary of GCL internal shear tests

GCL	Normal stress (kPa) at peak	Shear stress (kPa) at peak	Displacement (mm) at peak	Normal stress (kPa) at 60mm displacement	Shear stress (kPa) at 60mm displacement	Bentonite moisture content (%)
A	131	85	14	157	19	180.0
A	192	90	13	230	20	179.0
A	244	96	13.6	301	20	157.0
B	199	182	19.6	228	28	115.0
B	252	183	20.6	328	28	98.8

The failure plane was located at the woven geotextile / bentonite interface. Examination of the woven geotextile failure surface showed fibre pullout as the predominant failure mechanism for GCL A and fibre breakage for GCL B. The higher non-woven geotextile density of GCL B may contribute to more and longer fibres being punched and anchored in the woven geotextile resulting in higher shear strengths. The large displacement shear strengths for GCL A and B given in table 9.3 are relatively high. This is because at that limited displacement most of the fibres are still pulling out of the woven geotextile and through the bentonite itself.

Due to the closeness of the curves the normal stress at peak shear stresses are labelled on Figure 8.2 for clarity. The pre-peak shear strength reduction for each test is believed to be caused by the fibres within the hydrated bentonite tilting to one side and becoming taut before the shearing force is transferred directly to the GCL.

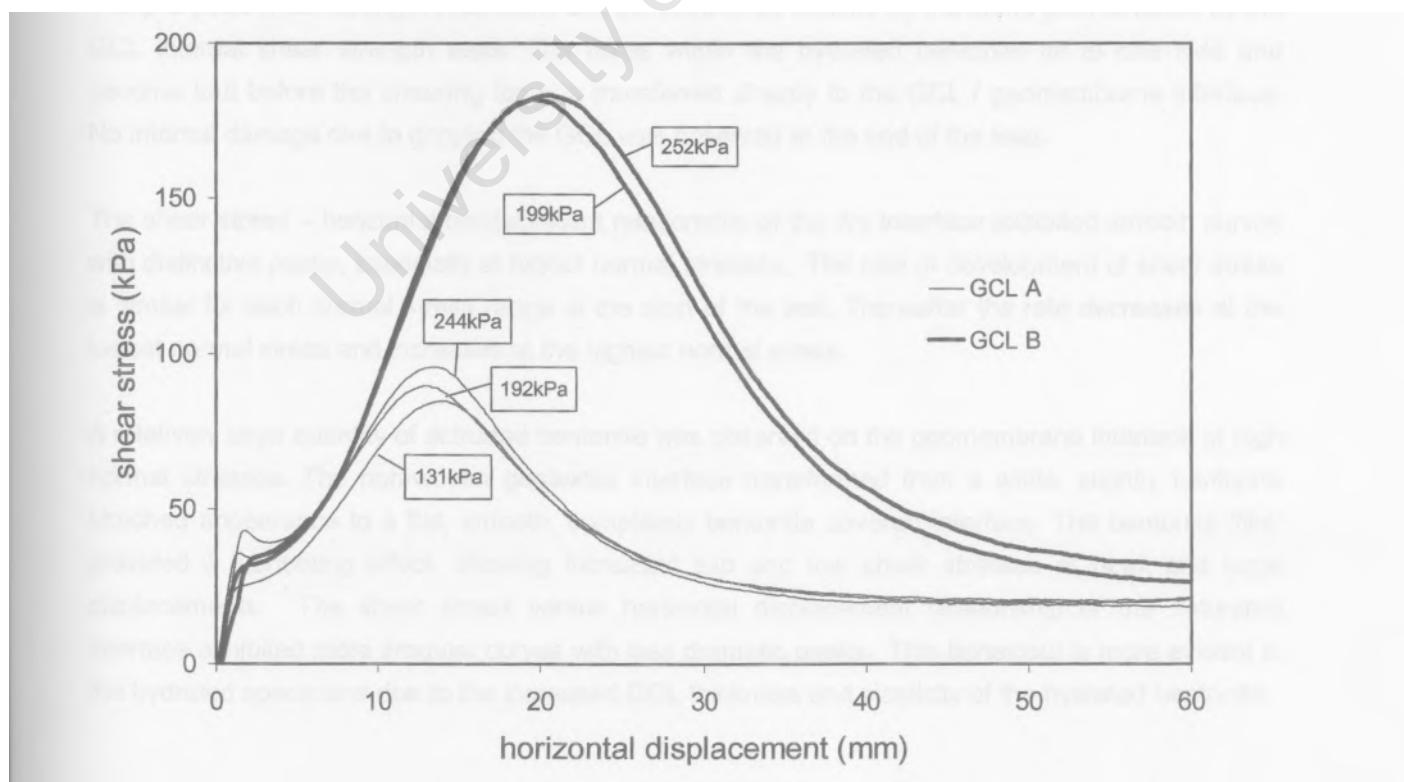


Figure 8.2 Shear stress versus horizontal displacement of the GCL internal interface at indicated peak normal stresses

8.3.1.2 GCL/smooth geomembrane interface

The smooth Geomembrane / GCL interface was investigated under two conditions. The in-situ "dry" state simulates the initial placement of the GCL. The other extreme, the hydrated condition, is considered more applicable as the critical test condition, due to hydrated bentonite providing a lubricating effect.

Table 8.7 Summary of GCL / smooth geomembrane shear tests

GCL condition	Shear stress		Normal stress (kPa) at 50mm displacement	Shear stress (kPa) at 50mm displacement	Bentonite moisture content (%)
	Normal stress (kPa) at peak	Displacement (mm) at peak			
In-situ	49	15	53	12	-
In-situ	215	69	251	51	-
In-situ	427	147	493	105	-
hydrated	26	8	33	8	236
hydrated	52	15	58	14	232
hydrated	107	31	125	30	211
hydrated	206	58	238	56	175
hydrated	433	115	494	87	141
Hydrated - long	50.95	16	63.9	15.8	237
Hydrated - long	218.5	61.2	257.9	57.4	163
Hydrated - long	450.3	120	571.3	96.7	115

Both saturated and dry tests showed dramatic softening after peak stress at higher normal stresses (see Figure 8.3). The in-situ moisture content tests displayed distinctive peaks at relatively small displacements. Stick and slip behaviour was observed at low normal stresses.

The pre-peak shear strength reductions are believed to be caused by the same phenomenon as the GCL internal shear strength tests. The fibres within the hydrated bentonite tilt to one side and become taut before the shearing force is transferred directly to the GCL / geomembrane interface. No internal damage due to gripping the GCL was observed at the end of the tests.

The shear stress — horizontal displacement relationship of the dry interface exhibited smooth curves with distinctive peaks, especially at higher normal stresses. The rate of development of shear stress is similar for each normal stress range at the start of the test. Thereafter the rate decreases at the lowest normal stress and increases at the highest normal stress.

A relatively large quantity of extruded bentonite was observed on the geomembrane interface at high normal stresses. The non-woven geotextile interface transformed from a white, slightly bentonite blotched appearance to a flat, smooth, completely bentonite covered interface. The bentonite 'film' provided a lubricating effect, allowing increased slip and low shear stresses at peak and large displacements. The shear stress versus horizontal displacement relationship of the saturated interface exhibited more irregular curves with less dramatic peaks. This behaviour is more evident in the hydrated specimens due to the increased GCL thickness and plasticity of the hydrated bentonite.

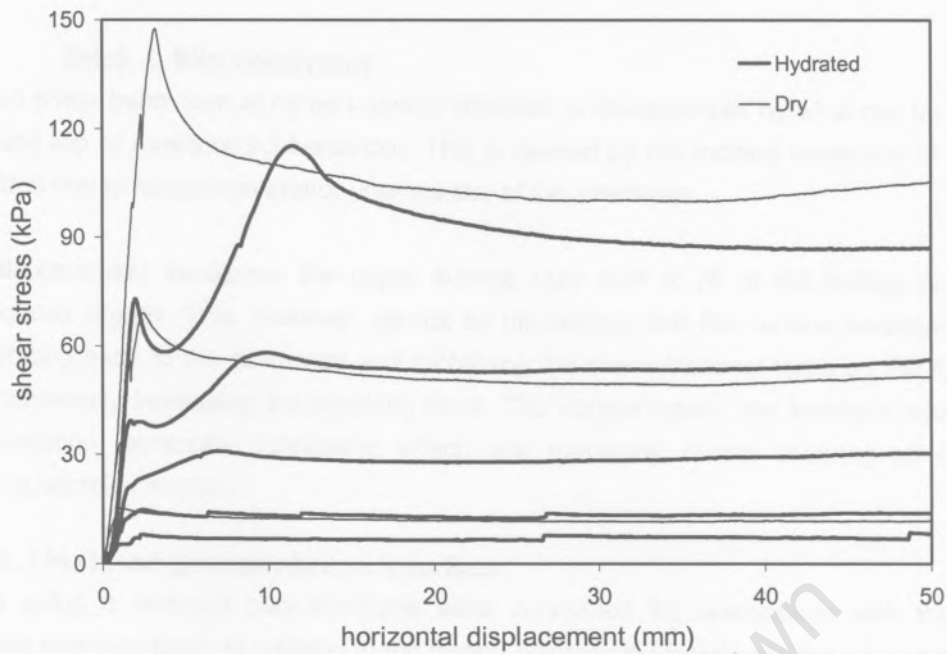


Figure 8.3 Shear stress versus horizontal displacement of the GCL / smooth geomembrane interface

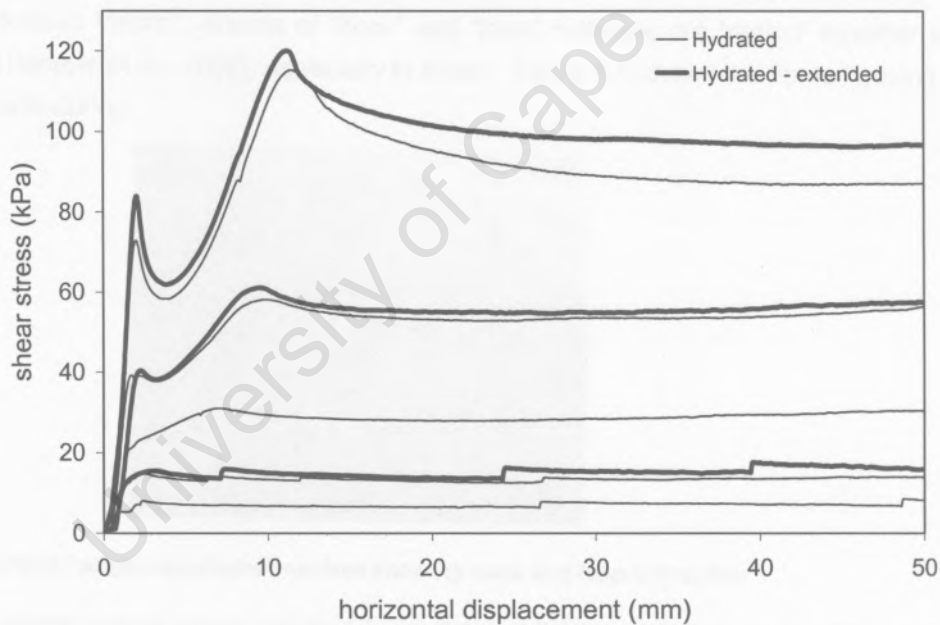


Figure 8.4 Shear stress versus horizontal displacement of the GCL / smooth geomembrane interface after long hydration periods

The effect of extended hydration of the bentonite on the interface behaviour was investigated by hydrating the GCL for 3 months before conducting tests between 50kPa and 400kPa normal stress (Figure 8.4). Although the test at the highest normal stress in the figure appears higher, it is noted that the normal stress was not exactly the same as the regular hydration test. No significant impact on the measured shear strength was observed.

8.3.1.2.1 Stick & Slip behaviour

The interface shear behaviour, at certain normal stresses, is characterized by what can be described as a stick and slip or saw-toothed behaviour. This is caused by the rocking behaviour of the upper shear interface due to roughness and/or unevenness of the interfaces.

As shear displacement increases, the upper surface may start to lift at the trailing end, i.e the specimen rotates slightly. This, however, cannot be maintained and the surface eventually slips at the front, rotating back to the horizontal and mobilizing the shear frictional force on the full contact area, instantaneously increasing the shearing force. The normal stress, the interface structure, the hydration condition, bentonite (lubricating effect) and damaging during shearing all affect this behaviour in a complex manner.

8.3.1.3 GCL / textured geomembrane interface

Three tests using a textured geomembrane were conducted for comparison with the smooth geomembrane interface tests. In addition to the friction between the interfaces, the structured surface interacts with the non-woven geotextile increasing the interface shear strength compared with the smooth geomembrane. This hook and loop interaction is most commonly associated with the commercial product Velcro®. Sheets of "hook" and "loop" materials are "mated" together to form a strong bond (Hebeler et al., 2005), especially in shear. Figure 8.5 shows the fibres hooking onto the geomembrane texturing.

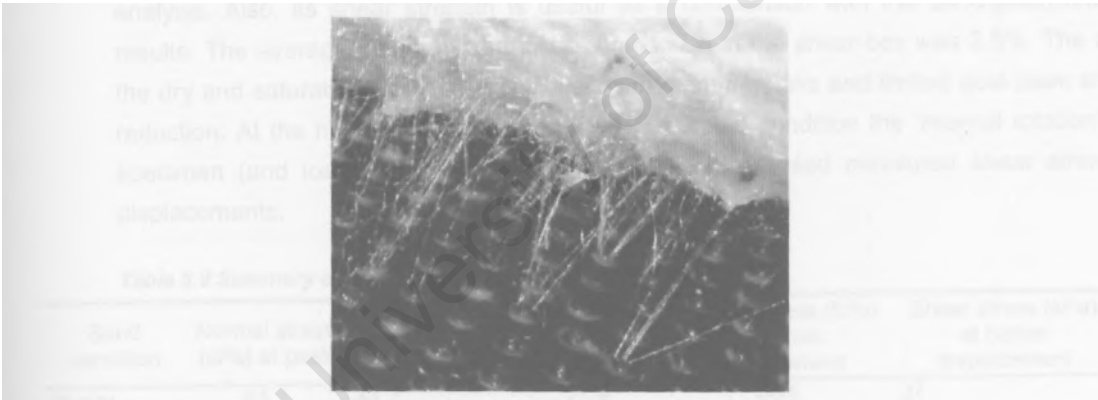


Figure 8.5 GCL/textured geomembrane interface showing hook and loop interaction

Tests above 36kPa normal stress resulted in partial or full internal failure of the GCL instead of a failure of the geomembrane / GCL interface. The curves are not smooth due to the irregular hook and loop behaviour. Post-peak softening is apparent, probably due to the damaged fibres after tearing away from the geomembrane texturing.

Table 8.8 Summary of GCL/textured geomembrane shear tests

GCL condition	Normal stress (kPa) at peak	Shear stress (kPa) at peak	Displacement (mm) at peak	Normal stress (kPa) at 50mm displacement	Shear stress (kPa) at 50mm displacement	Bentonite moisture content (%)
hydrated	11.72	10.9	10.06	13.72	9.7	290
hydrated	20	15.8	6.19	24.08	14.4	268
hydrated	35.57	25.9	11.2	37.38	24	255

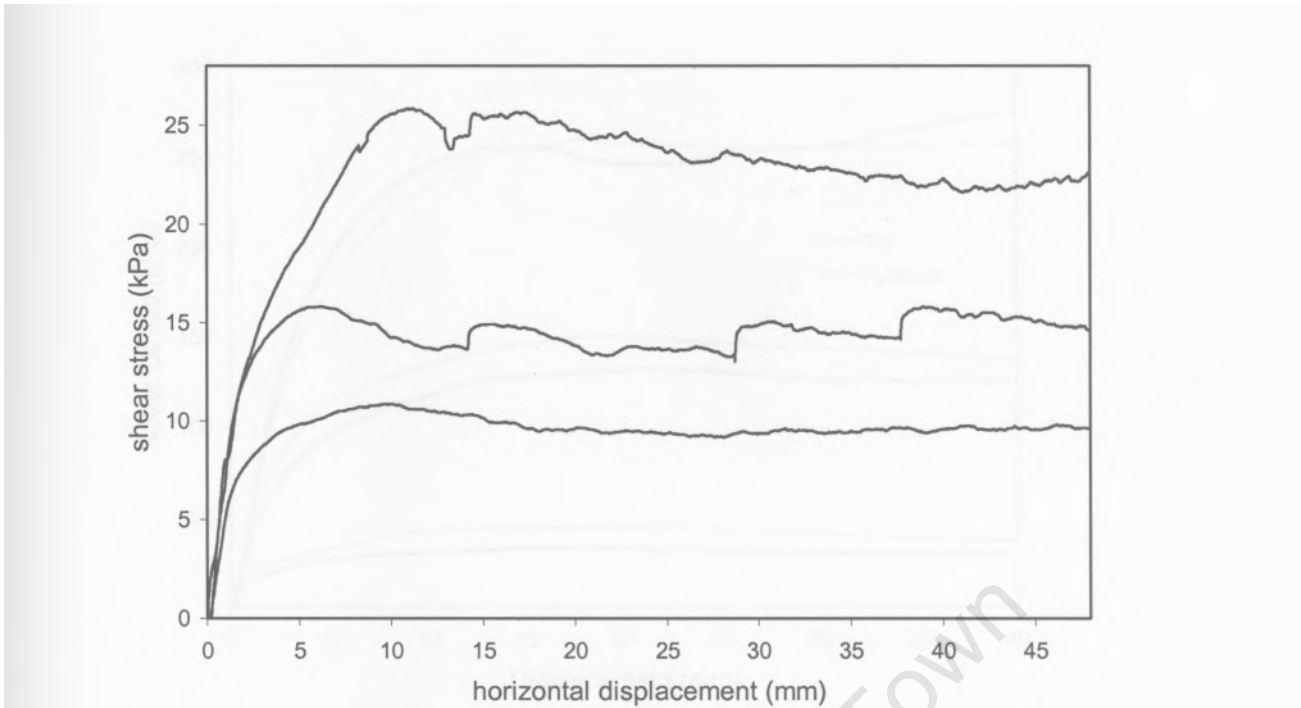


Figure 8.6 Shear stress versus horizontal displacement of the GCL textured geomembrane interface

8.3.1.4 Sand

Shear failure of the lightly compacted sand may be a factor to consider in the liner system safety analysis. Also, its shear strength is useful as a comparison with the sand/geosynthetic interface results. The average moisture content at compaction in the shear-box was 2.5%. The responses of the dry and saturated condition are similar, with gradual peaks and limited post-peak shear strength reduction. At the highest normal stress in the saturated condition the 'internal rotation' of the sand specimen (and load platen) was large resulting in increased measured shear strength at large displacements.

Table 8.9 Summary of sand shear tests

Sand condition	Normal stress (kPa) at peak	Shear stress (kPa) at peak	Displacement (mm) at peak	Normal stress (kPa)	Shear stress (kPa)	Dry density at compaction (kg/m ³)
				at 50mm displacement	at 50mm displacement	
In-situ	55.7	44.2	21.9	56.6	37	1518
In-situ	201.7	150.2	19.2	208.1	137.3	1515
In-situ	394.9	260.8	18.1	406.2	257.8	1519
Hydrated	45.9	32.9	15.9	45.6	30.4	1510
Hydrated	193.5	151.1	19.2	192.3	127	1509
Hydrated	393.7	255.5	13.5	393.9	255	1512

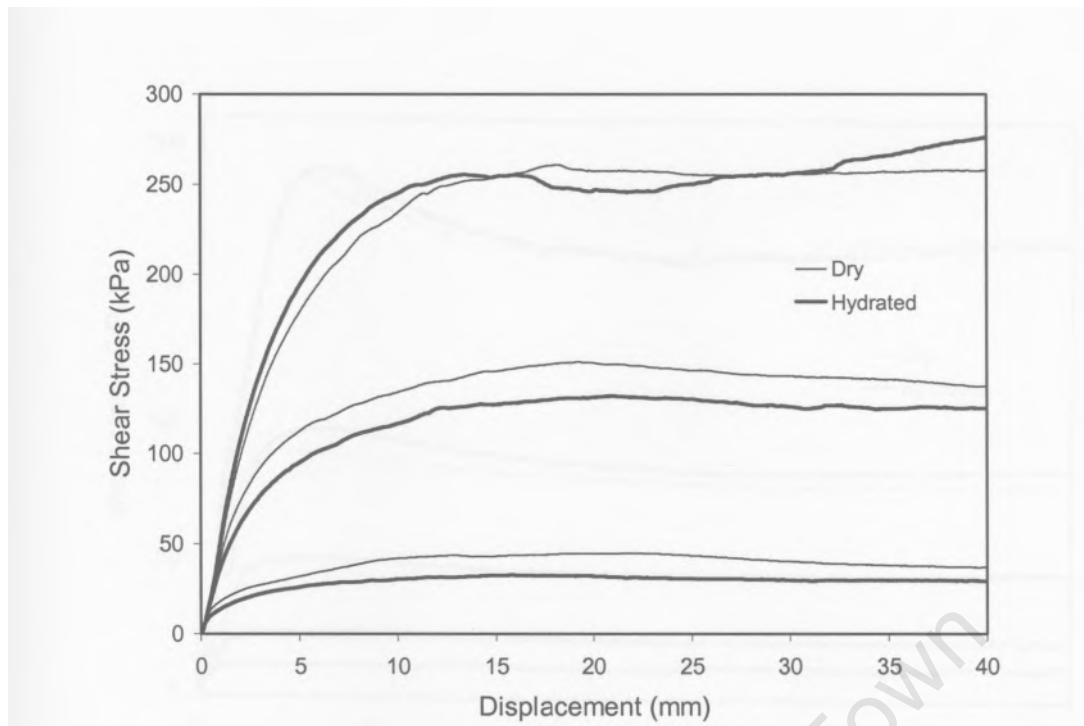


Figure 8.7 Shear stress versus horizontal displacement of the tests on sand

8.3.1.5 Geomembrane / sand interface

The geomembrane / sand interface was investigated in the natural moisture content ("dry") and hydrated state. The average moisture content at compaction in the lower shear-box was 2.5%. The rate of development of shear stress increases with increasing normal stress at the start of the test, leading to gradual peaks (see Figure 8.8). Stick and slip behaviour occurred only at the 25kPa normal stress. Sudden and short lived drops in shear stress were observed before reaching peak stress for both test conditions. It is believed that the lightly compacted sand grains re-orientate - "seat" - themselves due to shear displacement. Post-peak shear strength softening generally increased with increasing normal stress.

Table 8.10 Summary of geomembrane /sand shear tests

Sand condition	Normal stress (kPa) at peak	Shear stress (kPa) at peak	Displacement (mm) at peak	Normal stress (kPa)	Shear stress (kPa)	Dry density at compaction (kg/m ³)
				at 50mm displacement	at 50mm displacement	
In-situ	52.72	21.2	4.19	51.6	21.5	1513
In-situ	221.8	89.6	4.78	232.25	78.5	1521
In-situ	432.88	189.2	5.48	471.28	169.3	1518
Hydrated	29.14	11.9	4.1	29.8	12.4	1496
Hydrated	54.87	24.2	9.26	55.55	21.6	1504
Hydrated	113.68	50.2	5.89	118.19	46	1505
Hydrated	221.23	92.6	6.82	235.5	84.2	1499
Hydrated	436.14	192.3	6.4	468.07	166.2	1511

The dry interface tests exhibit similar behaviour to the saturated tests except there are slightly more accentuated peaks and stick and slip at the maximum normal stress. Particle crushing and geomembrane damage probably contribute to the bigger post-peak softening at high normal stresses. Significant damage to the geomembrane was observed and is discussed in Section 8.3.1.8.

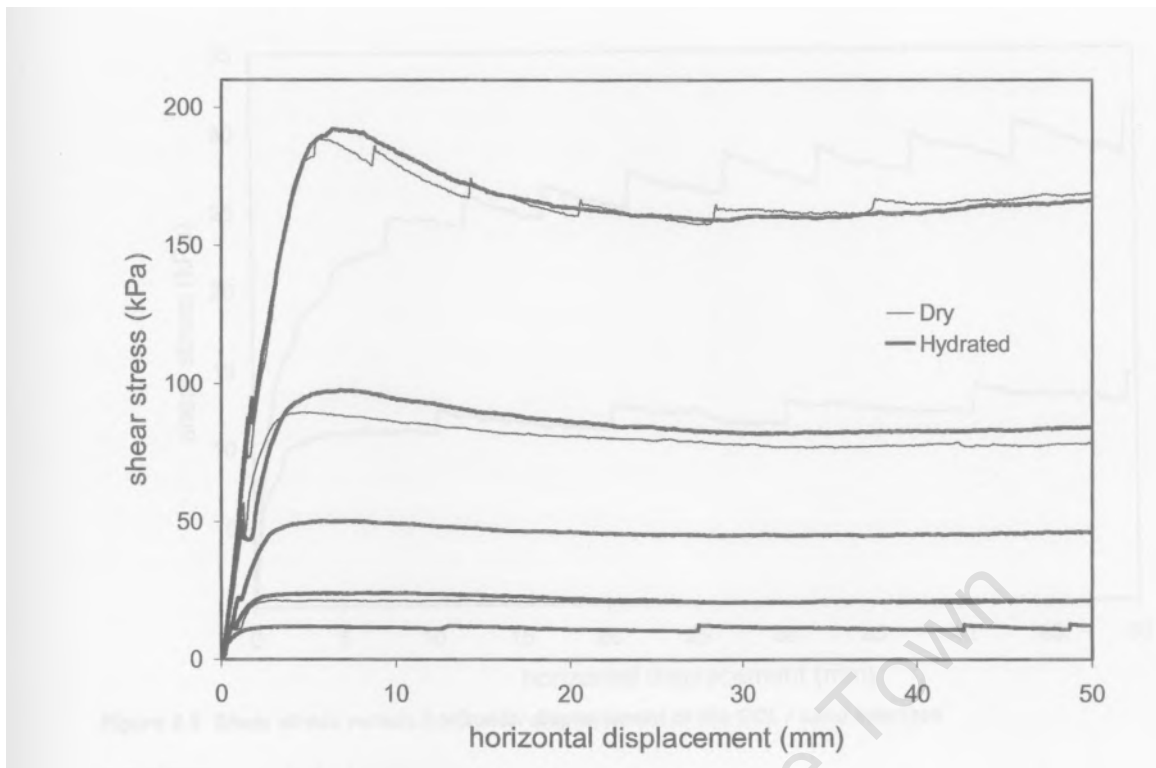


Figure 8.8 Shear stress versus horizontal displacement of the geomembrane / sand interface

8.3.1.6 GCL / sand interface

These interface behaviour are characterised by no post-peak shear strength softening as well as repeated stick and slip behaviour (see Figure 8.9). The probable reasoning is that the woven geotextile and sand interface is relatively uneven and soft allowing relatively easy rotation along the interface.

Table 8.11 Summary of GCL / sand shear tests

GCL condition	Normal stress (kPa) at peak	Shear stress (kPa) at peak	Displacement (mm) at peak	Normal stress (kPa) at 38mm	Shear stress (kPa) at 50mm	Bentonite moisture
Hydrated (1)	20.97	11.2	8.99	23.1	14.3	241
Hydrated (2)	45.47	25	45.8	55	31	236

Table 8.12 Summary of sand properties of the GCL / sand shear tests

GCL condition	Soil properties at compaction		Sand moisture content after	
	Moisture content %	Dry Density (kg/m ³)	Deep sample	Surface sample
Hydrated (1)	1.6	1501	3	6.7
Hydrated (2)	1.4	1497	3.9	6.1

Tests at normal stresses higher than 45kPa resulted in partial or full internal failure of the GCL. Although the moisture content at the compaction of the sand was kept to a minimum there is an increase in the sand moisture content due to the fact that as the hydrated GCL is placed on top of the sand consolidation water is expelled. Sand samples taken on the surface of the interface, as apposed to a dug out sample, showed higher moisture contents due to close proximity with the GCL.

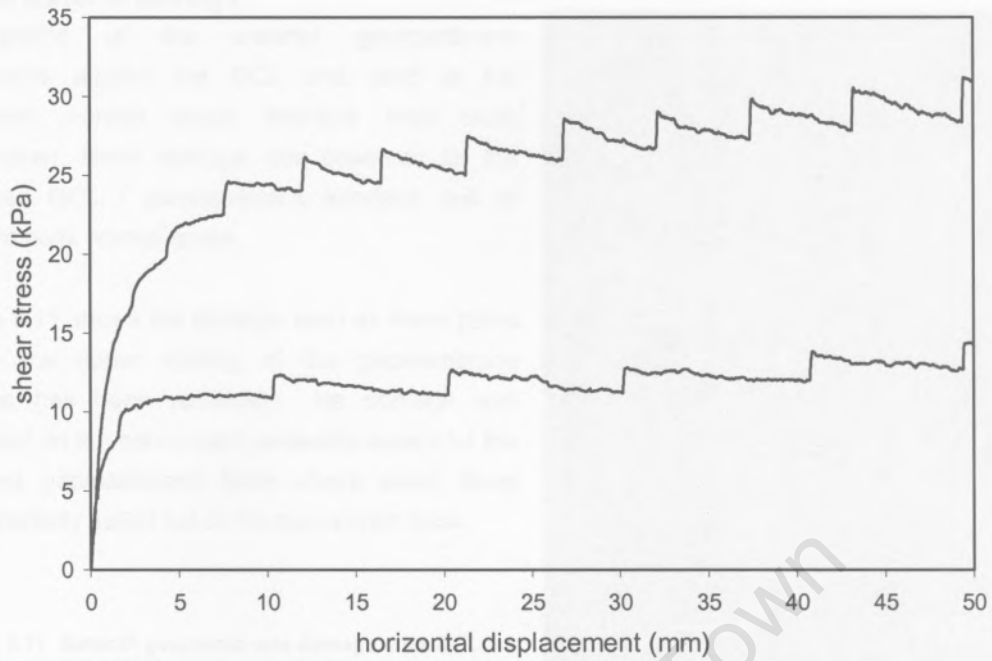


Figure 8.9 Shear stress versus horizontal displacement of the GCL / sand interface

8.3.1.7 Pre-peak behaviour

The initial shear stress reduction before reaching peak conditions is due to the tilting and reorientation of the needle-punched fibres before full tensioning begins. Figure 8.10 shows the normal stress shear stress relationship of this pre-peak shear strength reduction.

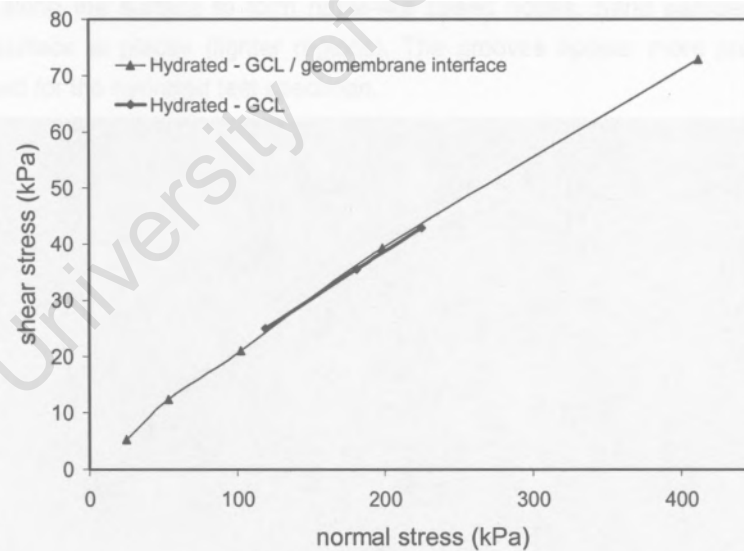


Figure 8.10 Normal stress versus shear stress relationship of the pre- peak shear stress reduction of the GCL and GCL /smooth geomembrane interface

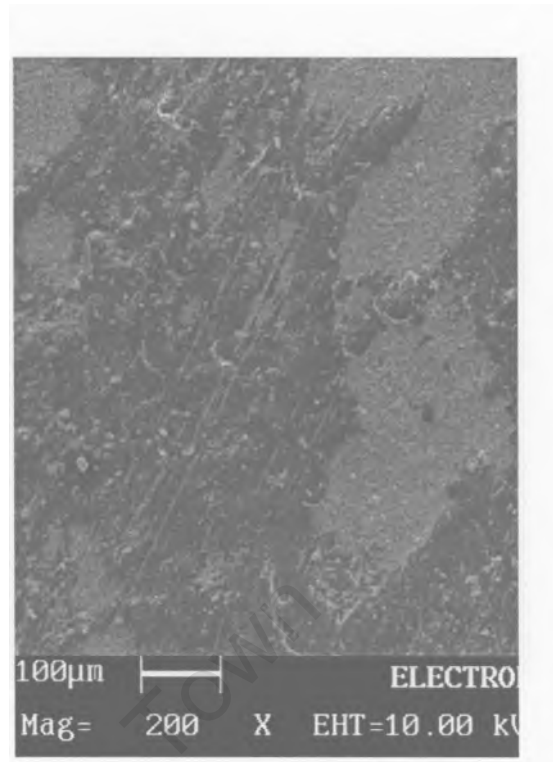
The diagram, shown in Figure 8.10, can be interpreted as a failure envelope for minor "internal failures" in the material before reaching full shear stress mobilisation. This relationship can be linearly approximated; the gradient of the GCL and GCL / geomembrane interface pre-peak reductions are 10° . This is approximately twice the shear strength of bentonite.

8.3.1.8 Material damage

Micrographs of the sheared geomembrane specimens against the GCL and sand at the maximum normal stress interface tests were undertaken. Minor damage was observed for the hydrated GCL / geomembrane interface test at 433kPa peak normal stress.

Figure 8.11 shows the damage seen as linear paths where the upper coating of the geomembrane surface has been removed. No damage was apparent on the non-woven geotextile except for the textured geomembrane tests where some fibres were partially pulled out of the non-woven mass.

Figure 8.11 Smooth geomembrane damage after GCL interface test at 433kPa peak normal stress



The dry and hydrated smooth geomembrane / sand interface tests displayed similar damage patterns in the shearing direction (see Figure 8.12 a) and b)). Scraping and rolling behaviour of the sand particles against the geomembrane results in long grooves of varying depths. The HDPE material is also displaced along the surface to form ripple-like raised ridges. Sand particles also pierce and adhere to the surface at places (lighter regions). The grooves appear more pronounced and the ridges less jagged for the hydrated test specimen.

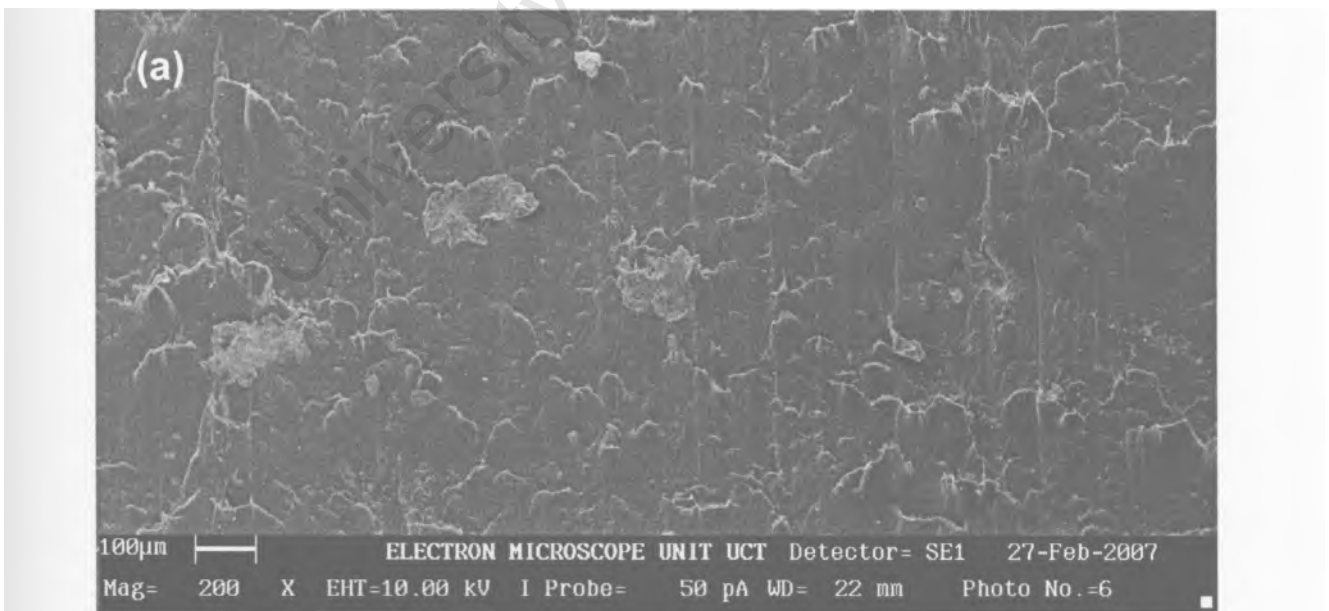


Figure 8.12 a) Geomembrane damage after dry sand interface test (433kPa peak normal stress)

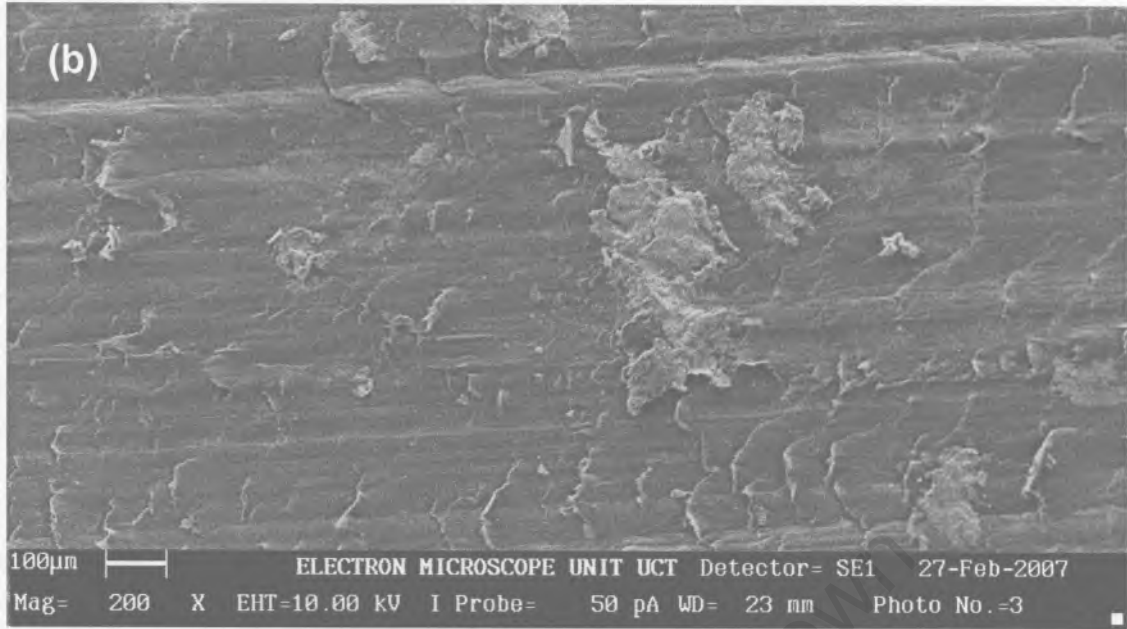


Figure 8.12 b) Geomembrane damage after hydrated sand interface test (436kPa peak normal stress)

8.3.1.9 Displacement at peak

The displacement at peak shear strength is important as it shows the displacement at which shear strength reduction will begin in the field at a specific normal stress. This relationship can be irregular due to minor specimen variations and sample preparation.

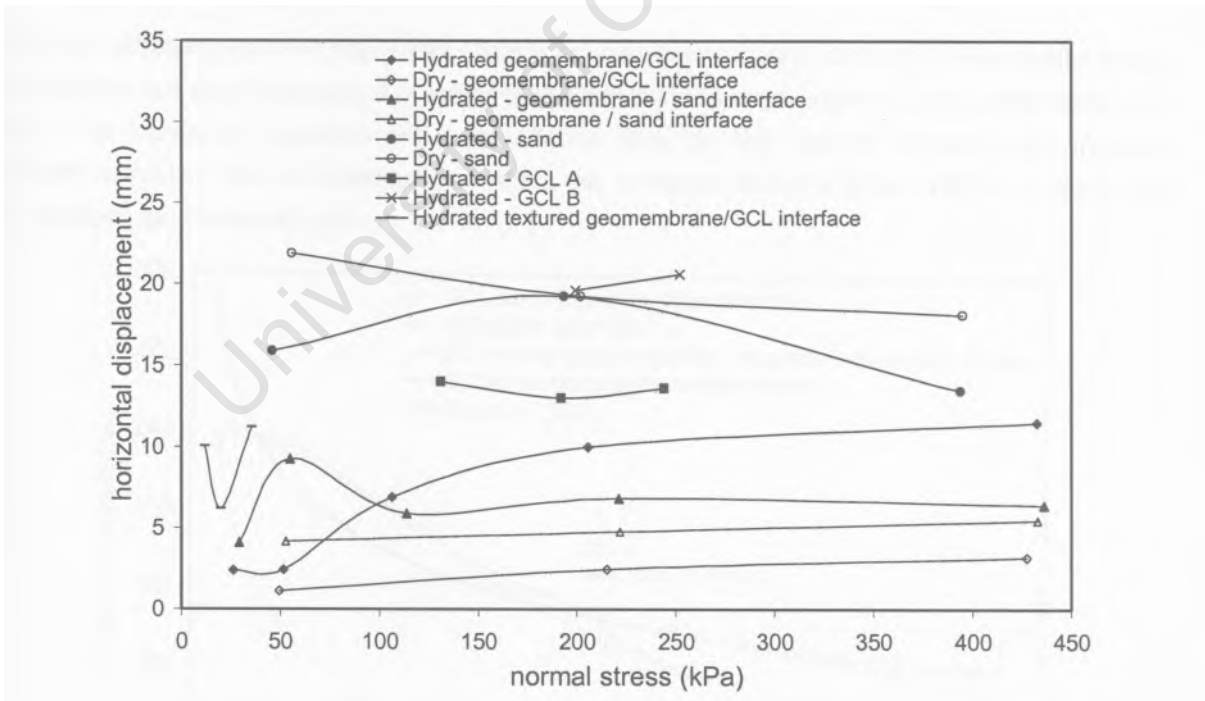


Figure 8.13 Displacement versus normal stress at peak shear stress conditions of all investigated interfaces

In sand the largest displacements are required to reach peak conditions. This is due to the relatively thick layer of sand of the enforced failure plane which is progressively mobilized as opposed to a thin

interface. The GCL itself also requires above 10mm to reach peak shear strength. The fibre pullout and stretch behaviour depends on the fibre length and stiffness. GCL B requires larger displacement due to higher shear strength. The textured geomembrane/GCL interface shows an erratic relationship due to the irregularity of the 'hook and loop' behaviour. The other interfaces display a general increase of displacement with increasing normal stress.

8.3.1.10 Bentonite moisture content

The bentonite as received from site had a moisture content of 17%. The average moisture content of the bentonite after a minimum of 48 hours hydration outside the machine was 540% for all interface tests incorporating the GCL. A slightly higher moisture content of 582% was recorded for the long hydration specimens.

The swell index indicates the capacity for water absorption of the bentonite and therefore the type of bentonite affects the final water content of the specimens. All shear tests conducted with GCL A show the same trend (see Figure 8.14). This relationship (between 10kPa and 430kPa normal stress) can be approximated by a power law regression:

$$w_f = 464 \sigma_n^{-0.1867}$$

where: w_f is the water content after shear failure and σ_n is the normal stress at peak.

Extended hydration (up to 90 days) may slightly increase the moisture content of the bentonite before consolidation but also increases the ability of the bentonite to expel water during compression and shear. The increased hydration and consolidation time for high normal stresses may increase bentonite extrusion onto the interface and affect the measured shear strength. Higher swelling may also increase bentonite extrusion.

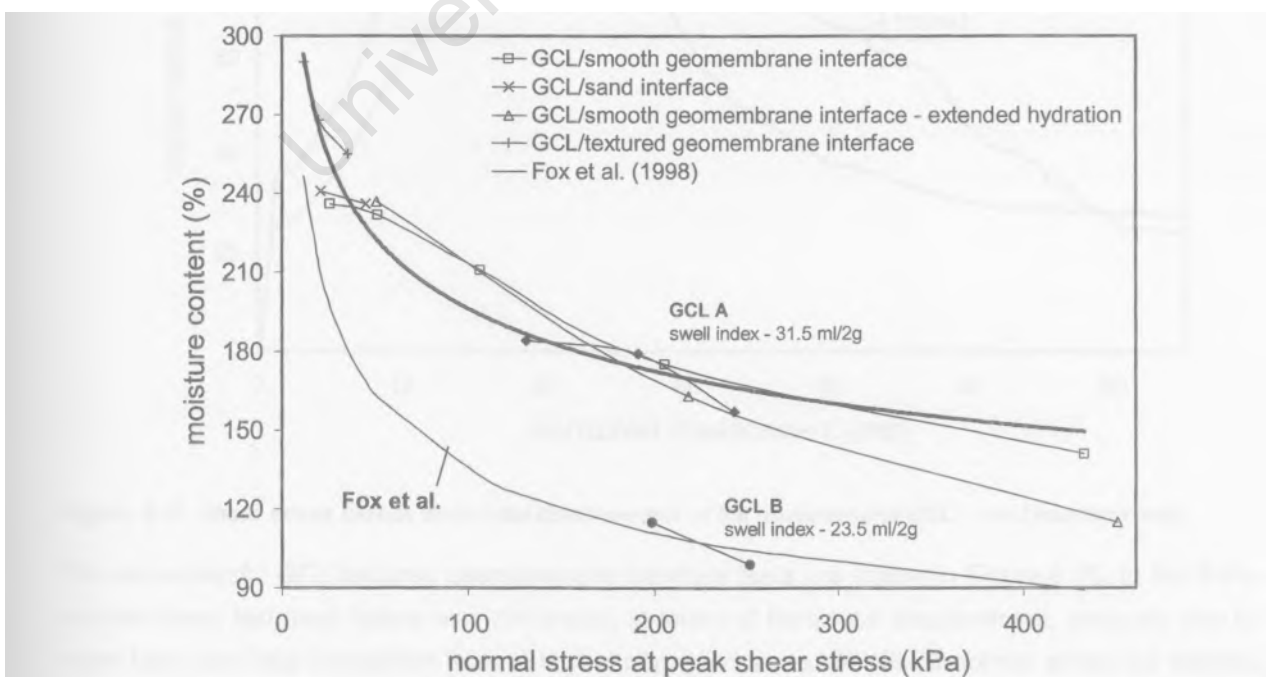


Figure 8.14 Bentonite moisture contents after direct shear interface tests.

The observed higher moisture content of GCL A, compared with GCL B, after shearing may contribute to lower shear strength due to the fact that the fibres are more lubricated thus pullout more easily.

8.3.1.11 'Unique' tests

Not all the interface tests were successful in the sense that they produced the classical result on the intended interface. In certain tests failure occurred at an interface not intended by the set up and yielded different information regarding the behaviour of the materials.

Table 8.13 Summary of unsuccessful shear tests

GCL contact material	Normal stress (kPa) at peak	Displacement at peak (mm)	Bentonite moisture content (%)	Comments
Cape Flats sand	107.46	48.6	196	Partial failure in GCL
<u>Cape Flats sand</u>	<u>222.2</u>	<u>17.5</u>	<u>162</u>	<u>Failure in GCL</u>
Textured geomembrane	7.7	42	290	Damaged geomembrane
Textured geomembrane	48.6	17.5	261	Failure in GCL

Figure 8.15 shows the GCL/sand interface tests. At a normal stress of 107kPa the woven geotextile failed in tension, accumulated in the opposite direction of shear, and allowed internal failure of GCL. This internal failure began at 38mm; thus the more irregular graph after this displacement. At 222kPa the GCL failed internally from the outset.

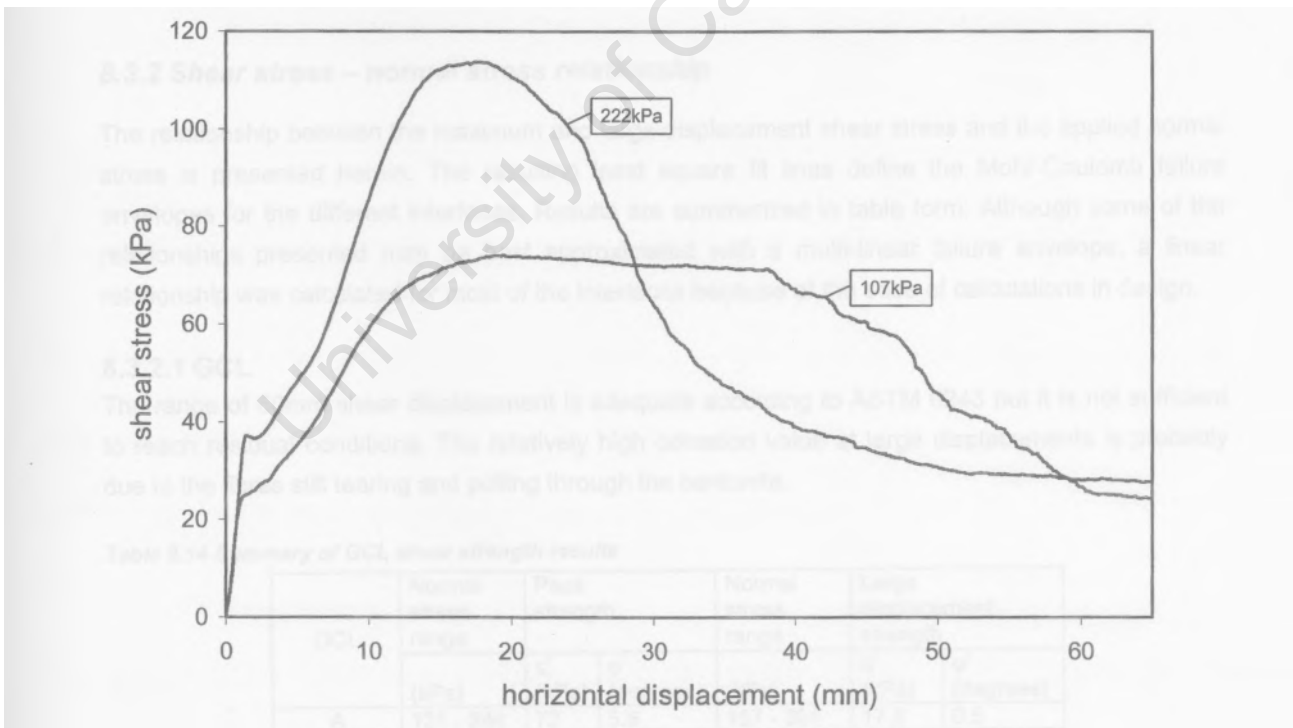


Figure 8.15 Shear stress versus horizontal displacement of the unsuccessful GCL / sand interface tests

The unsuccessful GCL/textured geomembrane interface tests are shown in Figure 8.16. In the 8kPa normal stress test peak failure was prolonged, in terms of horizontal displacement, probably due to more hook and loop interaction than at higher normal stresses. At 49kPa normal stress full internal failure of the GCL occurred.

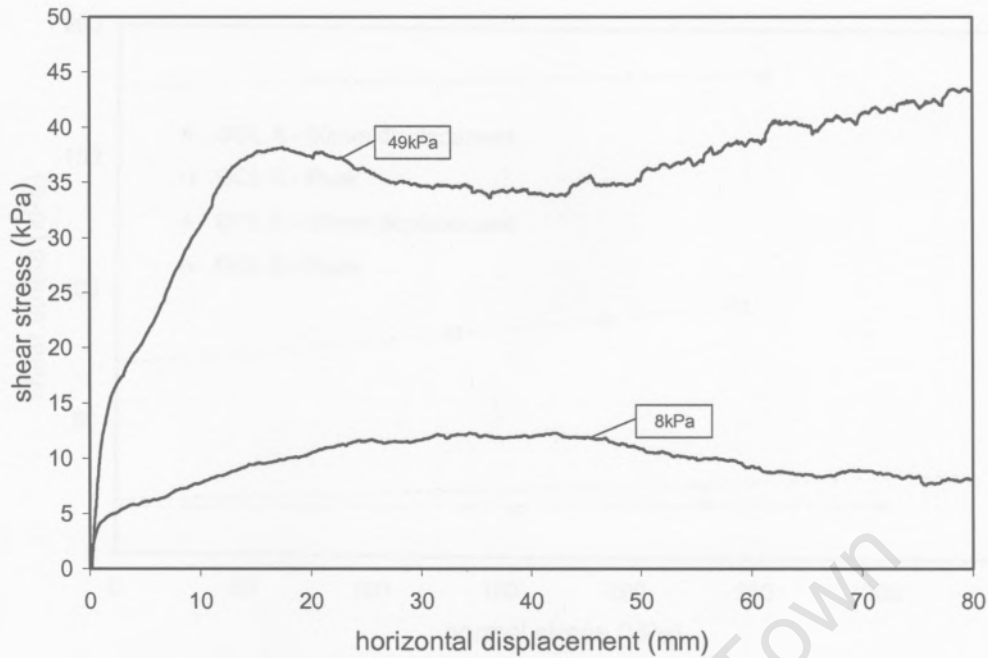


Figure 8.16 Shear stress versus horizontal displacement of the unsuccessful GCL / textured geomembrane interface tests

The peak and large displacement failure shear stress may not be a true reflection of either interface due to a partial failure scenario.

8.3.2 Shear stress – normal stress relationship

The relationship between the maximum and large displacement shear stress and the applied normal stress is presented herein. The resulting least square fit lines define the Mohr-Coulomb failure envelopes for the different interfaces. Results are summarized in table form. Although some of the relationships presented may be best approximated with a multi-linear failure envelope, a linear relationship was calculated for most of the interfaces because of the ease of calculations in design.

8.3.2.1 GCL

The range of 60mm shear displacement is adequate according to ASTM 6243 but it is not sufficient to reach residual conditions. The relatively high cohesion value at large displacements is probably due to the fibres still tearing and pulling through the bentonite.

Table 8.14 Summary of GCL shear strength results

GCL	Normal stress range	Peak strength		Normal stress range	Large displacement strength	
	(kPa)	c' (kPa)	ϕ' (degrees)	(kPa)	c' (kPa)	ϕ' (degrees)
A	131 - 244	72	5.6	157 - 301	17.5	0.5
B	199 - 252	196	1.6	228 - 328	20	2

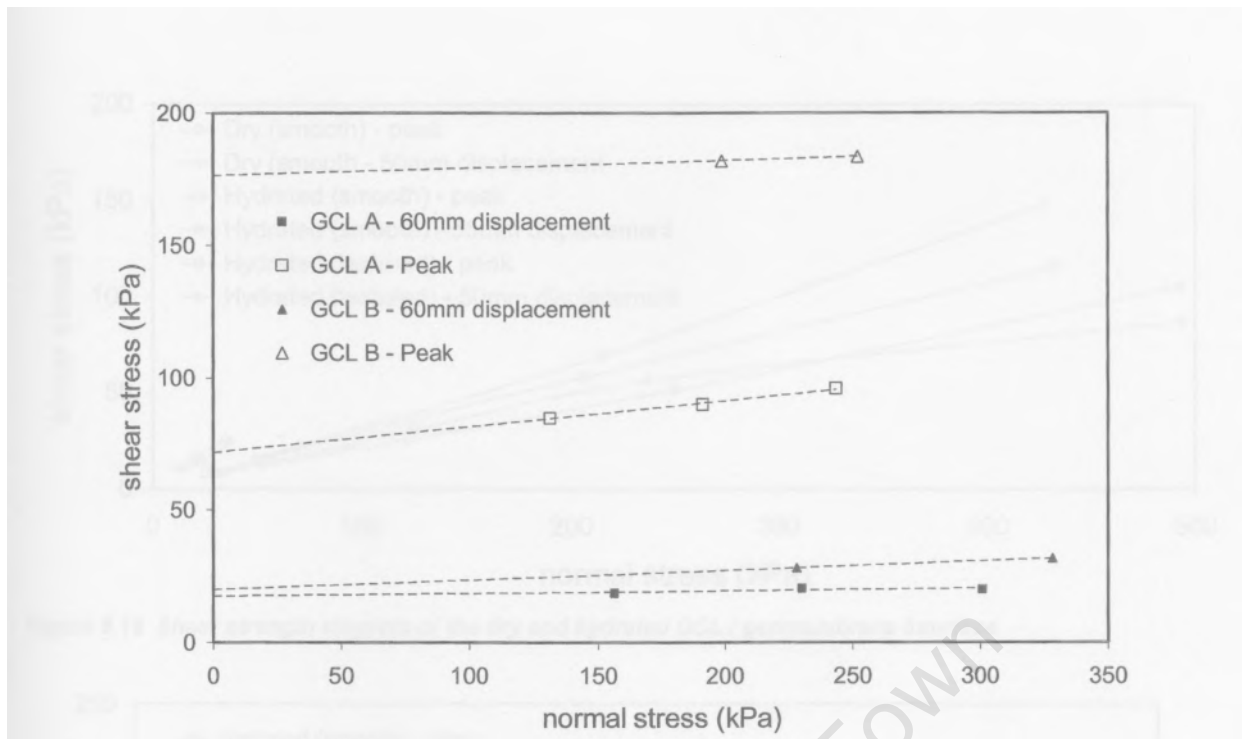


Figure 8.17 Shear strength diagram of GCLs

8.3.2.2 GCL / geomembrane interface

Table 8.15 Summary of GCL / geomembrane shear strength results

Interface condition	Normal stress range (kPa)	Peak strength		Normal stress range (kPa)	Large displacement strength	
		c' (kPa)	(ϕ') (degrees)		c' (kPa)	(ϕ') (degrees)
Dry	49 - 427	0	18.7	53 - 494	0	12
Hydrated	26 - 432	2.1	14.8	33 - 238	0.5	13.3
				238 - 494	28	6.8
Hydrated - extended	51 - 450	3.3	14.6	64 - 258	2.1	12.1
				258 - 571	25	7.1

The relationship for the geomembrane / GCL interface, where significant softening occurs at higher normal stresses necessitates a bi-linear approximation. Above 240kPa normal stress the friction angle drops to 6.8°. This is due to the extrusion of bentonite at higher normal stresses.

Table 8.16 Summary of GCL / textured geomembrane shear strength results

Interface condition	Normal stress range (kPa)	Peak strength		Normal stress range (kPa)	Large displacement strength	
		c' (kPa)	(ϕ') (degrees)		c' (kPa)	(ϕ') (degrees)
Hydrated	12 - 36	3.3	32.2	14 - 38	0.7	31.3

No significant shear strength difference between the regular and long hydration tests was observed (see Figure 8.19).

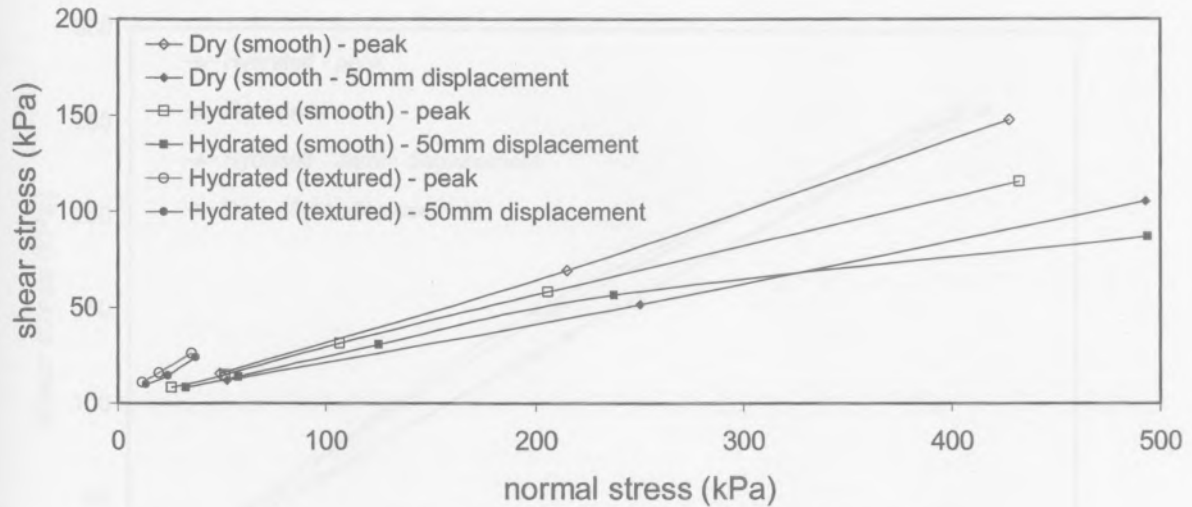


Figure 8.18 Shear strength diagram of the dry and hydrated GCL / geomembrane interface

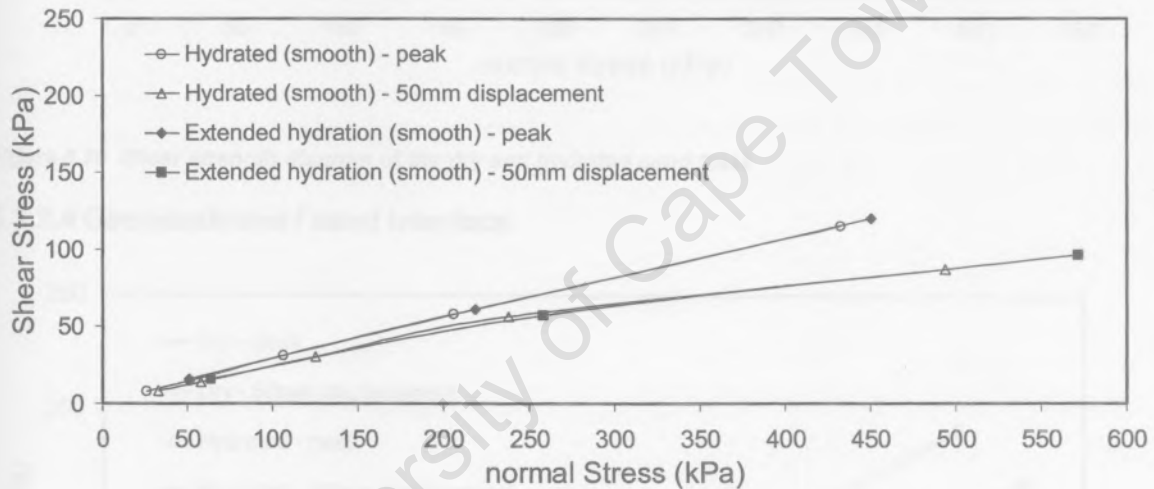


Figure 8.19 Shear strength diagram of the GCL / geomembrane interface investigating extended hydration

8.3.2.3 Sand

Table 8.17 Summary of sand shear strength results

Sand condition	Normal stress range	Peak strength		Normal stress range	Large displacement strength	
	(kPa)	c' (kPa)	ϕ' (degrees)	(kPa)	c' (kPa)	ϕ' (degrees)
Dry and hydrated	30 - 436	3.8	34	30 - 470	3.0	32

No significant difference between the dry and hydrated shear strength results was observed.

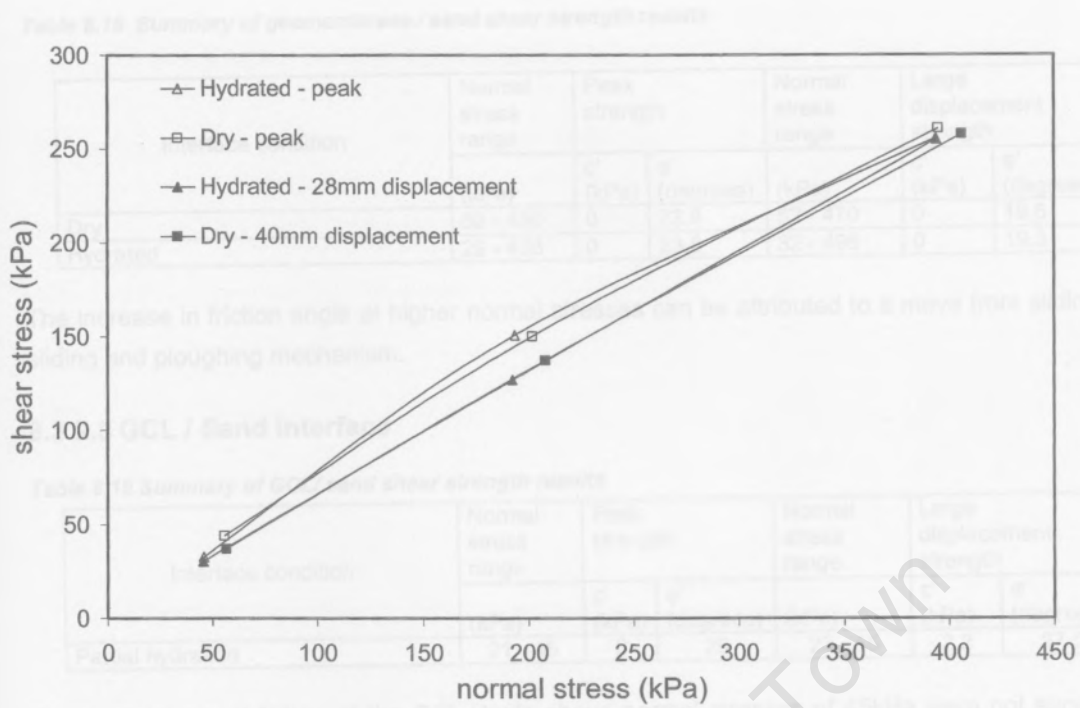


Figure 8.20 Shear strength diagram of the dry and hydrated sand tests

8.3.2.4 Geomembrane / sand Interface

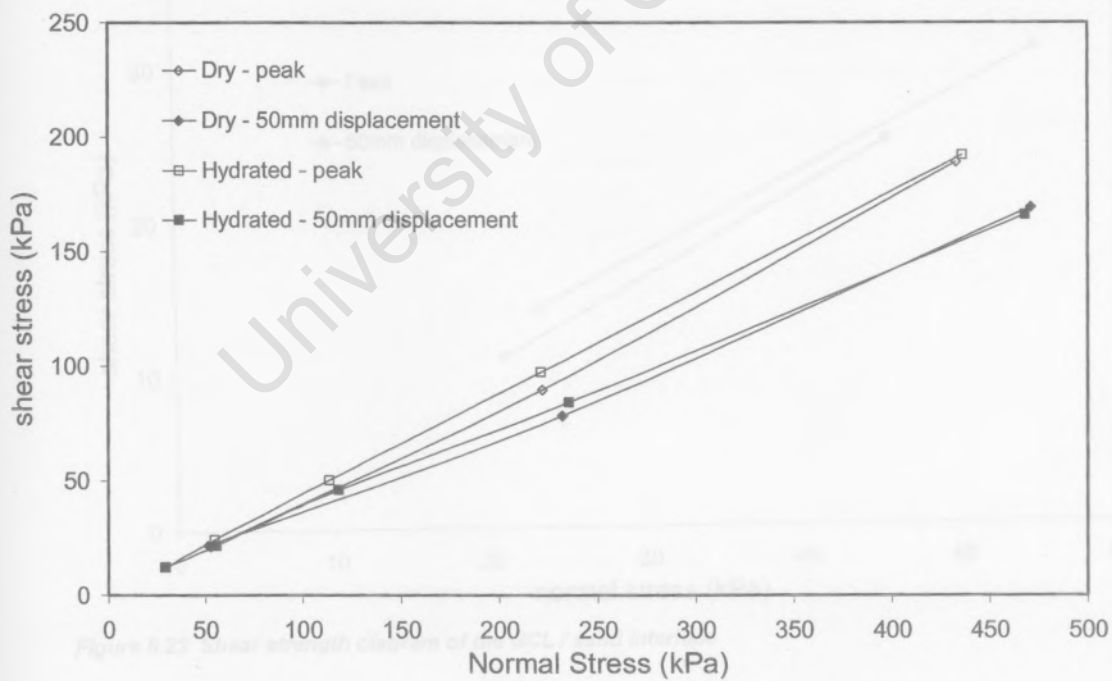


Figure 8.21 Shear strength diagram of the dry and hydrated geomembrane / sand interface

Table 8.18 Summary of geomembrane / sand shear strength results

Interface condition	Normal stress range (kPa)	Peak strength		Normal stress range (kPa)	Large displacement strength	
		c' (kPa)	ϕ (degrees)		c' (kPa)	ϕ (degrees)
Dry	52 - 430	0	23.9	52 - 470	0	19.5
Hydrated	29 - 436	0	23.8	32 - 496	0	19.3

The increase in friction angle at higher normal stresses can be attributed to a move from sliding to a ploughing mechanism.

8.3.2.5 GCL / Sand Interface

Table 8.19 Summary of GCL/ sand shear strength results

Interface condition	Normal stress range (kPa)	Peak strength		Normal stress range (kPa)	Large displacement strength	
		c' (kPa)	ϕ (degrees)		c' (kPa)	ϕ (degrees)
Partial hydration	21 - 45	0	29	23 - 55	2.2	27.5

Due to the internal failure of the GCL, tests above normal stresses of 45kPa were not successful. There was a slight post peak shear strength increase because of the complex interaction of the sand grains and woven geotextile. A much greater horizontal displacement is probably required to reach a residual failure condition.

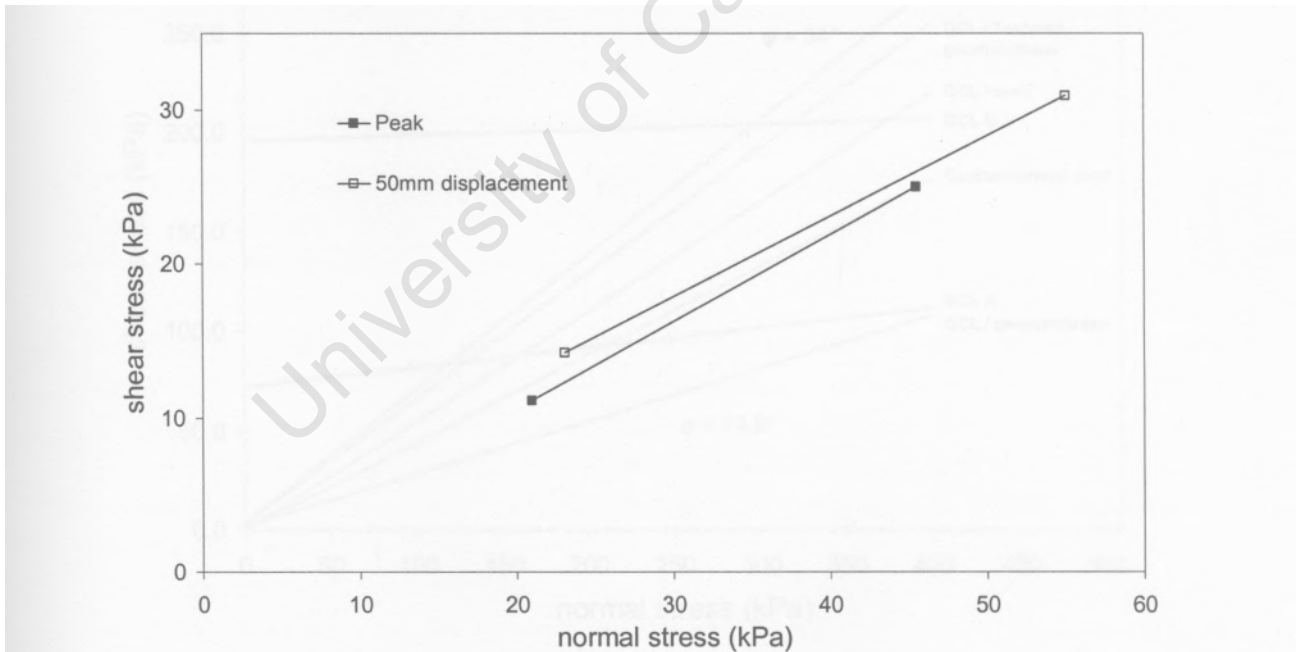


Figure 8.22 Shear strength diagram of the GCL / sand interface

8.3.3 Comparison of direct shear interface tests

The interface shear strength parameters for all the interfaces of the liner system were determined. These are summarized in Table 8.20. The comparison of the individual failure envelopes allows the

development a combined failure envelope for a chosen system of geosynthetic materials and sand — depending on the design of the lining system.

The cases presented here are based on the short term shear strength results presented earlier. Reductions of GCL internal shear strength over time may significantly affect these strengths and may change the combined failure envelope adopted as critical.

Table 8.20 Summary of interface shear strength results

Interface	Normal stress range	Peak strength		Normal stress range	Large displacement strength	
	(kPa)	c' (kPa)	ϕ' (degrees)	(kPa)	c' (kPa)	ϕ' (degrees)
GCL A internal	131 - 244	72	5.6	157 - 301	17.5	0.5
GCL B internal	199 - 252	196	1.6	228 - 328	20	2
GCL/smooth geomembrane dry	49 - 427	0	18.7	53 - 494	0	12
GCL/smooth geomembrane hydrated	26 - 432	2.1	14.8	33 - 238	0.5	13.3
GCL/smooth geomembrane hydrated				238 - 494	28	6.8
GCL/textured geomembrane	12 - 36	3.3	32.2	14 - 38	0.7	31.3
Cape Flats sand	30 - 436	3.8	34	30 - 470	3.0	32
GCL/Cape Flats sand	21 - 45	0	29	23 - 55	2.2	27.5
Cape Flats sand/geomembrane	29 - 436	0	23.8	32 - 496	0	19.3

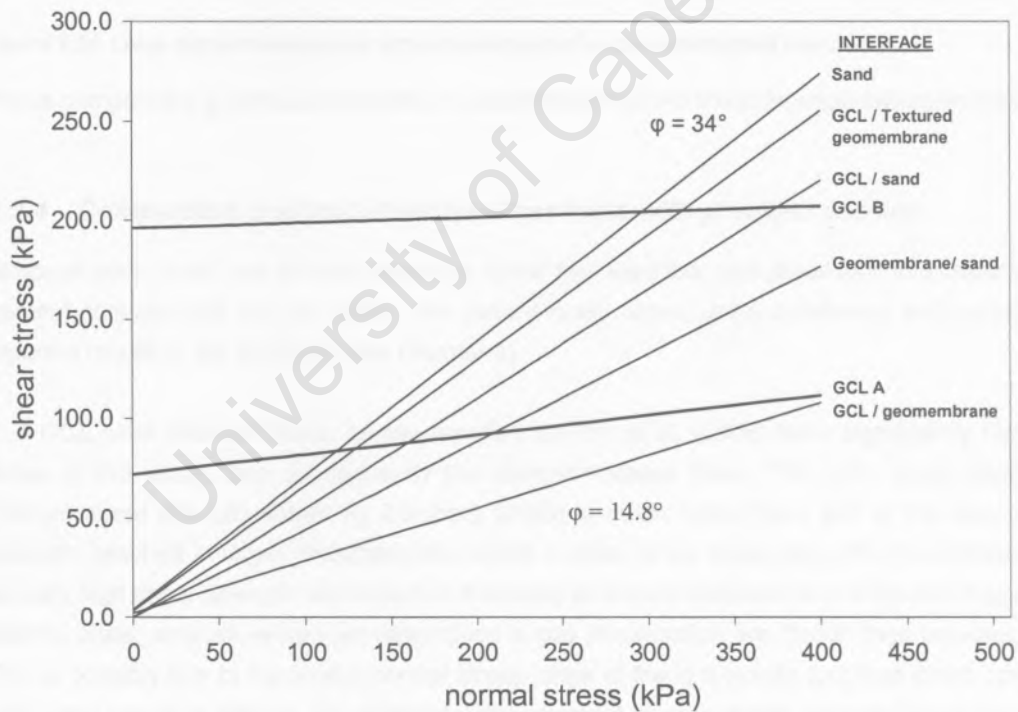


Figure 8.23 Peak shear strength diagram summary of all the investigated interfaces

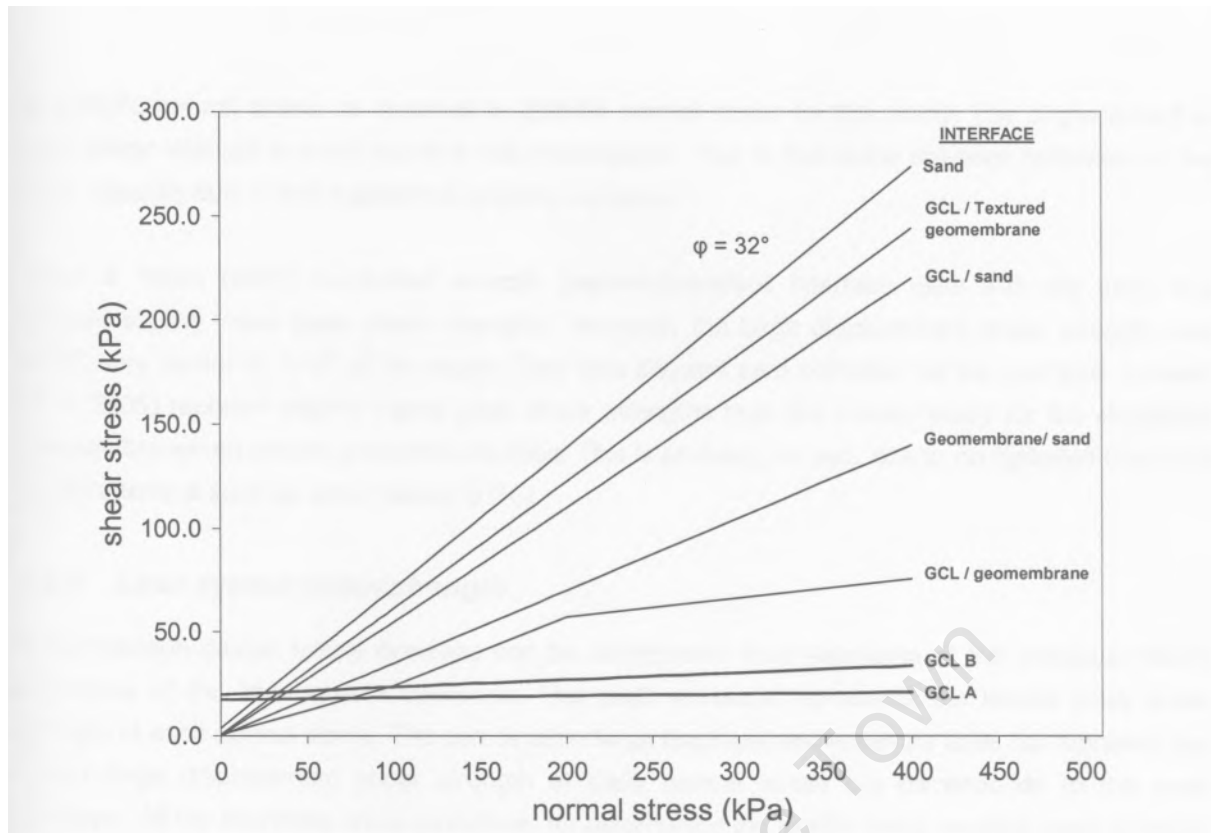


Figure 8.24 Large displacement shear strength diagram of all the investigated interfaces

These comparative graphs can be used to determine combined shear strength failure envelopes

8.3.4 Comparison of direct shear interface tests with previous studies

Although each study has its own particular shear test machine, test procedure and material batch, general comparisons can be made. The current study shows good agreement with certain of the reported results in the literature (see Chapter 4).

The GCL peak internal friction angles reported by Fox et al. (1998) were significantly higher than those of this study, and subsequently the cohesion values lower. The GCL large displacement (75mm) shear strength shown by Zornberg (2005) is much higher than that of the residual shear strength, reached at larger displacements, which is close to the shear strength of bentonite itself. A similar high shear strength was shown in this study at a shear displacement of 50mm. In general the internal shear strength envelopes determined in this investigation are 'flatter' than previous studies. This is possibly due to the limited normal stress range of the test results and thus direct comparison with other results is difficult. The horizontal displacement at peak shear strength falls in the range of both Fox et al. (1998) and Zornberg (2005).

Triplett and Fox (2001) showed a lower peak shear strength for the GCL/smooth geomembrane interface. The lower large displacement shear strength is probably in part due to higher displacements than those of this study, thus approach residual conditions. However, the same bi-linear large displacement shear strength envelope was reported. The shear strength softening began

at 127kPa normal stress, as opposed to 238kPa normal stress for this study. The displacement at peak shear strength is much higher in this investigation. This is due to the pre-peak behaviour of the GCL, possibly due to less aggressive gripping surfaces.

Hsieh & Hsieh (2002) conducted smooth geomembrane/soil interface tests with dry sand and showed slightly lower peak shear strengths. However, the large displacement shear strength was 18.9° , very similar to 19.3° of this study. They also showed zero cohesion for the interface. Hebel et al. (2005) reported slightly higher peak shear strengths than the current study for the structured geomembrane/non-woven geotextile interface. This is probably, in part, due to no hydrated bentonite on the interface such as when testing a GCL.

8.3.5 Liner system shear strength

A combination design failure envelope can be constructed from segments of the individual failure envelopes of the liner system interfaces. The peak envelope represents the lowest peak shear strength at each normal stress. The combination large displacement envelope does not represent the lowest large displacement shear strength at each normal stress but corresponds to the peak envelope. All the interfaces were considered for determining the landfill liners possible shear strength (short term) combination failure envelopes (see Figures 25 to 27). The following cases were considered:

1. Smooth geomembrane and GCL A or GCL B
2. Single sided textured geomembrane and GCL B
3. Single sided textured geomembrane and GCL A

In case 1 the GCUsmooth geomembrane exhibits the lowest peak shear strength over the full normal stress range. Thus, the large displacement shear strength is related to this interface only. Similarly for case 2, but the GCL/sand interface is the lowest peak and residual shear strength envelope due to the GCUtextured geomembrane shear strength being much higher than the smooth interface.

Case 3 is different because the internal shear strength of GCL A is relatively low, resulting in different interfaces failing at different normal stresses. Thus, a combined failure envelope must be constructed, with the discontinuity at 209kPa normal stress.

at 127kPa normal stress, as opposed to 238kPa normal stress for this study. The displacement at peak shear strength is much higher in this investigation. This is due to the pre-peak behaviour of the GCL, possibly due to less aggressive gripping surfaces.

Hsieh & Hsieh (2002) conducted smooth geomembrane/soil interface tests with dry sand and showed slightly lower peak shear strengths. However, the large displacement shear strength was 18.9° , very similar to 19.3° of this study. They also showed zero cohesion for the interface. Hebel et al. (2005) reported slightly higher peak shear strengths than the current study for the structured geomembrane/non-woven geotextile interface. This is probably, in part, due to no hydrated bentonite on the interface such as when testing a GCL.

8.3.5 Liner system shear strength

A combination design failure envelope can be constructed from segments of the individual failure envelopes of the liner system interfaces. The peak envelope represents the lowest peak shear strength at each normal stress. The combination large displacement envelope does not represent the lowest large displacement shear strength at each normal stress but corresponds to the peak envelope. All the interfaces were considered for determining the landfill liners possible shear strength (short term) combination failure envelopes (see Figures 25 to 27). The following cases were considered:

1. Smooth geomembrane and GCL A or GCL **B**
2. Single sided textured geomembrane and GCL B
3. Single sided textured geomembrane and GCL A

In case 1 the GCUsmooth geomembrane exhibits the lowest peak shear strength over the full normal stress range. Thus, the large displacement shear strength is related to this interface only. Similarly for case 2, but the GCUsand interface is the lowest peak and residual shear strength envelope due to the GCUtextured geomembrane shear strength being much higher than the smooth interface.

Case 3 is different because the internal shear strength of GCL A is relatively low, resulting in different interfaces failing at different normal stresses. Thus, a combined failure envelope must be constructed, with the discontinuity at 209kPa normal stress.

8.4 CONCLUSIONS

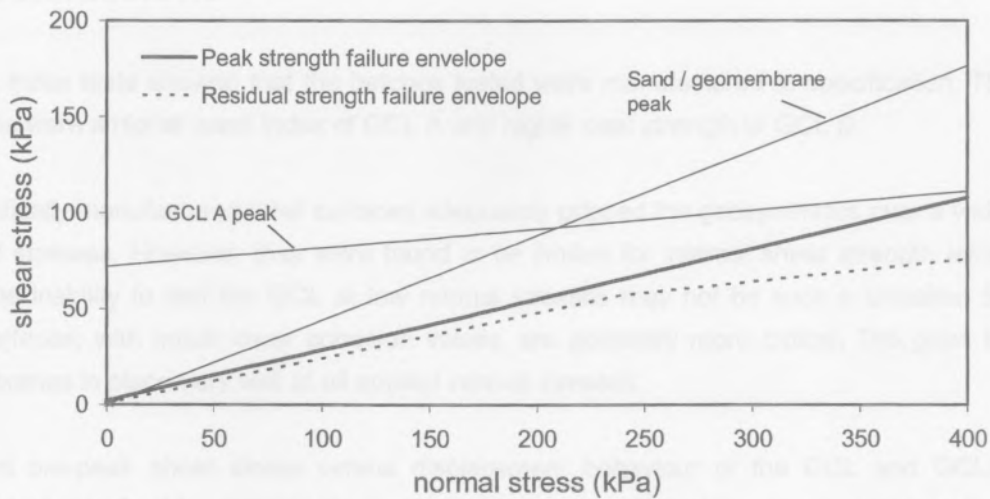


Figure 8.25 Combined shear strength diagram of case 1

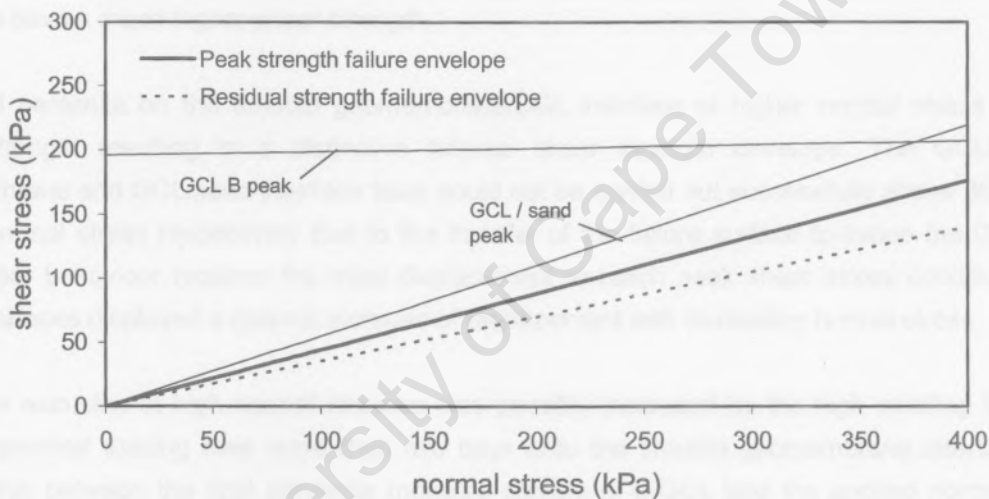


Figure 8.26 Combined shear strength diagram of case 2

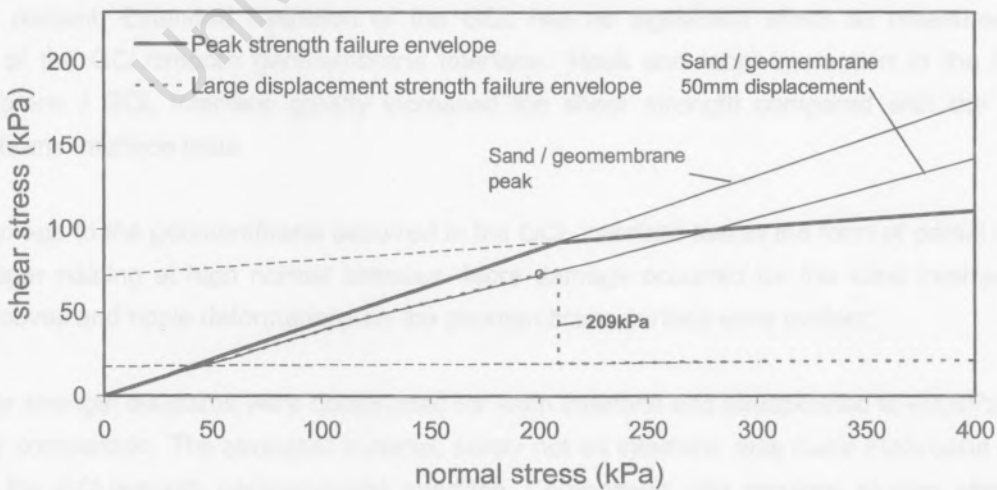


Figure 8.27 Combined shear strength diagram of case 3

8.4 CONCLUSIONS

The GCL index tests showed that the batches tested were manufactured to specification. The main differences were a higher swell index of GCL A and higher peel strength of GCL B.

The specifically manufactured steel surfaces adequately gripped the geosynthetics over a wide range of normal stresses. However, they were found to be limited for internal shear strength tests of the GCLs. The inability to test the GCL at low normal stresses may not be such a limitation because other interfaces, with much lower cohesion values, are generally more critical. The grips kept the geomembranes in place very well at all applied normal stresses.

Consistent pre-peak shear stress versus displacement behaviour of the GCL and GCU smooth geomembrane interface is related to the bentonite shear strength and fibre reorientation before shear stresses begin to fully mobilize on the intended interface. GCL B, which had high peel strength, was shown to have a much higher shear strength.

Extruded bentonite on the smooth geomembrane/GCL interface at higher normal stress reduces shear strength resulting in a distinctive bilinear shear strength envelope. The GCL/textured geomembrane and GCL/sand interface tests could not be carried out successfully above 36kPa and 46kPa normal stress respectively due to the transfer of the failure surface to inside the GCL. The sand shear behaviour requires the most displacement to reach peak shear stress conditions. The other interfaces displayed a general increase of displacement with increasing normal stress.

Bentonite extrusion at high normal stresses was possibly increased by the high swelling bentonite and incremental loading over more than two days onto the smooth geomembrane interface. The relationship between the final bentonite moisture content of a GCL and the applied normal stress may be approximated with a power function. Also, the swell index of the bentonite affects the final moisture content. Extended hydration of the GCL has no significant effect on measured shear strength of the GCL/smooth geomembrane interface. 'Hook and loop' interaction in the textured geomembrane / GCL interface greatly increased the shear strength compared with the smooth geomembrane interface tests.

Minor damage to the geomembrane occurred in the GCL interface test in the form of partial removal of the upper coating at high normal stresses. More damage occurred for the sand interface tests where grooves and ripple deformations on the geomembrane surface were evident.

The shear strength diagrams were constructed for each interface and extrapolated to 400kPa normal stress for comparison. The strongest material, surely not an interface, was Cape Flats sand and the weakest the GCL/smooth geomembrane interface. Comparison with previous studies show good agreement of results. However, due to limited studies, especially for the sand/GCL and GCL/smooth geomembrane interfaces, it is difficult to fully understand the differences between results.

Combined shear strength failure envelopes were determined for different liner material choices. If a smooth geomembrane is chosen then the GCL/geomembrane interface will be the failure plane. If the single-sided textured geomembrane is used, the failure plane will be shifted from the GCL/geomembrane interface to the sand/geomembrane interface at low normal stresses but will force GCL A to fail internally above 209kPa applied normal stress.

University of Cape Town

CHAPTER 9

LIMIT STATE ANALYSIS OF LANDFILL LINING SYSTEM

9.1 Introduction

The shear strength parameters of the GCL and liner interfaces were characterised for the materials of a local landfill lining system. This chapter makes use of these parameters for the safe design of a landfill liner incorporating a relatively steep slope for South African conditions. The main purpose of this work is to propose and demonstrate a method which could set the groundwork for a comprehensive South African standard for the stability analysis of varying landfill cross-sectional geometries. DWAF minimum standards are considered the benchmark for developing nations and should ensure up to date design and testing requirements.

In time, landfill location options may reduce due to stricter legislation and more urban development. Therefore sites with steeper slopes could become attractive options. Designers would be more inclined to consider these alternatives if a safe design methodology and testing protocol was available.

DWAF (1998) stipulate the use of residual shear strengths on all interfaces and require a global factor of safety of 1.3. This, however, may not be applicable to a liner incorporating a GCL, since the residual shear strength is essentially that of bentonite, which is very low. Thus, design adhering to these standards is essentially overconservative and too restrictive for designers.

9.2 Analysis methods

The results of the experimental investigation provide adequate information to determine the static balance of forces for a given liner slope geometry. A typical landfill must satisfy an appropriate factor of safety for two critical design cases (see Section 3.8) to ensure the integrity of the landfill. These are the considerations of the:

- Constructed liner system itself
- Landfill at the end of the design life

In Chapter 4 different methods of analysis were reviewed, the most complex being finite elements. Previous finite element studies, as discussed in Section 4.11.5, showed the effect of waste settlement and its associated large displacements along the liner slope interfaces. The use of residual shear parameters on the slope and peak shear parameters on the base was shown to be valid for assessing global stability of the waste body.

Ultimate limit state approaches from Giroud et al. (1996) and SANS 207 (2006) were modified to assess the safety of the liner system. Serviceability limit states, in terms of allowable displacements,

are not required from an analytical perspective since very large settlements are inevitable and acceptable (see Section 4.11.5).

This initial condition can readily be assessed by existing methods such as the two wedge analysis by Giroud et al. (1995). This method was developed for the design of sloped geosynthetic-soil layered systems. A diagrammatic representation and the equation for the factor of safety is explained and presented in Appendix F.1. The aim is to determine the factor of safety against sliding along a plane failure surface of a geosynthetic-soil layered system of uniform thickness on a given slope. The method considers a two-wedge analysis independent of pore water pressures. This will be used with the defined input parameters for the design cases presented in this chapter.

Since no formal manual calculation method for the limit state of the full landfill scenario was found, a two-wedge analyses was developed which is a logical extension of Giroud et al. (1995). A summary of the design equations, including diagrams, is in Appendix F.2. Simplicity in the approach was considered essential. The proposed analysis does not purport to take all aspects of the system into account, and further refinements are recommended.

Even though the limit state method has certain limitations, as discussed in Section 4.11.3, selected measures are taken into account indirectly. This includes the incorporation of the waste shear strength and the settlement of the waste by the option to assign residual conditions on the side slopes. Also, the run-out trench is assumed to be designed in such a way that pullout is allowed prior to tensile failure of the liner system.

9.2.1 Partial factors of safety

Traditionally, global factors of safety are used and are adequate for most geotechnical safety analyses. The characteristic parameters of a given problem are used directly in the calculations and the overall (global) factor of safety must satisfy a recommended safe value larger than unity. Partial safety factors, on the other hand, are applied to the characteristic values, to either reduce strengths and/or increase loads, before the balance of forces is considered. In this way partial factors of safety make it possible to take all risks into account individually. The precautionary principle states that where a risk is unknown, the worst case situation is assumed and provisions are made for such a situation. This is done by adopting appropriate partial safety factors.

In a landfill the geosynthetics do not play a reinforcing role, but a containment function. However, the geosynthetics are extensible and must sustain shear forces over an extended period to maintain the integrity of the lining system. Also, the materials degrade over time and there are possible economic ramifications of failure. SANS 207 (2006) is addressing soil reinforced structures. However, in view of the abovementioned conditions, lining systems have similarities that warrant the same approach.

The choice of these partial safety factors is project specific and an implicit understanding of the full life, loading, installation and operational activities and conditions, is essential to determine appropriate partial factors. SANS 207 (2006) uses the following partial factors. Factors considered

not directly applicable to the landfill situation, are not listed (eg. live loads). The notation is taken directly from SANS 207 (2006).

f_{fs} = load factor applied to soil unit weight

= soil material factor applied to $\tan(\phi)$

$f_{ms|c}$ = soil material factor applied to cohesion

f_r = reinforcement material factor applied to reinforcement base strength, composed of:

L_{vn} = *manufacture*: variation of material strength, modeling errors in assessment of material resistance

f_{m2} *extrapolation of test data*: confidence of long-term capacity assessment

f_{m21} = *susceptibility to damage*: damage during construction

f_{m22} = *environment*: rate of material degradation due to environmental conditions

f_i = interaction factor applied to sliding across surface of reinforcements

f_e = economic ramifications of failure factor applied to all reinforcement base strengths

f_m is considered in detail in the code since the tensile strength of the reinforcements is critical for the safety of a reinforced soil system. This also requires careful attention in a landfill situation, however interface shear strengths are probably a more important consideration. Thus, instead of applying f_s to the tensile shear strength, applying it to the interface shear strength for the post waste fill situation is recommended and carried out for this analysis. Prior to waste filling the tensile strength does play a significant role for the slope stability, thus the original use was maintained.

To take account of the landfill specific aspects additional factors are proposed:

f_{oul} = GCL material factor applied to combined shear strength failure envelope

f_{le} = environmental ramifications of failure factor applied to all interface shear strengths

f_n is applicable to a landfill but many liner failures will not drastically affect other infrastructure and could be left as is. Thus, apart from possible minor landscape rectifications, major repair is unlikely to be financially warranted. However, the environmental consequences are very important since liner rupture could release a great deal of leachate into the groundwater. Such failures may go unnoticed or will be prohibitively expensive to repair. However, there will be an indirect "cost" to society due to the pollution. Thus, the separate environmental partial factor, f_e , is recommended to take care of this risk. This factor will be applied to the shear strengths of the interfaces like the economic factor for the long term scenario.

Table 9.1 Summary of partial safety factors

Partial Factor	Factor type	Modified for Landfill		
		SANS minimum	analysis short-term	analysis long-term
f_{fs}	Load	1.5	1.5	<u>1.5</u>
$f_{ms[\phi]}$	Soil material	1.0	1.0	1.0*
$\%I_{sm}$		1.6	1.6	1.6*
f_{GCL}	GCL material	-	1.0	3.3
f_{s}	Interaction	1.3	1.3	<u>1.3</u>
	<u>Economic</u>	1.0	1.0	<u>1.1</u>
f_e	<u>Environmental</u>	1.0	1.0	<u>1.1</u>
<u>Total factor applied to interface shear strength:</u>				1.6
		1.0	1.0	1.0
f_{m12}	Geosynthetic	1.0	1.0	1.0
f_{m21}	material	1.0	1.1	1.1
f_{m22}	(tension)	1.0	1.0	<u>1.5</u>
<u>Total factor (f_m) applied to geosynthetics:</u>			1.1	1.7

*Waste material

Table 9.1 compares the partial factors recommended by SANS 207 (2006) with the factors, highlighted in bold, adopted for this study. These are tentative values to demonstrate the application of the method. A brief reasoning or arguments for these increased factors are as follows:

- f_{m21} is changed from 1.0 to 1.1 for the short term analysis. This is to allow for aggressive construction practices due to low skilled labour in South Africa.
- f_{m22} is doubled due to expected creep and durability concerns over the long design life.
- f_n and f_e are to ensure sustainability - future generations do not have to suffer economically or be concerned about pollutants affecting their water supply.

9.3 Design parameters

The cross-sectional geometry chosen as a basis for this analysis is similar to the Kettleman Hills case, as shown in Section 3.4 and detailed in Appendix F.2. Although the design method can take a head on the liner into account, it is not considered in this example. Table 9.2 lists the landfill cases considered in the analysis. The objective is to determine which slope angle design is safe for the full life of the landfill.

Table 9.2 Landfill cases

Case	side slope gradient	Common parameters
L = 100m		
1	1:3	Waste height = 30m
2	1:4	Waste slope = 1:3
3	1:5	Base gradient = 1:50 Head = 0m

Table 9.3 summarizes the interface shear strengths applicable to this assessment. For each slope gradient the material option cases, as discussed in Section 8.3.4, are applied.

Table 9.3 Interface shear strength properties

Interface	Normal stress range	Peak strength		Normal stress range	Large displacement strength	
		(kPa)	(kPa) (degrees)		(kPa)	c' (kPa)
GCL A intenal	131 - 244	72	5.6	157 - 301	17.5	0.5
GCL B intenal	199 - 252	196	1.6	228 - 328	20	2
GCL/smooth geomembrane hydrated	26 - 432	2.1	14.8	33 - 238	0.5	13.3
GCL/smooth geomembrane hydrated				238 - 494	28	6.8
GCL/textured geomembrane	12 - 36	3.3	32.2	14 - 38	0.7	31.3
Cape Flats sand/geomembrane	29 - 436	0	23.8	32 - 496	0	19.3

For the long term assessment a partial factor of safety of $f_{GCL} = 3.3$ must be applied to the GCL peak shear strength. The background to the resulting values, listed in Table 9.4, is detailed in Section 4.9.3 Also, since excessive displacements should be expected in the field, the residual shear strengths of the GCL (not the large displacements shear strength as determined in this study) are used.

Table 9.4 Revised interface shear strength properties

Interface	Normal stress range	Peak strength		Normal stress range	Large displacement strength	
		c' (kPa)	(p' (degrees))		(kPa)	c' (kPa)
GCL A intenal	131 - 244	34	2.1	157 - 301	0	4.5
GCL B intenal	199 - 252	73.3	1.9	228 - 328	0	4.5

Table 9.5 lists the material properties assumed for this investigation. According to Giroud et al. (1995) (see Section 4.11.1), a weighted cohesion of 40.7kPa is calculated if the full strength of the cement stabilized sand is used. This, though, is not conservative since it is highly likely that the layers are not uniform, cement not distributed evenly and are (to some extent) damaged during construction and initial waste placement. Thus, the lowest cohesion value of the materials i.e. the sand, was adopted for the cement stabilized layer and the weighted shear strength calculated, as shown in Table 9.6.

Table 9.5 Material properties

Material	Property	Unit	Value
Cement stabilized sand	Bulk Density	kg/m ³	1600
	Friction angle	degrees	33
	Cohesion	kPa	100
Crushed gravel	Bulk Density	kg/m ³	1800
	Friction angle	degrees	45
	Cohesion	kPa	10
Philippi Dune sand	Bulk Density	kg/m ³	1540
	Friction angle	degrees	34
	Cohesion	kPa	3.8
Waste	Bulk Density	kg/m ³	1200
	Saturated density	kg/m ³	1600
	Friction angle	degrees	25
Geomembrane GCL	Cohesion	kPa	5
	Max. axial force	kN/m	32
	Max. axial force	kN/m	6

A waste internal friction angle of 15°, as recommended by DWAF (1998) (see also Section 4.11.3), was used and is considered conservative and low enough to take shear strength reduction due to waste degradation into account.

The waste saturated density shown in Table 9.5 is based on a porosity of 50%, as recommended by Koerner & Soong (2000). Ismail (2005) investigated cement stabilized retaining walls and deemed cement stabilized sandy soil with properties of 100kPa cohesion and 33° internal shear strength, and unit weight of 1600kg/m³ as representative. Thus these parameters were used since no shear strength tests or density determinations were done for the material used in the Belleville South landfill.

Table 9.6 Weighted material properties

Material	Property	Unit	Weighted average
All soil material above interface	Bulk Density	kg/m ³	1645
	Friction angle	degrees	35
	Cohesion	kPa	4.6

9.4 Analysis

The shear strength of the slope interface is the large displacement shear strength. However, for a combined failure envelope, this is not the same over the entire surface. Since the limit state method requires a single input for the slope, a weighted value is calculated based on the normal stress range along the slope. Figure 9.1 presents the situation, combining a shear strength diagram and the slope profile to demonstrate the regions in which the different shear strength parameters are applicable. The following example shows the calculation for a 1:4 slope. The GCL B and GCL/sand interface shear strength properties, listed in Table 9.5, are used. This approach is also used for a bilinear

failure envelope of a single interface, such as for the GCL/smooth geomembrane interface in this study.

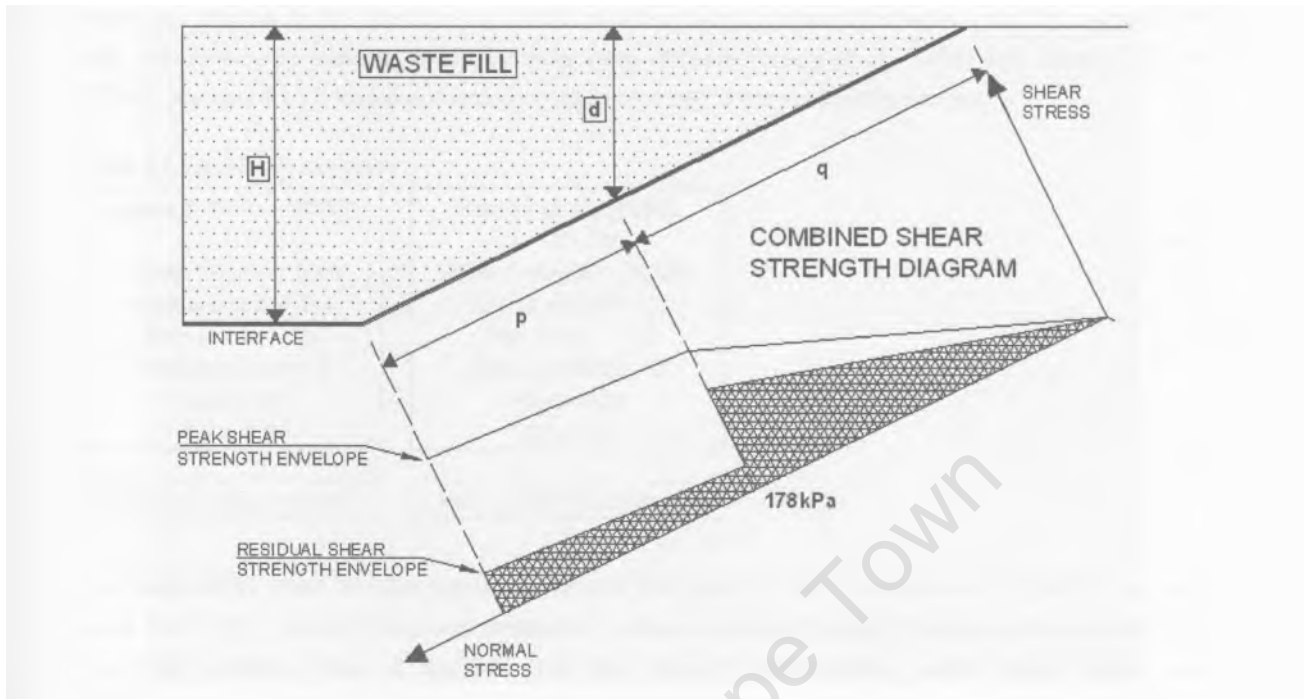


Figure 9.1 Determination of side slope interface shear strength

Where:

H = height of waste

d = depth to critical normal stress along slope interface

p = length parallel to interface where lower residual shear strength at high normal stresses applies

q = length parallel to interface where higher residual shear strength at low normal stresses applies

If H = 30m then by geometry:

$$d = 15.3\text{m}$$

$$p = 60.65\text{m}$$

$$q = 63.04\text{m}$$

Therefore the calculated weighted interface friction angle, β_{id} :

$$\beta_{id} = \frac{60.65\text{m} \cdot 4.5^\circ + 63.04\text{m} \cdot 19.3^\circ}{60.6\text{m} + 63.04\text{m}} = 12.04^\circ$$

This interface shear strength is then incorporated into equation [F.2] in Appendix F to determine the factor of safety for the slope.

9.4.1 Verification

No access to a numerical limit state analysis program was available at the time of this investigation. However, studies in the literature of similar cross-sectional geometries were used for comparison with the developed method. Two examples were chosen: Reddy et al. (1996) and Jones & Dixon (2005). Section 4.11.3 lists the computer programs used in the respective studies.

Table 9.7 Verification examples

<p>Jones & Dixon (2005) L = 100m Waste height = 30m Waste slope = 1:3 Side slope = 1:3 Base gradient = 0 Head = 0m FS = 2.6</p>	<p>Reddy et al. (1996) L = 91.5m Waste height = 30.5m Waste slope = 1:3 Side slope = 1:2 Base gradient = 0 Head = 0m FS= 1.0</p>
<p>FS = 2.4 (Rouncivell)</p>	<p>FS = 0.85 (Rouncivell)</p>

The parameters used and the results in terms of the factor of safety are listed in Table 9.7. In each case the in this research proposed method is in close proximity but less than the values obtained in the other studies. Thus, it appears that this method incorporating partial safety factors can adequately be used for the analysis of similar landfill geometries and using unity as the partial factors of safety in this comparative study produces conservative results

9.5 Results

The results of numerous analyses are listed in Table 9.8 where critical values are shown in bold. They indicate that a slope of 1:4 for the pre-fill situation is safe. The restricting interface is the geomembrane/GCL interface. If the textured geomembrane is used instead of the smooth geomembrane the critical interface will move from this interface to the geomembrane/sand interface (pre-fill) and the GCL itself (post-fill).

Table 9.8 Summary of results

Design	Pre fill			Post fill		
	1:5	1:4	1:3	1:5	1:4	1:3
Liner slope						
Smooth GM/Sand	1.85	1.49	1.12	1.98	1.54	1.1
Smooth GM/GCL	1.24	1.02	0.79	1.94	1.65	1.3
Textured GM/GCL B	2.68	2.16	1.65	1.32	1.12	0.91
Textured GM/GCL A				0.95	0.81	0.65

The safety factors calculated for the pre-fill scenario utilized the strength of the textured geomembrane/GCL interface thus these factors are relatively high. However1 for the post-fill scenario the internal shear strength of the GCL and the sand/geomembrane combined failure envelope is used. Thus, the effect of the internal shear strength of the GCL is critical. As shown, if GCL A is used

all the cases will not be safe. This however is a very brief assessment and a great deal more analyses of different configurations and material properties should be carried out to solidify the findings.

9.6 Conclusion

In a liner system, the slip surface is already known thus implementing a manual calculation technique is acceptable from a time perspective. The proposed design method for the full landfill case appears to be conservative compared with other studies. Partial factors of safety can easily be incorporated into the limit state analysis and the determination of the weighted residual shear strength on the side slope is straightforward for combined or multi-linear shear strength envelopes.

In general, the pre-fill stability is the limiting factor for the smooth geomembrane/sand and smooth geomembrane/GCL interface. However, if a textured geomembrane is used the post-fill situation is critical. Thus, it is imperative that the GCL internal shear strength is reliably established, particularly since GCL products are not consistently of the same shear strength.

University of Cape Town

CHAPTER 10

CONCLUSION

10.1 Introduction

A comprehensive study into the history, previous research, shear strength characteristics and design of landfill liner systems was conducted. The experimental investigation produced various new insights and recommendations regarding the determination of the internal and external shear strength of a GCL and other liner interfaces.

The use of these parameters in a limit state analysis considering the full design life of a typical critical landfill geometry and showed the influence of the different input parameters and the effectiveness of the partial safety factor approach.

This chapter summarises these conclusions and makes recommendations for further investigations.

10.2 Experimental investigation

- The GCL index tests showed that the batches tested were manufactured to specification.
- The specifically manufactured steel surfaces adequately gripped the geosynthetics over a wide range of normal stresses. However, they were found to be limited for internal shear strength tests of the GCLs. The grips kept the geomembranes in place very well at all applied normal stresses.
- GCL B, which had high peel strength, was shown to have a much higher shear strength. Consistent pre-peak shear stress versus displacement behaviour of the GCL and GCL/smooth geomembrane interface is related to the bentonite shear strength and fibre reorientation before shear stresses begin to fully mobilize on the intended interface.
- Extruded bentonite on the smooth geomembrane/GCL interface at higher normal stress reduces shear strength resulting in a distinctive bilinear shear strength envelope. The GCL/textured geomembrane and GCL/sand interface tests could not be carried out successfully above 36kPa and 46kPa normal stress respectively due to the transfer of the failure surface to inside the GCL. The tested interfaces displayed a general increase of displacement with increasing normal stress.
- Bentonite extrusion at high normal stresses was possibly increased by the high swelling bentonite and incremental loading over more than two days onto the smooth

geomembrane interface. The relationship between the final bentonite moisture content of a GCL and the applied normal stress may be approximated with a power function. Also, the swell index of the bentonite affects the final moisture content. Extended hydration of the GCL has no significant effect on measured shear strength of the GCL/smooth geomembrane interface. 'Hook and loop' interaction in the textured geomembrane/GCL interface greatly increased the shear strength compared with the smooth geomembrane interface tests.

- Minor damage to the geomembrane occurred in the GCL interface test in the form of partial removal of the upper coating at high normal stresses. More damage occurred for the sand interface tests where grooves and ripple deformations on the geomembrane surface were evident.
- The shear strength diagrams were constructed for each interface. The strongest material was Cape Flats sand and the weakest the GCL/smooth geomembrane interface. Comparison with previous studies show good agreement of results. However, due to limited studies, especially for the sand/GCL and GCL/smooth geomembrane interfaces, it is difficult to fully understand the differences between results.
- Combined shear strength failure envelopes were determined for different liner material choices. If a smooth geomembrane is chosen then the GCL/geomembrane interface will be the failure plane. If the single-sided textured geomembrane is used, the failure plane will be shifted from the GCL/geomembrane interface to the sand/geomembrane interface at low normal stresses but will force GCL A to fail internally above 209kPa applied normal stress.

10.3 Limit state analysis

- In a liner system, the slip surface is already known thus implementing a manual calculation technique is acceptable from a time perspective.
- The proposed design method for the full landfill case appears to be conservative compared with other studies. Partial factors of safety can easily be incorporated into the limit state analysis and the determination of the weighted residual shear strength on the side slope is straightforward for combined or multi-linear shear strength envelopes.
- In general, the pre-fill stability is the limiting factor for the smooth geomembrane/sand and smooth geomembrane/GCL interface. However, if a textured geomembrane is used the post-fill situation is critical. Thus, it is imperative that the GCL internal shear strength is reliably established, particularly since GCL products are not consistently of the same shear strength.

10.4 Recommendations

- Further testing in the large direct shear device to determine the interface shear strength parameters for landfill lining interfaces between other possible lining materials. These include, among others, geogrids, geodrains and other types of textured geomembranes.
- Investigate the modification of the geosynthetic gripping surfaces to allow internal shear strength testing of needle-punched GCLs at low and very high normal stresses.
- Propose that DWAF consider using peak shear strengths on the base and residual shear strengths on the side slopes for landfill stability calculations. Also, make provision for dealing with GCL internal shear strength — its reduction for long term analyses and caution when using the residual shear strength over an entire liner slope. Also, propose that preference for shear strength testing with a large direct shear device rather than a ring shear device for all liner interface testing be stated.
- It is hoped to amend a chapter to SANS 207 (2006) or create a new South African National Standard for a formalized method incorporating partial factors of safety for the design of landfill liner systems in the SA environment and conditions. The method could also easily be extended to assess landfill cover systems containing geosynthetics. The established approaches used in 'First World' countries could provide guidance in terms of the methodology, in the selection of the appropriate partial factors of safety and their magnitudes.

REFERENCES

1. ASTM D 3080, 1990. Direct Shear Test of Soils Under Consolidated Drained Conditions. *ASTM International*, West Conshohocken, PA, USA.
2. ASTM D 698, 1991. Laboratory Compaction Characteristics of Soil Using Standard Effort. *ASTM International*, West Conshohocken, PA, USA.
3. ASTM D 5321, 1992. Determining the Coefficient of Soil and Geosynthetic or Geosynthetic and Geosynthetic Friction by the Direct Shear Method. *ASTM International*, West Conshohocken, PA, USA.
4. ASTM D 6243, 1998. Standard Test Method for Determining the Internal and Interface Shear Resistance of Geosynthetic Clay Liner by the Direct Shear Method. *ASTM International*, West Conshohocken, PA, USA.
5. ASTM D 5993, 1999. Standard Test Method for Measuring Mass per Unit Area of Geosynthetic Clay Liners. *ASTM International*, West Conshohocken, PA, USA.
6. ASTM D 5890, 2001. Standard Test Method for Swell Index of Clay Component of Geosynthetic Clay Liners. *ASTM International*, West Conshohocken, PA, USA.
7. ASTM D 4439, 2004. Standard Terminology for Geosynthetics. *ASTM International*, West Conshohocken, PA, USA.
8. ASTM D 5890, 2001. Standard Test Method for Determining Average Bonding Peel Strength Between the Bottom and Top Layers of Needle-punched Geosynthetic Clay Liners. *ASTM International*. West Conshohocken, PA, USA.
9. Babuska, I., Strouboulis, T. 2001. *The Finite Element Method and its Reliability*. Oxford University Press Inc, New York.
10. Bell, J. R., Yoder, E. J, 1957. *Plastic Moisture Barrier for Highway Subgrade Protection*. Proc. Highway Research Board, Washington. DC. 36, 713 - 35.
11. Bentler, D. J., Morrison, C. S., Esterhuizen, J. J. B., and Duncan, J. M, 1999. *Sage User's Guide*, Virginia Polytechnic Institute and State University, Blacksburg, USA.
12. Bogchi, A., 1994. *Design, Construction and Monitoring of Landfills*. 2nd edition. John Wiley and Sons, Ltd., New York.
13. Bouazza, A., 2002. Geosynthetic clay liners. *Geotextiles and Geomembranes*, 20, 3-17
14. British Medical Association, 1991. *Hazardous Waste and Human Health*. Oxford University Press, Oxford.
15. BS 1377: Part 2: 1990, British Standard Methods of Test for Soils for Civil Engineering Purposes., *Classification tests*, British Standards Institution.
16. BS 8006: 1995. *Code of Practice for Strengthened / Reinforced Soils and other Fills*. British Standards Institution.
17. Byrne J.R., 1994. Design issues with displacement softening interfaces in landfill liners. Proceedings of Waste Technology 1994, Charleston, South Carolina, USA.
18. Cetco Poland., 2006. Sodium Bentonite: Its Structure and Properties, Including a Discussion of Cetco's Contaminant Resistant Bentonites. *Colloid Environmental Technologies Company*. [Online] Available: <http://www.cetco.pl/e/volclay.htm> [2007, January 15]

19. Cetco. 2002. *Geosynthetic Clay Liners*. Cetco Lining Technologies. Arlington Heights, IL 60004 USA.
20. Cetco. 2007. Geosynthetic Clay Liner Product Range. [Online] Available: <http://www.cetco.com/LT/products/GCLasp> [2007, May 10]
21. Cetco. 2004. *Bentomat ST Certified Properties*. Cetco Lining Technologies. Arlington Heights, IL 60004 USA. [Online] Available: http://www.cetco.com/Groups/lining/LTE/Content/pdf/ST_prop.pdf [2006, August 10]
22. Chang, M., 2005. Three-dimensional stability analysis of the Kettleman Hills landfill slope failure based on observed sliding-block mechanism. *Computers and Geotechnics* 32 (2005) 587-599.
23. Daniel, D.E., Koerner, R.M., Bonaparte, R., Landreth, R.E., Carson, D.A., Scranton, F.B. 1998. Slope Stability of Geosynthetic Clay Liner Test Plots. *Journal of Geotechnical and Geoenvironmental Engineering*, July 1998, 628 - 637.
24. Daniel, D. E., 1993. *Geotechnical Practice for Waste Disposal*. St. Edmundsbury Press, Great Britain.
25. Davies, P.L. and Legge, K.R. (2002). Geosynthetic clay liners in developing countries: an African perspective. *Geosynthetics - 7th - ICG*, Nice, France. Delmas, Gourc & Girard (eds), Swets & Zeitlinger.
26. De Jong, J.T., Westgate, Z.J., 2005. Role of Over-Consolidation on Sand-Geomembrane Interface Response and Material Damage Evolution. *Geotextiles and Geomembranes*, 23, 486-512
27. DiBiagio, E., Flaate, K., eds. 2000. Ralph B. Peck: Engineer, Educator, A Man of Judgement. Norwegian Geotechnical Institute. Publication 207. Oslo.
28. DWAF.1994. Minimum Requirements for Waste Disposal by Landfills. *Waste Management Series*. Department of Water Affairs and Forestry. Pretoria, South Africa.
29. DWAF.1998. Minimum Requirements for Waste Disposal by Landfills. 2nd edition. *Waste Management Series*. Department of Water Affairs and Forestry. Pretoria, South Africa.
30. Eid, H.T. 2002. Interactive Shear Strength Behavior of Landfill Composite Liner System components. *7th International Conference on Geosynthetics - Delmas, Gourc & Girard* (CD-ROM). Nice, France. Vol.2, pp. 587-590.
31. Eid, H.T., Stark, T.D., Doerfler, C.K., 1999. Effect of Shear Displacement Rate on Internal Shear Strength of Reinforced Geosynthetic Clay Liner. *Geosynthetics International*, 6(3), 219-239.
32. Rathje, E.M., Bray, J.D., 2001. One- and Two-dimensional Seismic Analysis of Solid-Waste Landfills. *Canadian Geotechnical Journal*. 38: 850-862.
33. Environment Conservation Act, No.73, 1989. Section 20 (5) (b). The Control and Management of General Communal and General Small Waste Disposal Sites. South Africa
34. Environmental Protection Agency. 2000. Landfill Site Design. *Landfill Manuals*. Environmental Protection Agency, Wexford, Ireland. [Online] Available: http://www.epa.ie/downloads/advice/waste/waste/epaJandfill_site_design_guide.pdf [2007, May 28]
35. Esterhuizen, J. J. B., Filz, G.M., Duncan, J.M. 2001. Constitutive Behaviour of Geosynthetic Interfaces. *Journal of Geotechnical and Environmental Engineering*.

36. Fang, H.Y., Slutter, R.J. and Koerner, R.M., 1977, "Load Bearing Capacity of Compacted Waste Materials", *Proceedings of the Ninth International Conference on Soil Mechanics and Foundation Engineering*, Specialty Session on Geotechnical Engineering and Environmental Control, Vol. 4, Tokyo, Japan, July 1977, pp. 265-278.
37. Filz G.M., Esterhuizen J.J.B., Duncan J.M. 2001. Progressive failure of lined waste impoundments. *Journal of Geotechnical and Geoenvironmental Engineering*, ASCE: 127, 841-848.
38. Fox, P.J., OIsta, J.T., Chiu, P., 2002. Internal and Interface Shear Strengths of Needle-Punched Geosynthetic Clay Liners. *7th International Conference on Geosynthetics - DeImes, Gourc & Girard* (CD-ROM). Nice, France. Vol.2, 667-670
39. Fox, P.J., Rowland, M.G., Scheithe, J.R., 1998. Internal Shear Strength of Three Geosynthetic Clay Liners. *Journal of Geotechnical and Geoenvironmental Engineering*, 933 - 944.
40. Fox, P.J., Stark, T.D., 2004. State-of-the-art report: GCL Shear Strength and its Measurement. *Geosynthetics International*, 11(3), 141-175.
41. German Geotechnical Society., 1993. *Geotechnics of Landfill Design and Remedial Works Technical Recommendations*. 2nd edition. Ernst & Sohn. Germany.
42. Gilbert RB, Wright SG, Liedtke E., 1998. Uncertainty in Back Analysis of Slope: Kettleman Hills **case history**. *Journal of Geotechnical and Environmental Engineering*, ASCE,124(12):1167-76.
43. Giroud, J.P., Williams, N.D., Pelte, T., Beech, J.F. 1995. Stability of Geosynthetic-Soil Layered Systems on Slopes. *Geosynthetics International*, 2(6), 1115-1148.
44. Giroud, J.P. and Ah-Line, C., 1984, Design of Earth and Concrete Covers for Geomembranes, *Proceedings of the International Conference on Geomembranes*, IFAI, Vol. 2, Denver, Colorado, USA, 487-492.
45. Giroud, J.P. and Beech, J.F., 1989. Stability of Soil Layers on Geosynthetic Lining System, *Proceedings of Geosynthetics*, IFAI, Vol. 1, San Diego, California, USA, 35-46.
46. Goodhue M.J., Edil TB., Benson, C.H. 2001. Interaction of Foundry Sands with Geosynthetics. *Journal of Geotechnical and Geoenvironmental Engineering*, 353 - 362.
47. Grim, R.E., 1968. Clay Minerology. 2nd edition. *McGraw-Hill International Series in the Earth and Planetary Sciences*. McGraw-Hill Book Company, USA.
48. Head. K. 1982. *Manual of Soil Laboratory Testfng*. Robert Hartnol Limited, Bodmin, Cornwall. Great Britain. Vol. 2, 509 - 580.
49. Hendricks, S, B., 1942. Lattice Structure of Clay Minerals and Some Properties of Clays, *J. Geol.* 50: 276 - 290
50. Hickey, M. E., 1957. Evaluation of Plastic Films as Canal Lining Materials. *US Bureau of Reclamation Lab Report*, B - 25.
51. Hofmann, U., Endell, K., Wilm, D., 1933. Kristallstruktur and Quellung von Montmorillonit, *Z. Krist.*, 86: 340 - 348.
52. Hsieh, C., Hsieh, M. 2003. Load Plate Rigidity and Scale Effects on the Frictional Behavior of Sand/Geomembrane Interfaces. *Geotextiles and Geomembranes*, 21 (1), 25-47.

70. Lovell, C.W., Sharma, S. and Carpenter, J.R., 1983, '*Introduction to Slope Stability Analysis with STABL4*', Report prepared for Federal Highway Administration, U.S. Department of Transportation, 109 p.
71. Marr, WA., Christopher, B., 2004. Slope Design using Geosynthetic Clay liners. *Third European Geosynthetics Conference*. Munich, Germany. 189-192
72. Marshall, C. E., 1935. Layer Lattices and Base-Exchange Clays, *Z. Krist.* 91: 433 - 449.
73. Martin, J.P. and Koerner, R.M., 1985, Geotechnical Design Considerations for Geomembrane Lined Slopes: Slope Stability, *Geotextiles and Geomembranes*, Elsevier, Vol. 2, No. 4, 299-321.
74. Mcbean, E. A. et al. 1995. *Solid Waste Landfill Engineering and Design*. Prentice Hall, Englewood Cliffs, NJ., USA.
75. Mitchell JK, Seed RB, Seed HB. Kettleman Hills Waste Landfill Slope Failure, I: Liner System Properties. *Journal of Geotechnical Engineering*, ASCE, 116(4):647-68.
76. Morgenstern, N.R., Price, V.E., 1965. The Analysis of the Stability of General Slip Surfaces. *Geotechnique* 15, 79-93.
77. Naue, 2004. *The Bentonite Construction Waterproofing Manual*. Naue GmbH & Co. KG. Espelkamp-Fiestel. Germany.
78. Neal, H. A., Schubel, J, R., 1987. *Solid Waste Management and the Environment: The Mounting Garbage and Trash Crisis*. Prentice Hall. Englewood Cliffs, NJ., USA.
79. Orsmond, W., 2007. *Landfill Liner Design Practice in Europe*. [Personal communication] e-mail correspondence.
80. Reddy, KR., Kosgi, S., Motan, ES., 1996. Interface Shear Behaviour of Landfill Composite Liner Systems: A Finite Element Analysis. *Geosynthetics International*, 3(2), 247-275.
81. Reinhart, D.R., McCreanor, P.T., Townsend, T. 2002. The bioreactor landfill: its status and future. *Waste Management Research*, 20, 172.
82. SANS 207. 2006. The Design and Construction of Reinforced Soils and Fills. *South African National Standard*. Standards South Africa, Pretoria.
83. Seed RB, Mitchell JK, Seed HB., 1988. Slope Stability Failure Investigation: Landfill Unit B-19, Phase I-A, Chemical Waste Management, Inc. Facility, Kettleman Hills, CA, vol. *Report of Investigation*. University of California Berkeley.
84. Seed R.B., Mitchell J.K., Seed H.B. 1990. Kettleman Hills Waste Landfill Slope Failure, II: Stability Analyses. *Journal of Geotechnical Engineering*, ASCE, 116(4):669-90.
85. Shan, H, -Y. 1993. Stability of Final Covers Placed on Slopes Containing Geosynthetic Clay Liners. PhD Dissertation, University of Texas, Austin, TX
86. Sharma, H.D. and Lewis, S.P., 1994, *Waste Containment Systems, Waste Stabilization, and Landfills: Design and Evaluation*, John Wiley and Sons, Inc., New York, USA.
87. Siegel,R.A., Robertson, R.J. and Anderson,D.G., 1990, "Slope Stability Investigations at a Landfill in Southern California", *Geotechnics of Waste Landfills - Theory and Practice*, Landva, A. and Knowles, G.D., Editors, ASTM Special Publication 1070, proceedings of a symposium held in Pittsburgh, Pennsylvania, USA, pp. 259-284.
88. Staff, C.E., 1984. The Foundation and Growth of the Geomembrane Industry in the United States. *Proc. Intl. Conf. on Geomembranes, Denver. CO. IFAI*, 5 - 8.

89. Stark, T.D., Eid, H.T., 1996. Shear Behaviour of Reinforced Geosynthetic Clay Liners. *Geosynthetics International*, 3(6), 771-786
90. Triplett, E.J., Fox, P.J. 2001. Shear strength of HDPE Geomembrane/Geosynthetic Clay Liner Interfaces. *Journal of Geotechnical and Geoenvironmental Engineering*, June 2001, 543 - 552.
91. Vaid, Y.P. and Rinne, N., 1995. Geomembrane Coefficients of Interface Friction. *Geosynthetics International*. Vol. 2, No. 1 309 - 325.
92. Villard, P., Gourc, J. P., Feki, N. 1999. Analysis of Geosynthetic Lining Systems (GLS) undergoing Large Deformations. *Geotextiles and Geomembranes* 17 (1999). pp 17- 32.
93. Waste Management Paper 26B. 1995. Landfill Design, Construction and Operational Practice. *Department of the Environment*, HMSO, London.
94. Wasti, Y., Bahadir OzduzgUn, Z. 2001. Geomembrane-Geotextile Interface Shear Properties as determined by Inclined Board and Direct Shear Box Tests. *Geotextiles and Geomembranes*, 20 (1), 45-57.
95. Williams, P. T., 1998. *Waste Treatment and Disposal*. John Wiley & Sons Ltd. England
96. Wise, C. 2006. *Aspects of the Bellville South Landfill in the Western Cape*. [Personal Communication]. Cape Town. (Unpublished)
97. Wright, S. G., 1991. UTEXAS3: a computer program for slope stability calculations, *Shinoak Software*, Austin, Texas.
98. Zornberg, J.G., McCartney J.S., Swan Jr, R.H., 2005. Analysis of a Large Database of GCL Internal Shear Strength Results. *Journal of Geotechnical and Geoenvironmental Engineering*, 367 - 380.

APPENDICES

Appendix A. Test Procedures

The following tests are presented in Appendix A:

- A.1 Determination of Limiting Dry Densities
- A.1.1 Determination of Maximum Dry Density of Sand
- A.1.2 Determination of Minimum Dry Density of Sand
- A.2 Determination of Moisture Content
- A.3 Standard Compaction Test
- A.4 Standard Test Method for Measuring Mass per Unit Area of Geosynthetic Clay Liner
- A.5 Standard Test Method for Determining Average Bonding Peel Strength between the
Top
and Bottom Layers of Needle-Punched Geosynthetic Clay Liners
- A.6 Standard Test Method for Swell Index of Clay Component of Geosynthetic Clay
Liners
- A.7 Standard Test Method for Determining the Internal and Interface Shear Resistance
of Geosynthetic Clay Liner by the Direct Shear Method

Appendix B. Large Direct Shear Devices

The following Large Direct Shear Devices have been used by other researchers and are presented in Appendix B:

- B.1 Wykeham Farrance device — Hsieh & Hsieh, 2003
- B.2 Shear Pullout device — Triplett & Fox, 2001
- B.3 Soil-Geosynthetic Interaction laboratory device, GeoSyntec Consultants, SGI Testing
Services Laboratory — Zornberg, 2005

Appendix C. Scanning Electron Microscope Images

The following micrographs of the research materials are presented in Appendix C:

- C.1 Geomembrane:
 - (a) Smooth side sheared against GCL
 - (b) Smooth side sheared against sand
- C.2 Bentonite: 11% moisture content
 - (a) 500x magnification

- (b) 15000x magnification
- C.3 Bentonite: 150% moisture content (frozen sample)
 - (a) 5000x magnification
 - (b) 15000x magnification
- C.4 Bentonite: 3000% moisture content (frozen sample)
 - (a) 5000x magnification
 - (b) 15000x magnification

Appendix D. Test Work Sheets

The following test sheets were used and copies are given in Appendix D:

- Sheet 1 Determination of minimum and maximum densities
- Sheet 2 Compaction test
- Sheet 3 Sand preparation and compaction for direct shear test
- Sheet 4 Sand preparation and compaction for direct shear interface test
- Sheet 5 Direct shear interface test

Appendix E. Direct Shear Test Raw Data

The following example Zwick data sheet is given in Appendix E:

- Sheet 1 Geomembrane / GCL direct shear interface test

Appendix F. Landfill Design

The following limit state design methods are given in Appendix F:

- F.1 Design of sloped geosynthetic-soil layered systems
- F.2 Design of landfill liner systems incorporating a geosynthetic lining

University of Cape Town

Appendix A. Test Procedures

A. 1 DETERMINATION OF LIMITING DENSITIES

Aim: To determine the dry densities in the two extreme states of packing of the sand material.

A. 1.1 DETERMINATION OF MAXIMUM DRY DENSITY OF SAND

A.1.1.1 Apparatus

- Drying oven (105 — 110 °C)
- Compaction mould — Diameter 101.8 mm, Height 116.3 mm
- Drop hammer (2.5kg)
- Straight steel edge

A.1.1.2 Method

- Prepare sufficient oven dried sand to fill at least three moulds
- Cool oven dried sand sample in desiccator
- Weigh empty mould
- Place sand in mould to one third of its height
- Compact sand layer using 55 blows of hammer falling through a height of 300mm
- Repeat steps 4 and 5 until end of 3rd layer
- Remove collar from mould and trim excess sand using straight edge
- Weigh mould with the sand
- Repeat the test at least three times

A.1.1.3 Results

SAND TYPE: Philippi Dune sand

Test Number	Compacted (Maximum Density)		
	1	2	3
Mass + Tare (g)	6127	6140	6130
Tare (g)	4422	4422	4422
Mass of sample (g)	1705	1718	1708
Volume of sample (cm ³)	956.3	956.3	956.3
<u>Density of sample (Mg/m³)</u>	<u>1.783</u>	<u>1.797</u>	<u>1.786</u>
Average Maximum Density =	1.789	(Mg/m ³)	

A.1.2 DETERMINATION OF MINIMUM DRY DENSITY OF SAND

A.1.2.1 Apparatus

- a) Drying oven (105 °C — 110 °C)
- b) Compaction mould — Diameter 101.8 mm, Height 116.3 mm
- c) Funnel
- d) Drop hammer (2.5kg)
- e) Straight steel edge

A.1.2.2 Method

1. Prepare sufficient oven dried sand to fill at least three moulds
2. Cool oven dried sand sample in a desiccator
3. Weigh empty mould
4. Insert funnel inside mould
5. Pour sand in funnel
6. Carefully retract funnel, causing sand to slowly empty into mould. Care should be taken to ensure that sand does not 'fall' into the mould
7. Continue steps 5 and 6 until entire mould is full
8. Using straight edge, carefully trim excess sand above the mould
9. Weigh mould with the sand
10. Repeat the test at least three times.

A.1.2.3 Results

SAND TYPE: Philippi Dune sand

Test Number	Uncompacted (Minimum Dry Density)		
	1	2	3
Mass + Tare (g)	5885	5886	5889
Tare (g)	4422	4422	4422
Mass of sample (g)	1463	1464	1467
Volume of sample (cm ³)	956.3	956.3	956.3
Density of sample (Mg/m ³)	1.530	1.531	<u>1.534</u>
Average Minimum Dry Density =	1.532	(Mg/m ³)	

A.2 DETERMINATION OF MOISTURE CONTENT

(According to BS 1377: Part 2: 1990)

A.2.1 Aim

To determine the moisture content (w) of the sand material

A.2.2 Apparatus

- a) Drying oven (105°C — 110 °C)
- b) Drying container
- c) Weighing scale (accuracy of 0.1g)
- d) Desiccator

A.2.3 Method

1. Determine the mass of dry container, (W_1)
2. Place chosen sample in container
3. Determine the mass of the sample + container, (W_2)
4. Place container in oven to dry for about 24 hours
5. Remove container from oven and allow to cool in the desiccator
6. Determine mass of container and sample, (W_3)

A.2.4 Calculations

$$w = \frac{(W_2 - W_3)}{(W_3 - W_1)} \times 100 \%$$

A.3 STANDARD COMPACTION TEST

(According to BS 1377: 1975, Test 12)

A.3.1 Aim

To determine the maximum dry density and optimum moisture content of sand material.

A.3.2 Apparatus

- a) Compaction mould (Proctor), internal dimensions 101.8 mm diameter and 116.3 mm high.
- b) Detachable base-plate
- c) Removable extension collar
- d) Metal rammer with 50mm diameter face, weighing 2.5 kg, sliding freely in a tube which controls the height of drop to 300mm
- e) Measuring cylinder
- f) Metal tray 600mm x 500mm x 80mm deep
- g) Weighing scale
- h) Tins for moisture content determinations
- i) Drying oven (105 °C — 110 °C)

A.3.3 Test Procedure

A.3.3.1 Apparatus Preparation

The mould body and the base-plate were weighed to **the** nearest 1g (m_1). Diameter (**D**, mm) and height (L, mm) were measured in several places to 0.1mm using a Vernier caliper and the mean dimensions obtained. The internal volume (V, cm³) was then calculated with the equation;

$$V = \frac{\pi \cdot D^2 \cdot L}{4 \cdot 1000} \text{ Cm}^3$$

The mould body and base were weighed.

A.3.3.2 Sample collection

The bulk sample of sand was air dried and the mass required weighed. Because the sample contained granular material, and was likely to be broken by the action of the rammer, separate batches were prepared for compaction at each moisture content.

A.3.3.3 Batches Preparation

From the sand sample, about eight representative samples each of about 2 kg were taken. The samples were combined and thoroughly mixed with the amount of water to give the lowest moisture

content for the tests. Water was added after each tested sample to bring the rest of the batch to the next required moisture content.

A.3.3.4 Compaction

The mould assembly was placed on a solid base. Loose wet sand was added to the mould so that it was about half filled. A rigid circular steel plate, 100mm in diameter and 13 mm thick, was then carefully placed on top of the filled sand. This was to prevent the sand 'jumping' out of the mould during compaction. The sand was compacted by applying 25 blows of the rammer dropping from the controlled height of 300mm on to this plate. Care was also taken to make sure that the rammer was properly in place before it was released.

After compaction of the first layer of sand, an approximately equal amount of the second layer of sand was placed in the mould and compacted with 25 blows as before.

The procedure was repeated with the third layer, which brought the compacted surface in the extension collar to about 5mm above the level of the mould body.

A.3.3.5 Trimming of sample

The extension collar was carefully removed. Excess sand was cut away and leveled off to the top of the mould, checked with a straight-edge.

A.3.3.6 Weighing of sample

Because the sample was granular and would not hold together well, the base-plate was left on. The sample, the mould and the base-plate were then weighed to the nearest 1g (m2)

A.3.3.7 Removal of soil

The sample was removed from the mould using a soil specimen extractor.

A.3.3.8 Measurement of moisture content

Moisture content samples were taken, after compaction and weighing, one from the top and one from the bottom of the sample. Moisture content, w (%) was then measured using standard procedures. (Appendix A.2)

The above stages were repeated for each sample in turn.

A.3.3.9 Evaluations

The bulk density of each compacted specimen was calculated using:

$$\rho = \frac{m_2 - m_1}{V} \text{ Mg/m}^3$$

The moisture content, w (%) for each compacted specimen was also calculated as an average of the two samples taken. The corresponding dry density was then obtained using the equation:

$$\rho_D = \left(\frac{100}{100 + w} \right) \cdot \rho \text{ Mg/m}^3$$

Each dry density was plotted against the corresponding moisture content. A smooth curve was drawn through the points. The maximum dry density values and the corresponding optimum moisture content were then read off.

University of Cape Town

A. 4 STANDARD TEST METHOD FOR MEASURING MASS PER UNIT AREA OF A GEOSYNTHETIC CLAY LINER

(According to ASTM D 5993 — 99)

A.4.1 Aim

To determine the mass per unit area and dry bentonite mass component per unit area of a sample of a geosynthetic clay liner (GCL).

A.4.2 Apparatus

- a) Drying Oven, 105°C - 110°C
- b) Balance, 0.01 g readability
- c) Sample containers
- d) Desiccator
- e) Miscellaneous: razor knives, oven gloves, scoops, measuring instrument

A.4.3 Procedure (Assuming Moisture Present)

The sample received at the testing laboratory was in satisfactory condition and representative of the product. The work area was cleaned before cutting the specimens. Samples of the GCL were cut into five 0.02m² (100mm x 200mm) test specimens using a sharp razor knife. The five specimens were randomly selected from locations on the sample, but were distributed across the sample. One half the weight of the waste clay on the cutting board was added to the test specimen container and the other one-half was discarded.

The tare of the specimen containers were determined and recorded before placing each test specimen in an individual container. The mass of the container and GCL specimen was determined and recorded.

The containers were placed, with the GCL specimens, in the drying oven until dried to constant mass. The containers were removed from the oven and allowed to cool to room temperature in a desiccator.

The mass of the container and oven-dried material was determined using the same balance as used previously. The tare of the container was subtracted from the mass of the sample to determine the samples' constant dry mass. This value was recorded (*MGM*).

A.4.4 Calculation

The mass per unit area of each of the specimens was calculated as follows:

$$m_{GCL} = \frac{M_{GCL}}{A}$$

where:

m_{dried} = mass per unit *area* of the dried GCL product rounded to the nearest 0.1 g/m²,

m_{dried} = dried mass of GCL specimen measured to the nearest 0.01 g,

= (oven-dried specimen + container mass) - (tare mass of container), and

A = area of the specimen, m²

The mass per unit area of the clay component of the GCL was estimated as follows:

$$m_{\text{clay}} = m_{\text{GCL}} - m_s$$

where:

m_{clay} = mass per unit area of dry clay component rounded to the nearest 0.1 g/m², and

m_s = nominal mass per unit area of GCL synthetic component(s), g/m²

The average of the mass per unit area results for the five test specimens was calculated.

A.5 STANDARD TEST METHOD FOR DETERMINING AVERAGE BONDING PEEL STRENGTH BETWEEN THE TOP AND BOTTOM LAYERS OF NEEDLE-PUNCHED GEOSYNTHETIC CLAY LINERS

(According to ASTM D 6496 — 99)

A.5.1 Aim

To determine the average bonding strength between the top and bottom layers of a sample of a needle-punched Geosynthetic Clay Liner (GCL).

A.5.2 Apparatus

- a) Tensile Testing Machine - A constant rate of extension (CRE) type
- b) Clamps
- c) Razor knife
- e) Measuring instrument

ASS Test Specimen

The sample received at the testing laboratory was in satisfactory condition. Five 100mm x 200mm test specimens were cut from the sample such that it was representative of the entire roll width. All specimens were cut in machine direction.

A.5.4 Procedure

Using a razor knife, the top and bottom layer of the GCL was separated for the first 50 ± 3 mm. The testing machine was adjusted so that the distance between the clamps at the start of the test was 50 ± 3 mm and the CRE was set at 300mm/min.

Each specimen was mounted centrally in the clamps, which held the specimen over the full 100mm width. The specimen length in the machine direction was confirmed parallel to the direction of the application of force. The tensile testing machine was started; the start of the peel test representing zero grip separation. Readings of force and time occurred continuously through a computerized system at approximately 120 readings per second.

The test was run till the grip separation was at least 125mm, resulting in a 100mm recorded peeling length of the GCL.

A.5.5 Calculation

The Bonding Peel Strength was calculated for each individual specimen:

$$\alpha_f = \frac{F_{avg}}{W_s} \quad \text{N / 10cm}$$

where:

α_f = bonding peel strength, N/10cm of width.

F_{avg} = observed average force (N) over a grip separation of 25 mm to 125mm

W_s = specified specimen width, cm (generally 10cm).

The Average Bonding Peel Strength was calculated as follows:

$$\alpha_{avg} = \frac{(\alpha_{f1} + \alpha_{f2} + \dots + \alpha_{f5})}{5} \cdot 10 \quad \text{N / m}$$

where:

α_{avg} = calculated average bond strength for specimen, N/cm and

α = average bond strength of the GCL, N/cm.

A.6 STANDARD TEST METHOD FOR SWELL INDEX OF CLAY COMPONENT OF GEOSYNTHETIC CLAY LINERS

(According to ASTM D 5890 — 01)

A.6.1 Aim

To determine the swell index of the clay component of a Geosynthetic Clay Liner (GCL).

A.6.2 Apparatus

- a) Mortar and Pestle
- b) U.S. Standard Sieve: 100 mesh, 200 mesh
- c) Drying Oven, 105°C-110°C
- d) Desiccator
- e) Balance, 0.01g readability
- f) Weighing dish
- g) Cylinder, graduated TC (to contain), Class A volumetrically calibrated, with 1ml subdivisions and stopper, approximately 180 mm height from inside base to 100 ml mark.
- h) Wash bottle
- i) Spatula
- j) Ten-minute timer
- k) ASTM Calibration Immersion Thermometer, 0 to 105°C \pm 0.5°C

A.6.3 Reagents

Water prepared by distillation

A.6A Procedure

The clay mineral sample was ground to 100 % passing a 100 mesh U.S. Standard Sieve and a minimum of 65 % passing a 200 mesh U.S. Standard Sieve with a mortar and pestle. The sample was dried to a constant weight in the oven.

2.00 \pm 0.01 g of this dried and finely ground clay mineral was weighed onto a small weighing dish. 90 ml of reagent water was added to a clean 100 ml graduated cylinder. 0.1g of clay mineral was removed with a volumetric spoon from the weighing dish and carefully dusted over the entire surface of water in the graduated cylinder over a period of approximately 30 s. The clay mineral was allowed to wet, hydrate, and settle to the bottom of the graduated cylinder for a minimum period of 10 min.

Additional increments of the clay mineral powder were added as above until the entire 2.00 g sample was added. After the final increment had settled, adhering particles on the sides of the cylinder were carefully rinsed into the water column, raising the water volume to the 100 ml mark. The thermometer was carefully immersed into the water, without disturbing the settled clay mineral and the

temperature of the slurry recorded to $\pm 0.5^{\circ}\text{C}$. The cylinder was allowed to stand undisturbed for 16 h from the last incremental addition.

The volume level in milliliters at the top of the settled clay mineral was recorded to the nearest 0.5 ml. The temperature of the hydrated clay mineral to $\pm 0.5^{\circ}\text{C}$ was also recorded.

A.6.5 Calculation

The average of the five swell test results was calculated.

University of Cape Town

A. 7 STANDARD TEST METHOD FOR DETERMINING THE INTERNAL AND INTERFACE SHEAR RESISTANCE OF GEOSYNTHETIC CLAY LINER BY THE DIRECT SHEAR METHOD

(According to ASTM D 6243 - 98 and ASTM D 5321 - 92)

A.7.1 Aim

To determine the internal shear resistance of a Geosynthetic Clay Liner (GCL) or the interface shear resistance between the GCL and an adjacent material under a constant rate of displacement.

A.7.2 Apparatus

a) *Shear Device* - A rigid device to hold the specimen securely and in such a manner that a uniform force with limited torque can be applied to the specimen was used. The device consisted of both a stationary and moving container/shear-box, each of which was capable of containing dry or wet soil and was rigid enough to not distort during shearing of the specimen. Each shear-box had dimensions of 300mm x 300 mm, with a depth of 75mm. The traveling container was placed on firm bearings and rack to ensure that the movement of the container was only in a direction parallel to that of the applied shear force.

c) *Normal Stress Loading Device*, capable of applying and maintaining a constant uniform normal stress on the specimen for the duration of the test.

d) *Shear Force Loading Device*, capable of applying a shearing force to the specimen at a constant rate of horizontal displacement (strain controlled) in a direction parallel to the direction of travel of the lower container. The rate of displacement could be controlled to an accuracy of $\pm 10\%$ over a range of at least 6.35 mm/min to 0.025 mm/min.

e) *Displacement Indicators*, the shear force loading device incorporated a sufficiently sensitive displacement indicator.

f) *Specimen Clamping Devices*, required for fixing GCL and/or geomembrane specimens to the stationary section or container, the traveling container, or both, during shearing of the specimen.

g) *Miscellaneous Equipment* for preparing specimens. A timing device and equipment required for maintaining saturation of the GCL.

A.7.3 Specimen and machine preparation

- The direct shear device was calibrated to measure the internal resistance to shear inherent to the device. The shear device was completely assembled without placing a specimen inside and without any normal stress. The shear force was applied to the traveling container at a rate of 6.35 mm/min. The shear force was sustained for at least 50mm total horizontal displacement. The maximum shear force recorded was the internal shear correction to be applied to shear force data after the testing of specimens.
- The GCL samples were stored at the 'as-received' moisture content.

- At least three specimens for shearing in a direction parallel to the machine direction were carefully cut. All specimens were free of surface defects and not from near the edge of the GCL or geomembrane sample. The individual preparation methods for the three materials used is described below:

A.7.3.1 GCL

- The GCL was cut to dimensions of 46cm x 30cm. 8.5cm of the GCL on each side was separated with a razor knife and cleaned of the dry bentonite. Holes were made for the clamping screws and the geotextile surfaces cleared of bentonite particles. A sample of bentonite was taken from the edge loss to determine the moisture content.
- The specimen was placed with free access to water outside the shear machine, with no normal stress, for at least 48 hours.

A.7.3.1 Geomembrane

- The geomembrane was cut to dimensions of 59cm x 30cm. Holes were made for the clamping screws and the interface was cleaned with a moist soft cloth.

A.7.3.1 Sand

- For the direct shear test the halves of the shear-box were screwed together before compacting the sand inside. Approximately 20kg of wetted sand was needed. The sand was compacted in three layers into the shear-box at the required dry density and moisture content.
- For a sand interface test the sand was compacted in two layers into the lower half of the shear-box at the required dry density and moisture content to between 3mm and 5.5mm above the shearing plane, depending on the normal stress for the test. Approximately 11kg of wetted sand was needed.

A.7.4 Set-up procedures

A.7.4.1 GCL/geomembrane interface

- The geomembrane was attached to the lower shear-box grip plate. The GCL was carefully removed from the water and cleaned of swelling bentonite outside the specimen perimeter. Four bentonite samples were taken to determine the moisture content.
- The GCL was attached to the upper grip plate with the non-woven side facing down. The space between the shear-boxes was set at 5 mm. The box was flooded to above the interface.
- The specimen was incrementally loaded beginning with the weight of the load plate itself. Loading proceeded with a load increment ratio of approximately 1 to the test required normal stress. The minimum time of hydration and consolidation in the direct shear machine was 48 hours. At each load increment enough time was allowed to let the specimen settle to a large

extent. The final load step was given the most time to reach vertical equilibrium - at least 16 hours.

- After the test, the water was drained, the normal stress and the upper shear-box removed. The specimens were taken out and the interfaces photographed and documented for bentonite amount and damage, if any. Five bentonite samples were cut from the GCL through the woven geotextile (each corner region and the centre) to determine the moisture content at post test conditions.

A.7.4.2 Geomembrane/sand interface

- The geomembrane was attached to the upper grip plate and placed over the leveled sand surface. The gap was set to 5mm.
- The normal stress was increased to the test required value and allowed to settle for at least 30min. if the test was in saturated conditions water was added to above the interface level soon after loading.
- Sand samples were taken immediately after the test to determine the moisture content of the interface at near test conditions.

A.7.4.2 GCL/sand Interface

- The GCL was carefully removed from the water and cleaned of swelling bentonite outside the specimen perimeter. Four bentonite samples were taken to determine the moisture content.
- The sand was compacted at a lower moisture content ($\pm 0.5\%$) than the natural moisture content, since it would become more moist as water was squeezed out of the GCL during consolidation.
- The GCL was attached to the upper grip plate, with the woven side facing down, and placed over the leveled sand surface. The gap was set to 5mm.
- The specimen was incrementally loaded beginning with the weight of the load plate itself. Loading proceeded with a load increment ratio of approximately 1 to the test required normal stress. The minimum time of consolidation in the direct shear machine was 48 hours.
- Sand samples were taken immediately after the test to determine the moisture content of the interface at post test conditions. Five bentonite samples were also cut from the GCL through the woven geotextile (each corner region and the centre) to determine the moisture content at post test conditions.

A.7.4.2 Sand

- The space between the two halves of the shear-boxes was set at approximately 0.5mm.
- The normal stress was increased to the test required value and allowed to settle for at least 30min. If the test was in saturated conditions, water was added to above the interface level soon after loading.
- Sand samples were taken immediately after the test to determine the moisture content of the interface at post- test conditions.

A.7.5 Shearing

- The upper half of the shear-box was brought into position and the necessary spacer plates inserted. The loading plate was put in place and the normal stress applied to the specimen. The normal stress voltage indicator was checked and allowed to warm up for 30min.
- The shear force loading device was switched on and set to the required displacement rate and displacement and force data capture settings. The shear force loading device was assembled such that the loading ram was in contact with the stationary container, but no shear force was applied.
- The shear force was applied using a constant rate of displacement. The data was recorded continuously. Normal force readings were manually recorded throughout the test.
- The test was run until the horizontal displacement exceeded 50mm or another larger value depending on the interface requirement.
- At the end of the test, the normal stress was removed from the specimen and the device carefully disassembled. The failure surface and clamp area were carefully investigated.
- The difference between the recorded shear stress and the internal shear correction was the actual shear stress applied to the specimen.
- The test was repeated with at least three normal stress levels with new GCL, GM and sand specimens.

A.7.6 Calculation

- For tests involving sand the initial and final water content as well as unit weight were calculated.
- For tests involving the GCL the initial and final water content of the bentonite was calculated.
- The apparent shear stress applied to the specimen for each recorded shear force was calculated as follows:

$$\tau = \frac{F_s}{A_c}$$

where:

= shear stress (kN/m²),

F_s = shear force (kN), and

= corrected area (m²).

- Being a square container, the corrected area is calculated for each displacement reading using the following equation:

$$A_c = A_o - (d \times W)$$

where:

= corrected area (m²),

A_o = initial specimen contact area (m^2),

d = horizontal displacement of the traveling container (m), and

W = specimen contact width in a direction perpendicular to that of shear force application (m).

The area correction was applied to the normal stress calculation as well, as follows:

$$\sigma_n = \frac{F_n}{A_c}$$

where:

σ_n = total normal stress (kN/m^2),

F_n = normal force (kN) and

A_c = corrected area (m^2).

- The limiting values of shear stress versus applied normal stress for each test conducted were plotted. These values were at peak shear stress.
- The data points were connected with a best-fit straight line, which is referred to as the peak failure envelope. In some cases a bilinear envelope was used. The slope of the failure envelope is the coefficient of friction. The angle of friction is determined by way of using the following equation:

$$\tau = c + \sigma_n \times \tan(\phi)$$

where:

τ = peak shear stress,

σ_n = normal stress,

ϕ = angle of friction (degrees), and

c = cohesion intercept.

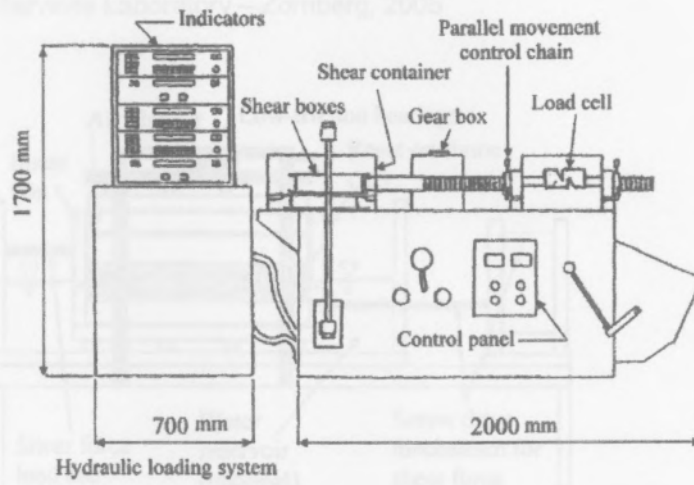
- The τ -intercept of the straight line with $\sigma_n = 0$ axis is the adhesion intercept, c_a , or cohesion intercept.
- Additionally, the coefficient of friction was calculated based on shear stresses at some larger displacement or at the end of the test — a large displacement friction angle and cohesion.

Appendix B. Large Direct Shear Devices

University of Cape Town

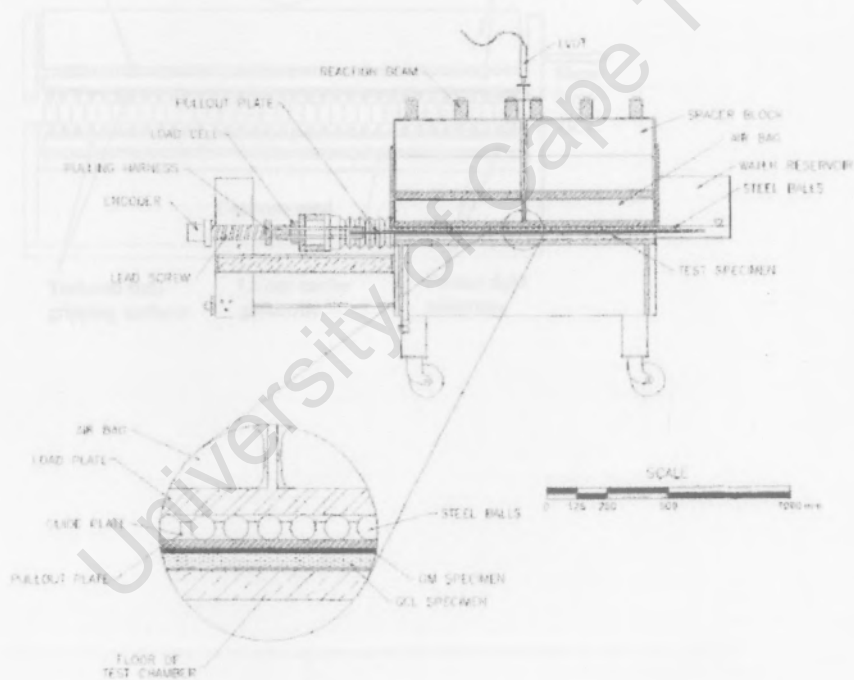
B.1

Wykeham Farrance device – Hsieh & Hsieh, 2003

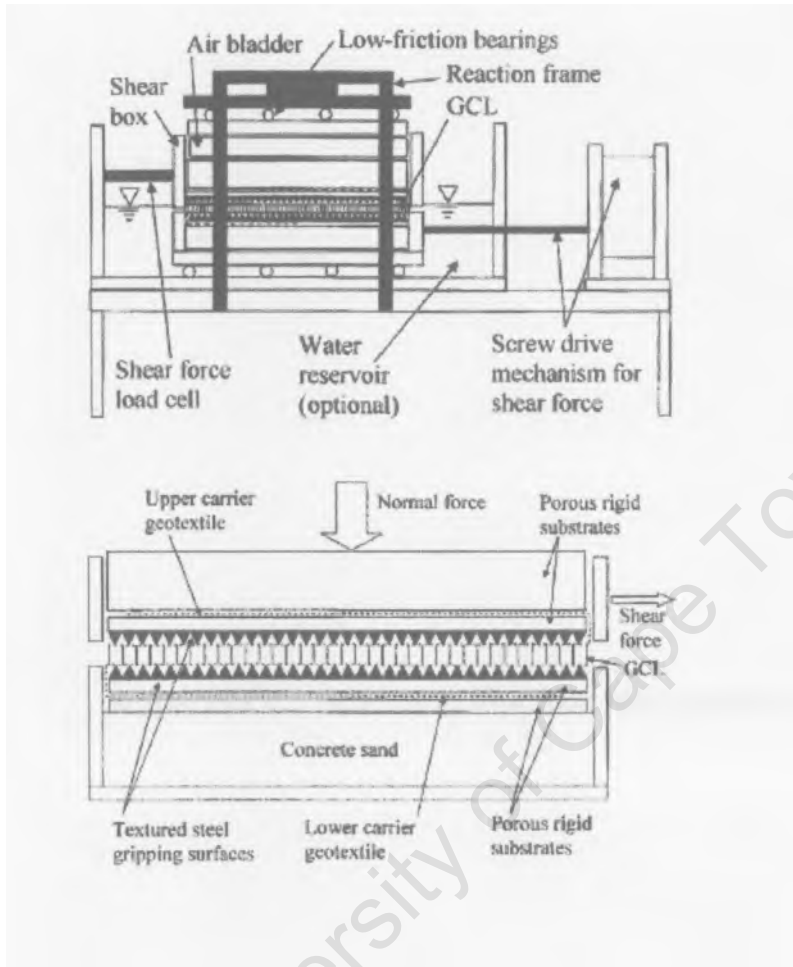


B.2

Shear Pullout device – Triplett & Fox, 2001



B.3 Soil-Geosynthetic Interaction laboratory device, GeoSyntec Consultants, SGI Testing Services Laboratory — Zorn berg, 2005



Appendix C. Scanning Electron Microscope Images

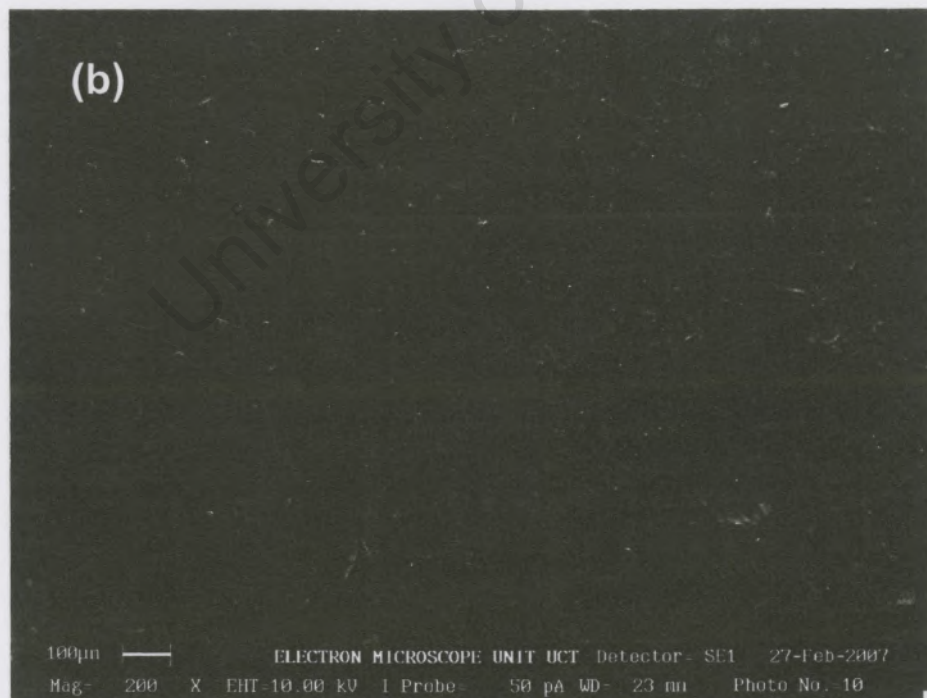
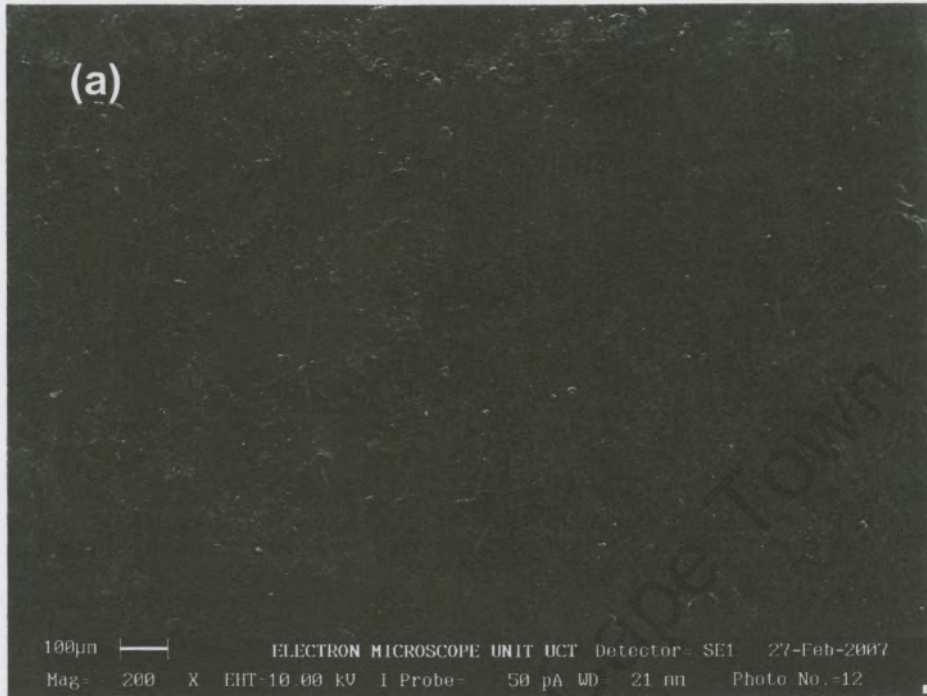
University of Cape Town

C.1

Geomembrane:

(a) Smooth side sheared against GCL

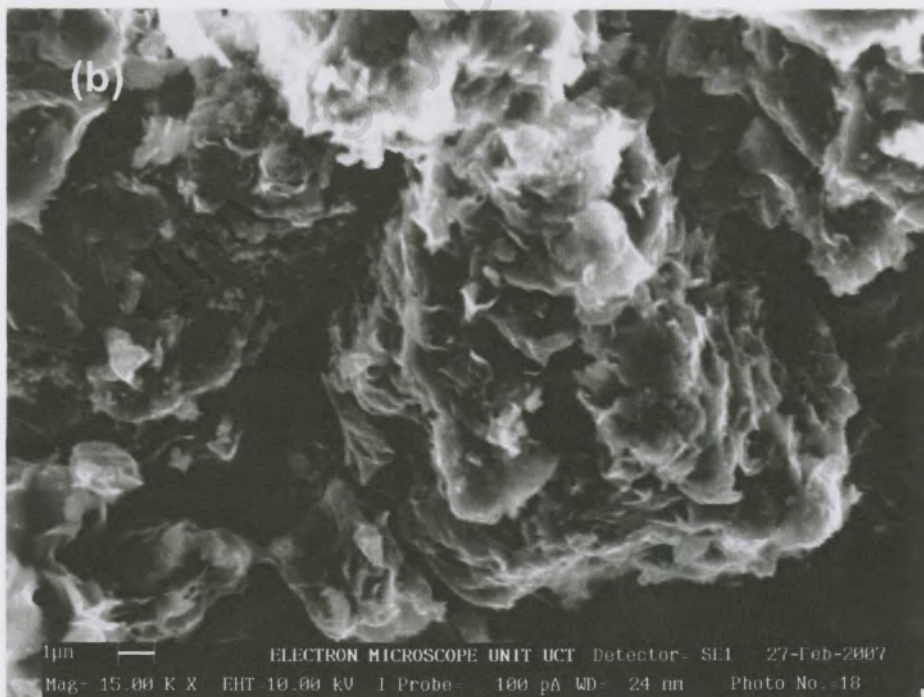
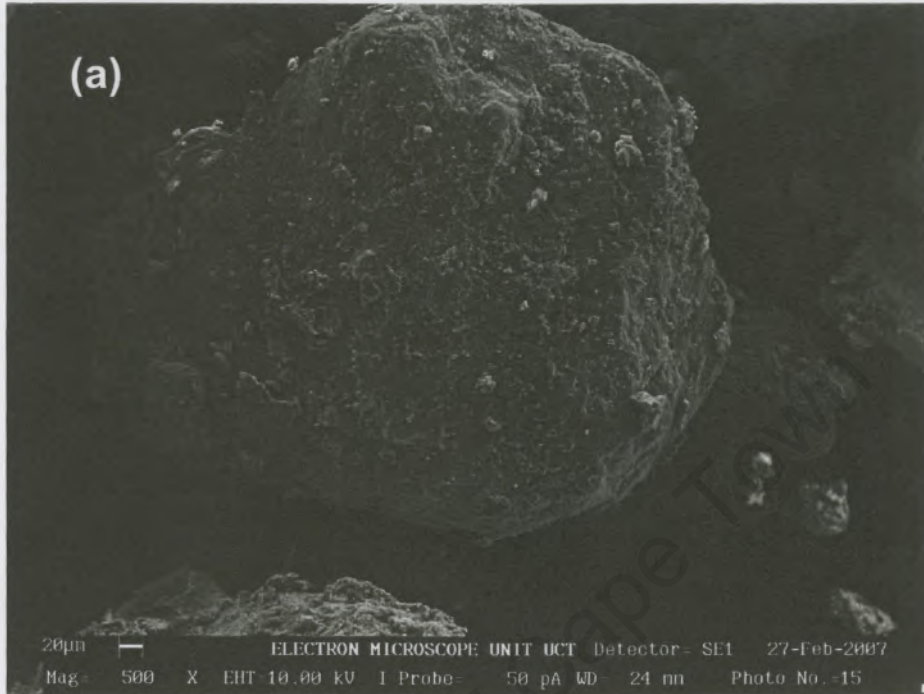
(b) Smooth side sheared against sand



C.2 Bentonite: 11 % moisture content

(a) 500x magnification

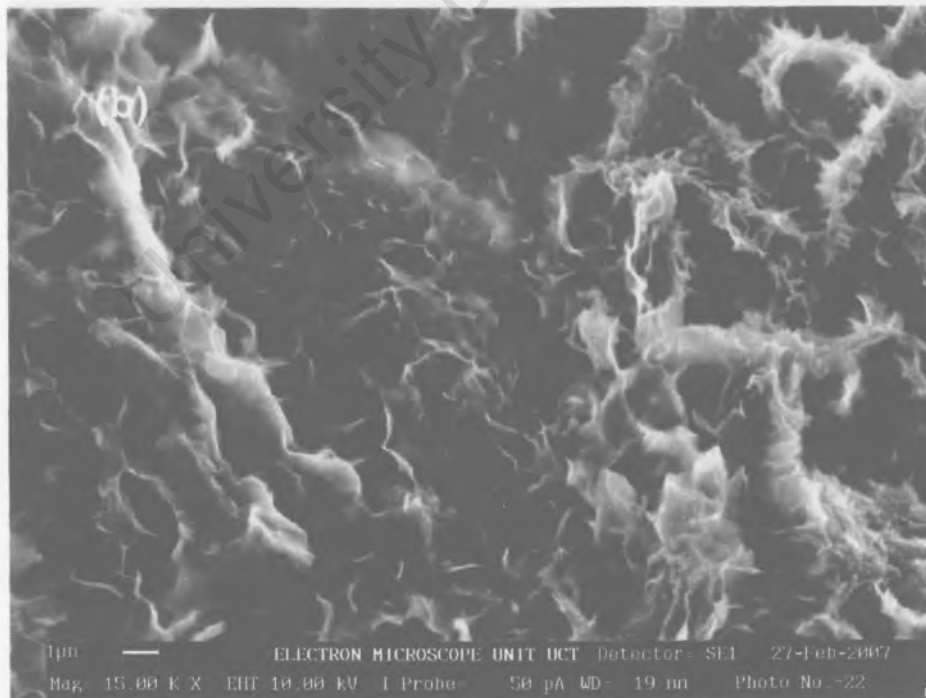
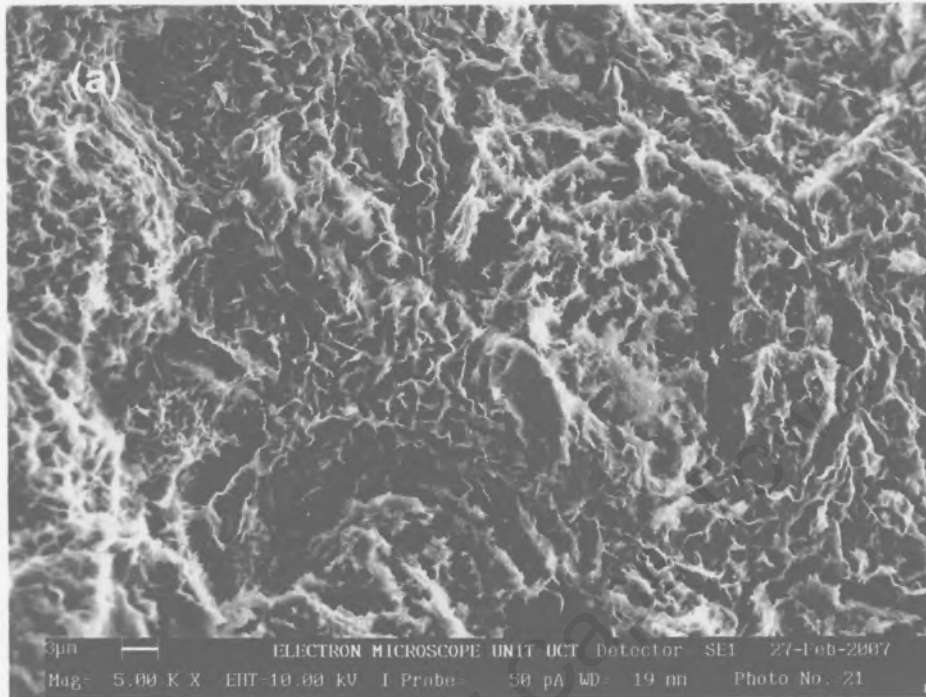
(b) 15000x magnification



C.3 Bentonite: 150% moisture content (frozen sample)

(a) 5000x magnification

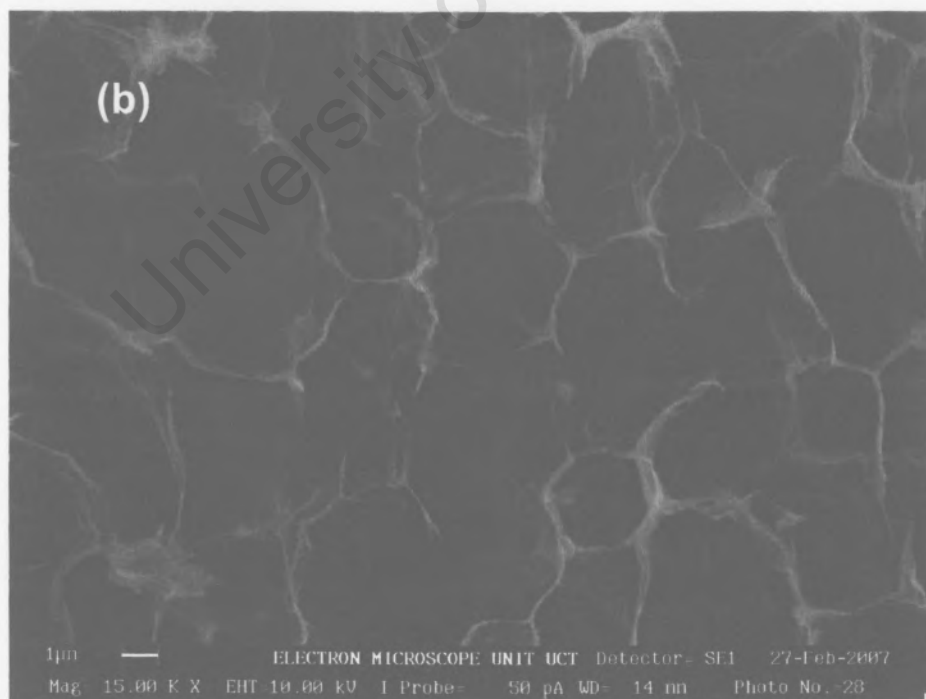
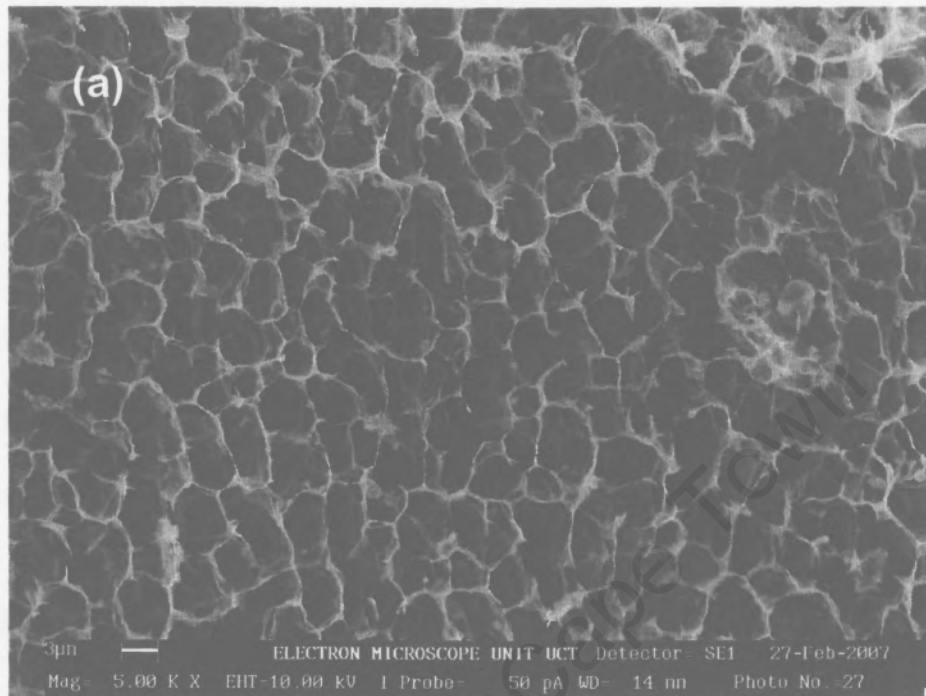
(b) 15000x magnification



C.4 Bentonite: 3000% moisture content (frozen sample)

(a) 5000x magnification

(b) 15000x magnification



Appendix D. Test Work Sheets

University of Cape Town

Sheet 1: Determination of minimum and maximum densities

Tested by: _____

Date: _____

1. SAND TYPE:

Test Number	_____	1	Compacted (Minimum Density)	_____
Mass + Tare (g)	_____			
Tare (g)	_____			
Mass of sample (g)	_____			
Volume of sample (cm ³)	_____			
Density of sample (Mg/m ³)	_____			

Average Minimum Density = _____ (Mg/m³)

1. SAND TYPE:

Test Number	_____	1	Compacted (Maximum Density)	_____	2	_____	3
Mass + Tare (g)	_____						
Tare (g)	_____						
Mass of sample (g)	_____						
Volume of sample (cm ³)	_____						
Density of sample (Mg/m ³)	_____						

Average Maximum Density = _____ (Mg/m³)

Sheet 3: Sand preparation and compaction for direct shear test

Soil Preparation for Shear Test

Date _____

Test Number:
Tester:
Soil type:
Time of mixing:

Sand Preparation

Moisture Content aimed at (%): _____ Water added to soil (ml): _____

Dry soil added to mixer:

Total:

Compaction in Shear box

Blows per layer:

Moisture content confirmation

Layer masses (g)

Layer 1:
Layer 2:
Layer 3:
Layer 4:

Bowl number
Bowl mass (g)
Mass bowl + wet soil (g)
Mass bowl + dry soil (g)
Mass water (g)
Mass dry soil (g)
Water content (%)

Lost during compaction (g):

Total mass sand in box (g):

Height of load plate (mm):

Thickness of load plate: 49.55mm
Depth of total box: 145.32mm (with base plate & mesh in place)
Depth of soil (mm):

Volume of soil (m³):

Estimated

Exact

Wet Density (kg/m³)
Dry Density (kg/m³)

Wet Density (kg/m³)
Dry Density (kg/m³)

Comments

Sheet 4: Sand preparation and compaction for direct shear interface test

Sand Preparation for Interface Test

Date _____

Test Number:
 Tester:
 Sand type:
 Time of mixing:

Sand Preparation

Moisture Content aimed at (%): _____ Water added to soil (ml): _____

Dry soil added to mixer:

Total:

Compaction in Lower Shear box

Blows per layer: T **Moisture content confirmation**

Layer masses (g)

Layer 1:
 Layer 2:

Bowl number
 Bowl mass (g)
 Mass bowl + wet soil (g)
 Mass bowl + dry soil (g)
 Mass water (g)
 Mass dry soil (g)

Height above lower box (mm):
 Soil removed to level (g):

Total mass soil in box (g):

Water content (%):

Volume of lower box (m³)
 Volume above level (m³)

Total Volume:

Estimated _____ Exact

Wet Density (kg/m³) _____ J Wet Density (kg/m³)
 Dry Density (kg/m³) _____ Dry Density (kg/m³)

Comments

Sheet 5: Direct shear interface test

Interface investigated:

Date _____

Test No:

Tester:

Sand:

GCL:

GM:

**Hydration of GCL
outside machine:**

Start:

Extraction: _____

GCL Interface investigated:

GM Interface investigated:

Gap between shear boxes (mm):

Area of Interface at start, I x b (mm):

Displacement rate (mm/min):

In LDS

Date	Time	Dead Load kg	Load on Hanger kg	Voltage mV	Normal stress kPa	Height - Front mm	Load Plate Back mm	Comments
-------------	-------------	------------------------	-----------------------------	----------------------	-----------------------------	-----------------------------	------------------------------	-----------------

START

Comments:

University of Cape Town

Appendix E. Direct Shear Test Raw Data

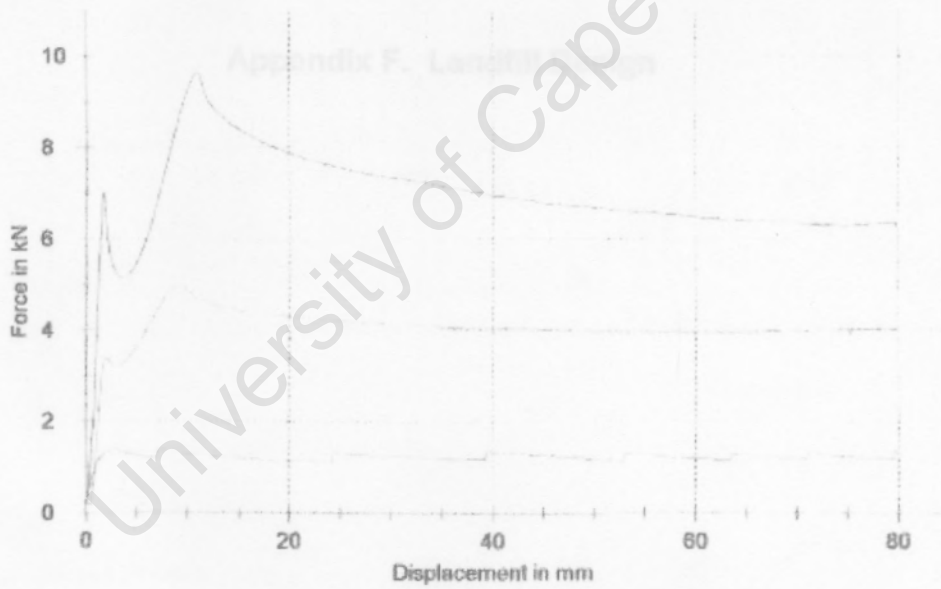
Parameter table:

Order number : Interface shear test series 2
 Charge : -
 Test standard : ASTM
 Tester : Wesley Rouncivell
 Customer : MSc. Thesis
 Material : Bentomat ST & 2mm smooth HDPE
 Extensometer (path) : -
 Load cell : 100 kN
 Specimen grips : Large Direct Shear Device
 Test speed : 1 mm/min

Results:

Legends	Nr	Rm N	c Rm %
	1	1372.17	16.25
	2	4958.55	20.75
	3	9623.62	24.38

Series graph:



Appendix F. Landfill Design

University of Cape Town

F.1 DESIGN OF SLOPED GEOSYNTHETIC-SOIL LAYERED SYSTEMS

(After Giroud et al., 1995)

F.1.1 Aim

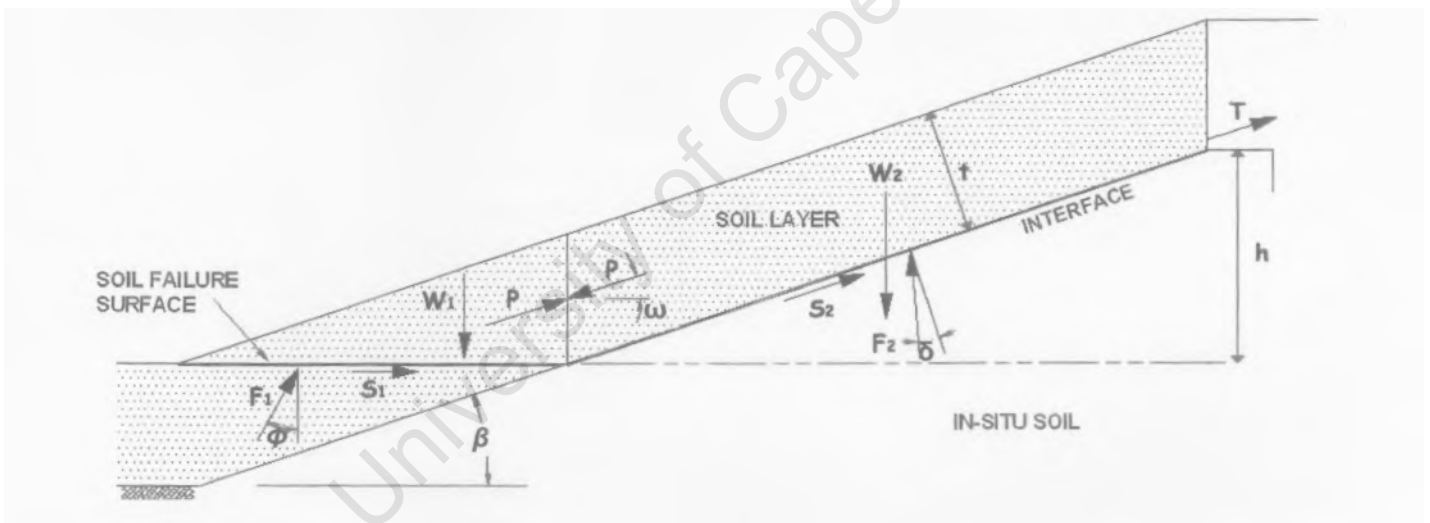
To determine the factor of safety against sliding along a plane failure surface of a geosynthetic-soil layered system of uniform thickness on a given slope.

F.1.2 Method

This method considers a two-wedge analysis independent of pore water pressures. Giroud et al. (1995) consider the balance of forces acting on these wedges based on a force polygon to develop equations to determine the factor of safety (FS).

F.1.3 Geometry

(not to scale)



Where,

t = thickness of soil layer above sliding interface

ϕ = internal angle of friction of the soil

β = slope angle

h = height of the geosynthetic interface considered

δ = interface friction angle

T = tension in any geosynthetics above the slip surface

P = force transmitted across the separation between the two wedges

W_1 = weight of wedge 1

W_2 = weight of wedge 2

F_1 = force due to soil frictional response at the lower boundary of wedge 1

F_2 = force due to interface frictional response at the lower boundary of wedge 2

S_1 = force due to soil cohesion at the lower boundary of wedge 1

S_2 = force due to adhesion at the lower boundary interface of wedge 2

F.1.4 Calculations (Giroud et al., 1995)

$$FS = \frac{\tan \delta}{\tan \beta} + \frac{a}{\gamma \cdot t \cdot \sin \beta} + \frac{t \cdot \sin \phi}{h \cdot \sin(2\beta) \cdot \cos(\beta + \phi)} + \frac{c \cdot \cos \phi}{\gamma \cdot h \cdot \sin \beta \cdot \cos(\beta + \phi)} + \frac{T}{\gamma \cdot h \cdot t}$$

[F.1]

Where,

FS = Factor of Safety

γ = unit weight of the soil

c = cohesion of the soil

a = interface adhesion along slip surface

University of Cape Town

F.2 DESIGN OF LANDFILL LINER SYSTEM INCORPORATING A GEOSYNTHETIC LINING

F.2.1 Aim

To determine the factor of safety against sliding of a landfill cross-section containing a geosynthetic lining system by considering the balance of forces per meter run.

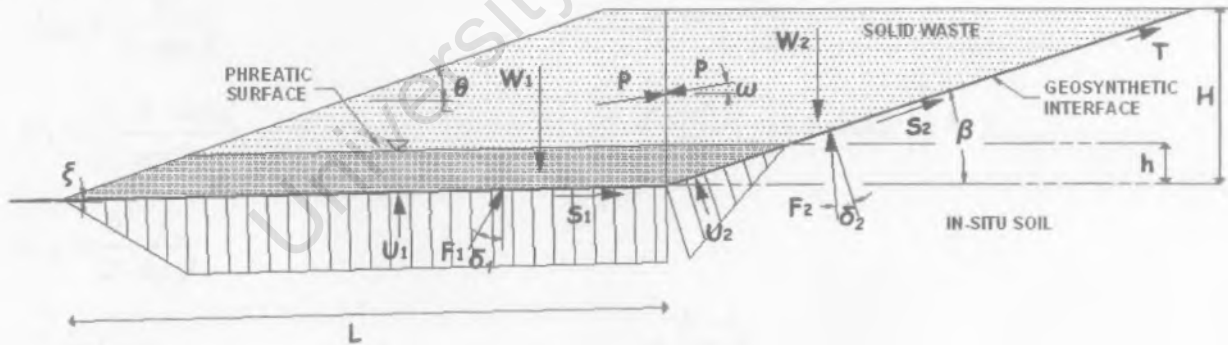
F.2.2 Method

This method considers a two-wedge analysis incorporating hydrostatic pressures and possibly different interface shear strength parameters on the base and side slopes. This method is a logical extension of the approach adopted by Giroud et al. (1995) for the design of sloped geosynthetic-soil layered systems. However, the waste material is added and the failure surface is considered to be along the geosynthetic interface only.

Also, forces are resolved in vertical and horizontal directions to determine the global factor of safety instead of constructing a force polygon — the method adopted by Giroud et al. (1995). The phreatic surface is assumed not to taper downward to the base liner at the waste slope region for the purposes of calculation. This approach is considered to a conservative one.

F.2.3 Geometry

(not to scale)



Where,

f_i = lining slope angle

θ = waste slope angle

β = base slope angle

ω = direction of inter-wedge force P (equivalent to internal friction angle of waste material)

H = height of the geosynthetic interface considered

L = length of base

h = height of phreatic surface above base liner at slope liner toe

T = tension in any geosynthetics above the slip surface

P = force transmitted across the separation between the two wedges
= weight of wedge 1

W₂ = weight of wedge 2

= force due to soil frictional response at the lower boundary of wedge 1

F₂ = **force** due to interface frictional response at the lower boundary of wedge 2

U₁ = hydrostatic force below wedge 1

U₂ = hydrostatic force below wedge 2

S₁ = force due to adhesion at the lower boundary interface of wedge 1

S₂ = force due to adhesion at the lower boundary interface of wedge 2

F.2.4 Calculations

$$\omega = \phi$$

$$W_1 = A_{sat1} \cdot \gamma_{sat} + A_{unsat1} \cdot \gamma_{unsat}$$

$$W_2 = A_{sat2} \cdot \gamma_{sat} + A_{unsat2} \cdot \gamma_{unsat}$$

$$A_{sat1} = \left(\frac{(h \cdot \cos \xi)^2}{2 \cdot \tan \theta} + \left(L - \frac{h \cdot \cos \xi}{\tan(\theta - \xi)} \right) \cdot h \cdot \cos \xi + \frac{h^2 \cdot \cos \xi \cdot \sin \xi}{2} \right)$$

$$A_{unsat1} = \left(\frac{(L \cdot \sin \xi + H)^2}{2 \cdot \tan \theta} + \left(L \cdot \cos \xi - \frac{(L \cdot \sin \xi + H)}{\tan \theta} \right) \cdot (L \cdot \sin \xi + H) - \frac{L^2 \cdot \cos \xi \cdot \sin \xi}{2} \right) - A_{sat1}$$

$$A_{sat2} = \frac{h^2}{2 \cdot \tan \beta}$$

$$A_{unsat2} = \frac{H^2}{2 \cdot \tan \beta} - A_{sat2}$$

$$U_1 = \left(\left(\frac{h \cdot \cos \xi}{\tan(\theta - \xi)} \right) - h \cdot \sin \xi \right) \cdot \frac{h \cdot \gamma_w}{2} + \left(L - \left(\frac{h \cdot \cos \xi}{\tan(\theta - \xi)} \right) - h \cdot \sin \xi \right) \cdot h \cdot \gamma_w$$

$$U_2 = \frac{h^2 \cdot \gamma_w}{2 \cdot \sin \beta}$$

$$C_1 = L \cdot a_1$$

$$C_2 = \frac{H \cdot a_2}{\sin \beta}$$

$$N_1 = W_1 \cdot \cos \xi - U_1$$

$$N_2 = W_2 \cdot \cos \beta - U_2$$

Where,

= internal angle of friction of the soil

γ_{unsat} = unit **weight** of the unsaturated soil

|||

γ_w = unit weight water

A_{sat1} = Area of saturated soil in wedge 1

A_{sat2} = Area of saturated soil in wedge 2



δ_1 = friction angle of interface at the base of wedge 1

δ_2 = friction angle of interface at the base of wedge 2

a_1 = interface adhesion along wedge 1 slip surface

a_2 = interface adhesion along wedge 2 slip surface

A_1 = interface adhesive force along wedge 1 slip surface

A_2 = interface adhesive force along wedge 2 slip surface

Consider **wedge 1**, balance forces in the horizontal direction:

$$P \cdot \cos \omega = \left(\frac{N_1 \cdot \tan \delta_1}{FS} + \frac{C_1}{FS} \right) \cdot \cos \xi \quad (1)$$

Consider **wedge 2**, balance forces in the vertical direction:

$$P \cdot \sin \omega = W_2 - N_2 \cdot \cos \beta - \left(\frac{N_2 \cdot \tan \delta_2}{FS} - \frac{C_2}{FS} - T \right) \cdot \sin \beta \quad (2)$$

Solve equation (1) and (2) simultaneously to determine the factor of safety, FS:

$$FS = \frac{\tan \omega \cdot \cos \xi (N_1 \cdot \tan \delta_1 + C_1) + N_2 \cdot \tan \delta_2 \cdot \sin \beta + C_2}{W_2 - N_2 \cdot \cos \beta - T \cdot \sin \beta} \quad [F.2]$$